Photosynthetic characteristics of *Arabidopsis* mutants, deficient in ascorbate, alternative oxidase and NADP-malate dehydrogenase, in relation to the redox status

A thesis submitted to the University of Hyderabad
for the award of Ph. D. degree in
Plant Sciences

By

Sai Krishna Talla

Department of Plant Sciences
School of Life Sciences
University of Hyderabad
Hyderabad 500 046, India

Regd. No: 06LPPH11

December 2012

University of Hyderabad
School of Life Sciences
Department of Plant Sciences
Hyderabad 500 046

DECLARATION

I, Sai Krishna Talla, hereby declare that this thesis entitled **"Photosynthetic characteristics of *Arabidopsis* mutants deficient in ascorbate, alternative oxidase and NADP-malate dehydrogenase, in relation to the redox status"** submitted by me under the supervision of Professor A. S. Raghavendra in the Department of Plant Sciences, School of Life Sciences, University of Hyderabad is an original and independent research work. I also declare that it has not been submitted previously in part or in full to this University or any other University or Institution for the award of any degree or diploma.

Date: Name: Sai Krishna Talla

Signature:

Regd. No.: 06LPPH11

University of Hyderabad
School of Life Sciences
Department of Plant Sciences
Hyderabad 500 046

CERTIFICATE

This is to certify that this thesis entitled **"Photosynthetic characteristics of *Arabidopsis* mutants deficient in ascorbate, alternative oxidase and NADP-malate dehydrogenase, in relation to the redox status"** is a record of bonafide work done by Mr. Sai Krishna Talla, a research scholar for Ph. D. programme in Plant Sciences, Department of Plant Sciences, School of Life Sciences, University of Hyderabad under my guidance and supervision.

Prof. A. S. Raghavendra
(Supervisor)

(Head of the Department) (Dean of the School)

Acknowledgements

I owe my gratitude to my supervisor, **Prof. A.S. Raghavendra**, for his constant encouragement, guidance and support.

I would like to thank **Prof. Attipalli R. Reddy,** Head, Department of Plant Sciences and **Prof. M. Ramanatham,** Dean, School of Life Sciences, for providing necessary facilities for my research. I extend my thanks to former Heads of Department **Prof. P.B. Kirti** and **Prof. Appa Rao Podile** and the former Dean, **Prof. A.S. Raghavendra.**

I am highly thankful to my doctoral committee members, **Dr. Saradadevi Tetali** and **Dr. K.P.M.S.V. Padmasree** for their helpful suggestions.

I am also thankful to all the faculty members of **Dept. of Plant Sciences/ School of Life Sciences**.

I would like to express my gratitude to **Prof. Prasanna Mohanty, Prof. Renate Scheibe, Prof. Erwin Grill** and **Prof. K.L. Kuchitsu** for helpful discussions during their visit to our laboratory.

I am thankful to my former labmates **Drs. Riazunnisa, Dinakar, Vijay, Uday, Bakshu** and present labmates **Dr. Sunil, Dr. Bindu, Dr. Poonam, Nupur, Mallikarjun, Rajsheel, Gayatri, Srinivas, Aswani and project students Hima Bindu, Swathi, Eshan, Raheem** and **Prathyusha** for the help and enjoyable company; **Mr. Venu** for help in lab and field.

I am also thankful to my friends **Karthik, Vijay, Shiva, Sankar, Arvind, Abhay Pratap, Srinivas, Suma** and **Sreedhar** for unconditional support and love they provided me all these years.

I am thankful to all my loving friends and colleagues in **School of Life Sciences** for their affection and moral support which will remain fresh forever in my memory.

I am also thankful to all the non teaching staff members of school of life sciences.

I gratefully acknowledge the financial assistance for me from the **UOH, UGC-SAP RFMS** and **CSIR**.

I also acknowledge funding from **UGC, CSIR, DBT, ICAR-NAIP, DST-DFG, DST-JC Bose** to the laboratory of **Prof. A. S. Raghavendra** as well as **DST-FIST, DBT-CREBB and UGC SAP-CAS** (for funding to Department and School).

I am thankful to the **Department of Plant Sciences, University of Hyderabad** for providing me an opportunity to pursue my Ph.D.

Last, but most important are the love and gratitude for my family members. I owe my deep respect for my father **Mr. Shanker Goud** and my mother **Mrs. Lakshmi Narsa** for their constant affection and encouragement. I owe my heartfelt thanks to my **brothers and sisters** for making my life happy with their lovely, enjoyable and memorable company.

I am heartily thankful to my wife **Mrs. Sujatha** who stood by my side in both good and bad circumstances and for her unconditional love and support.

Finally, I dedicate my entire research work to my sister **Mrs. Alekhya**.

Sai Krishna Talla

Dedicated to my beloved sister

Abbreviations

AAN	=	aminoacetonitrile
AOX	=	alternative oxidase
aox1a	=	alternative oxidase 1a lacking mutant of *Arabidopsis*
APX	=	ascorbate peroxidase
AsA	=	ascorbate (reduced form)
BSA	=	bovine serum albumin
CAT	=	Catalase
CCCP	=	carbonyl cyanide *m*-chlorophenylhydrazone
DAB	=	3,3-diaminobenzidine
DHA	=	dehydroascorbate (oxidized form)
DHAP	=	dihydroxyacetone 3-phosphate
GalL	=	L-galactono-1,4-lactone
GalLDH	=	L-galactono-1,4-lactone dehydrogenase
GHA	=	glycine hydroxamate
GR	=	glutathione reductase
GSH	=	glutathione (reduced form)
NADP-MDH	=	NADP-dependent malate dehydrogenase
nadp-mdh	=	NADP-MDH lacking mutant of *Arabidopsis*
OAA	=	oxaloacetic acid
PMSF	=	phenyl methane sulfonyl fluoride
ROS	=	reactive oxygen species
SHAM	=	salicylhydroxamic acid
vtc1	=	vitamin C deficient mutant of *Arabidopsis*

All the remaining abbreviations are standard ones and as indicated by the journal *Plant Physiology* on their website: http://www.aspb.org. under 'Instructions For Authors'.

Contents

Chapter 1

Introduction and Review of Literature

Chapter I

Introduction and Review of Literature

Plants encounter varying environmental stress conditions such as excess light, limited water and salinity. Since plants are sessile, they need to adapt to these stress conditions, so as to survive. These environmental stresses frequently cause a rise in intracellular ROS in plants. Such rise seems to be pronounced in photosynthetic organisms, particularly when photosynthetic electron transport outpaces the rate of electron consumption during CO_2 fixation (Scheibe et al., 2005; Oelze et al., 2008). Besides these extreme conditions, there are some indications that elevated CO_2 levels could also induce oxidative stress in plant cells (Kolla et al., 2007; Qiu et al., 2008). Under steady state conditions, the ROS molecules are scavenged by various antioxidative defense mechanisms. The equilibrium between the production and the scavenging of ROS may be perturbed by various biotic and abiotic stress factors. These disturbances in equilibrium lead to sudden increase in intracellular levels of ROS which can cause extensive damage of membrane components, proteins, lipids, and even DNA (Mittler et al., 2004; Halliwell, 2006).

The ROS at limited levels may act as signal molecules to regulate cell–cell interaction, long-distance signaling, and hormone action. However, if the ROS-levels are too high, they may cause damage to cell membranes and then to other compartments, as well. Plants have developed several poising systems to maintain a balanced electron flow and the required rate of ATP production under changing conditions. These include D1 turnover, state transitions, non-photochemical energy quenching, xanthophyll cycle, chlororespiration and cyclic electron transport (Scheibe et al., 2005; Oelze et al., 2008; Foyer and Shigeoka, 2011; Scheibe and Dietz, 2012). Antioxidants and antioxidative enzymes therefore play crucial role to minimize the risk of detrimental effects caused by excess ROS. The other important cellular components which help to keep ROS-levels low are: malate valve, alternative oxidase (AOX) and

photorespiratory reactions (Scheibe et al., 2005; Noguchi and Yoshida, 2008; Bauwe et al., 2010; Yoshida and Noguchi, 2010).

Antioxidant systems

An efficient multi-component antioxidant defense system has evolved in plants in order to cope up with oxidative damage caused by excess ROS. The antioxidant defense systems include both enzymatic and non-enzymatic elements. A typically tight cooperation between enzymatic and non-enzymatic antioxidant systems provides and efficient system to regulate ROS levels in plants (Foyer and Noctor, 2009; De Gara et al., 2010).

Non-enzymatic antioxidants

These include ascorbic acid (AsA), glutathione (GSH), α-tocopherol, carotenoids, flavonoids and even proline. The most abundant soluble antioxidants in plants are AsA and GSH, which play a key role in plant defense against oxidative stress (Foyer and Noctor, 2011). In plant cells, the AsA–GSH cycle is quite active and ensures the presence of AsA–GSH in reduced form.

AsA

Ascorbate (AsA) is the most abundant water-soluble antioxidant which plays a key role in protection against oxidative damage caused by enhanced level of ROS. AsA is considered powerful antioxidant because of its ability to donate electrons in a number of enzymatic and non-enzymatic reactions. AsA is present at high levels in all sub-cellular compartments. For example, the AsA are in the range of 20 mM or more in chloroplasts (Smirnoff and Wheeler, 2000). It has also become clear from extensive literature that AsA has multiple roles in metabolism, electron transport, control of the cell cycle, and even the responses of plants to biotic/abiotic stress (Ishikawa and Shigeoka, 2008).

The regulation by AsA of intracellular ROS levels becomes very effective when coupled with AsA/GSH cycle or Asada-Halliwell pathway. AsA peroxidase (APX) utilizes AsA as its electron donor to reduce H_2O_2 to water with the concomitant generation of

monodehydroascorbate (MDA), a univalent oxidant of AsA. MDA is either disproportionated to AsA and dehydroascorbate (DHA) or reduced to AsA by MDA reductase. DHA is also reduced back to AsA by the actions of GSH-dependent DHA reductase, and the resulting oxidized GSH which is then regenerated by GSH reductase.

AsA biosynthesis occurs in all plant tissues and eukaryotic algal cells. The major AsA biosynthetic pathway in higher plants has been elucidated. This pathway, designated as the D-Man/L-Gal pathway which occurs in cytosol proceeds from D-glucose to L-Gal via GDP-D-Man, and the final aldonolactone precursor of AsA is L-galactono-1, 4-lactone (L-GalL) (Figure 1.1). The final step of the pathway, occurs in the inner mitochondrial membrane involving L-GalL dehydrogenase enzyme to oxidize L-GalL to AsA and uses cytochrome c as its electron acceptor (Smirnoff and Wheeler, 2000; Ishikawa and Shigeoka, 2008; Linster and Clarke, 2009). The *vtc-1* mutant is the ascorbate deficient mutant in which the activity of GDP-mannose pyrophosphorylase is reduced.

GSH

The tripeptide GSH is a water-soluble antioxidant composed of cysteine, glutamic acid, and glycine. Its synthesis occurs in two ATP dependent steps. The first step is the formation of γ-glutamylcysteine from glutamic acid and cysteine, catalyzed by the enzyme γ-glutamylcysteine synthetase (γ-GCS) in chloroplast. The second step is catalyzed by the enzyme glutathione synthetase, which forms a peptide bond between glycine and the cysteine of the γ-glutamylcysteine intermediate in cytosol.

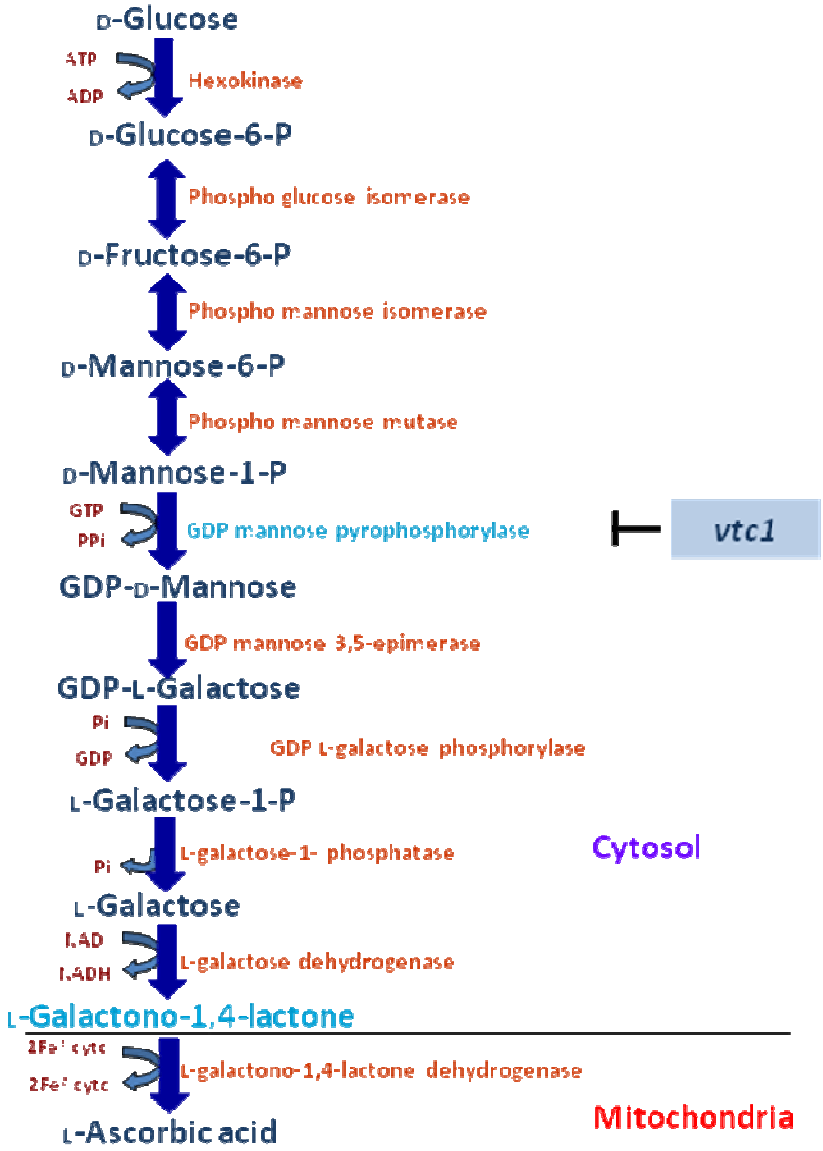

Figure 1.1. The D-Man/L-Gal pathway of ascorbate biosynthesis in plants, starting from D-glucose. Most of the reactions in this pathway are localized in cytosol, except the last step of ascorbate biosynthesis, which occurs in the inner-mitochondrial membrane. Photosynthesis can provide D-glucose.

Under physiological conditions, GSH predominantly exists in the reduced form. In response to stress, GSH can be oxidized into its disulphide form, GSSG, which can accumulate to high levels in plant cells. GSH redox status (GSSG/GSH ratio) reflects the level of oxidative stress, therefore GSH is frequently considered to be a suitable oxidative stress marker (Foyer & Noctor, 2009; Foyer & Noctor, 2011). Fernandez-García et al. (2009) have demonstrated that the chloroplast represents the major location of GSH during development of plants. The chloroplast alone has 62-75 % of total GSH, while the mitochondria account for 15-25 % of the total GSH in *Arabidopsis*. Other cellular compartments, such as the peroxisomes and nuclei, have low GSH contents.

Proline (Pro)

Besides being a well-known osmolyte, Pro is now considered as a potent antioxidant (Verbruggen and Hermans, 2008). Therefore, Pro can be regarded as non-enzymatic antioxidants that plants, microbes and animals, require to mitigate the adverse effects of ROS (Chen and Dickman, 2006). The synthesis of L-Pro from L-glutamic acid via Δ^1-pyrroline- 5-carboxylate (P5C) is catalyzed by the activities of the enzymes Δ^1-pyrroline-5-carboxylate synthetase (P5CS) and Δ^1-pyrroline-5-carboxylate reductase (P5CR) in plants (Verbruggen and Hermans, 2008). Pro biosynthesis occurs in the cytosol and in the plastids (chloroplasts) while Pro degradation takes place in mitochondria (Rayapati et al., 1989; Szoke et al., 1992). Mitochondrial enzymes Pro dehydrogenase (oxidase) (ProDH) and P5C dehydrogenase (P5CDH) metabolize L-Pro into L-Glu via P5C.

Others

Tocopherols (α, β, γ, and δ) represent a group of lipophilic antioxidants involved in scavenging of oxygen free radicals, lipid peroxy radicals, and $^1O_2$. Tocopherols are synthesized only by photosynthetic organisms and are present in only green parts of plants (Li et al., 2010). Tocopherols protects lipids and other membrane components by physically quenching and chemically reacting with O_2 in chloroplasts, thus protecting the structure and

function of PSII. Regeneration of the oxidized tocopherol back to its reduced form can be achieved by AsA and GSH.

Carotenoids also belong to the group of lipophilic antioxidants which detoxify excess ROS (Han et al., 2012). Carotenoids absorb light in the region between 400 and 550 nm of the visible spectrum and channel the captured energy to the Chl. Carotenoids scavenge $^1O_2$ to inhibit oxidative damage and quench triplet sensitizer and excited chlorophyll molecule to prevent the formation of $^1O_2$ to protect the photosynthetic apparatus. Carotenoids also serve as precursors to signaling molecules that influence plant development and biotic/abiotic stress responses.

Flavonoids occur widely in the plants at a concentration over 1 mM. Flavonoids, which function basically as pigments in flowers, fruits, and seeds, can also protect against UV light and phytopathogens. Flavonoids are the most bioactive plant secondary metabolites and serve as ROS scavengers of plants under adverse environmental conditions (Han et al., 2012). There is an increase in flavonoid levels under biotic and abiotic stresses, such as wounding, drought, metal toxicity and nutrient deprivation (Winkel-Shirley, 2002). Production of flavonoids in response to UV-B, cold and drought were reported earlier.

Antioxidant enzymes

The major antioxidant enzymes in plant cell are summarized in the Table 1. Superoxide dismutase (SOD), ascorbate peroxidase (APX) and catalase (CAT) are key enzymes involved in tight control of ROS levels by scavenging directly ROS and converting them into less reactive or less harmful species. They can be considered as intracellular ROS sensors due to their direct interaction with ROS. Another group of enzymes, monodehydroascorbate reductase (MDAR), dehydroascorbate reductase (DHAR) and glutathione reductase (GR), is involved in the reduction of oxidized AsA or GSH, thus, completing the cycles and balancing the redox status of the cell (Foyer & Noctor, 2011). Up-regulation of the enzymes involved in the antioxidant system both at the transcript and the

protein levels in response to ROS accumulation, occurs frequently under abiotic stress conditions (Gill & Tuteja, 2010).

Catalase

Catalase (CAT, 1.11.1.6) is a ubiquitous tetrameric heme-containing enzyme that dismutates the two molecules of H_2O_2 into water and oxygen. It has high specificity for H_2O_2. Plants contain several types of H_2O_2-degrading enzymes, however, CATs are unique as they do not require cellular reducing equivalent. CATs have a very fast turnover rate, but a much lower affinity for H_2O_2 than APX. The peroxisomes are major sites of H_2O_2 production. CAT scavenges H_2O_2 generated in this organelle during photorespiratory oxidation and β-oxidation of fatty acids, (Scandalios et al., 1997; Corpas et al., 2008). Though there are frequent reports of CAT being present in cytosol, chloroplast, and mitochondria, the presence of significant CAT activity in these is less well established (Mhamdi et al., 2010).

Willekens et al. (1995) proposed a classification of CAT based on the expression profile of the tobacco genes. Class I CATs are expressed in photosynthetic tissues and are regulated by light. Class II CATs are expressed at high levels in vascular tissues, whereas Class III CATs are highly abundant in seeds and young seedlings. Evidences suggest that Arabidopsis, CAT2, CAT3 and CAT1 correspond to Class I, Class II and Class III catalases, respectively (Mhamdi et al., 2010).

Ascorbate peroxidase (APX)

APX (APX, EC 1.1.11.1) is involved in scavenging of H_2O_2 in water-water and AsA-GSH cycles and utilizes AsA as the electron donor. APX is a widely distributed antioxidant enzyme and found in four distinct forms, corresponding to its intra-cellular location: stromal

Table 1. Major enzymes involved in ROS detoxification in plants.

Enzyme (Abbreviation)	**Reaction catalyzed**	**Sub-cellular localization**
Superoxide dismutase (SOD)	$O_2.^- + O_2.^- + 2H^+ \longrightarrow 2H_2O_2 + O_2$	Cytosol (Cu/Zn-SOD), chloroplast (Cu/Zn- SOD,Fe-SOD) mitochondria and peroxisome (Mn-SOD)
Catalase (CAT)	$H_2O_2 \longrightarrow H_2O + ½\ O_2$	Peroxisomes
Ascorbate peroxidase (APX)	H_2O_2 + AsA* $\longrightarrow H_2O$ + DHA*	Chloroplast, cytosol, mitochondria
Dehydroascorbate reductase (DHAR)	DHA + 2GSH* $\longrightarrow$ AsA + GSSG*	chloroplast, cytosol
Glutathione reductase (GR)	GSSG + NAD(P)H $\longrightarrow$ 2GSH + $NAD(P)^+$	cytosol, peroxisomes chloroplast, mitochondria
Monodehydroascorbate reductase (MDHAR)	MDHA* + NAD(P)H $\longrightarrow$ AsA + $NAD(P)^+$	chloroplast, mitochondria, cytosol

*Abbreviations: DHA, dehydroascorbate; MDHA, monodehydroascorbate; AsA, ascorbate; GSH, reduced glutathione; GSSG, oxidized glutathione

APX (sAPX) and thylakoid membrane-bound APX (tAPX) in chloroplasts, microbody (including glyoxysome and peroxisome) membrane-bound APX (mAPX), and cytosolic APX (cAPX). A fifth APX isoenzyme (mitAPX) occurs in a mitochondrial membrane-bound form (Noctor and Foyer, 1998; Gill and Tuteja, 2011). APXs have much higher affinity for H_2O_2 than CAT, making APXs efficient scavengers of H_2O_2 under stressful conditions.

Glutathione Reductase (GR)

GR (EC 1.6.4.2) is a flavo-protein oxidoreductase, found in both prokaryotes and eukaryotes (Romero-Puertas et al., 2006). It is localized predominantly in chloroplasts, with very small amounts found in mitochondria and cytosol (Edwards et al., 1990; Creissen et al., 1994). GR catalyzes the NADPH dependent reaction of disulphide bond of GSSG and is thus important for maintaining the GSH pool. GR and GSH play a crucial role in determining the tolerance of a plant under various stresses (Reddy and Raghavendra, 2006; Rao and Reddy, 2008).

Inter-organelle interactions and the major components

A delicate metabolic equilibrium exists between the key compartments within plant cells, including not only mitochondria and chloroplasts but also the peroxisomes and cytosol. Disturbance of any of these compartments perturbs the metabolism of whole cell (Raghavendra and Padmasree, 2003; Noguchi and Yoshida, 2008; Yoshida and Noguchi, 2010). A major factor for such metabolic stability is the exchange of several metabolites between the different cell organelles. Besides the metabolites there are other possible signals between mitochondria, chloroplasts, peroxisomes and cytosol, including AsA, nitric oxide (NO) and the cytosolic pH. For e.g. AsA can be key component during interorganelle interaction and optimizes the photosynthesis against photoinhibition and compensates the function of other protective mechanisms (Talla et al., 2011). Further, other cellular

components such as malate valve, AOX and photorespiratory pathway can also protect chloroplasts from over-reduction caused due to oxidative stress.

Malate valve and interorganelle metabolite movement

The chloroplastic NADP-malate dehydrogenase (NADP-MDH), a crucial enzyme of malate valve transports the excess reducing equivalents from chloroplasts as malate in exchange of OAA, via dicarboxylate translocator (Figure 1.2). Isoenzymes of MDH are present in different cellular compartments. Chloroplasts contain a redox-controlled NADP-MDH that is active only in the light. In contrast, a plastidic NAD-MDH that is permanently active and is present in all plastid types. Export of excess NAD(P)H through the malate valves will facilitate optimized production of ATP in photosynthesis, as well through oxidative phosphorylation (Scheibe, 2004). Along with malate-OAA shuttle, triose-P-PGA shuttle also participate in transferring reducing equivalents from chloroplasts and supplying triose-P for sucrose synthesis (Gardeström et al., 2002; Padmasree et al., 2002; Taniguchi and Miyake, 2012).

Photorespiratory reactions

Adjustments in extra-chloroplastic components of photorespiration offer an efficient outlet for dissipating excess reducing equivalents from chloroplasts (Figure 1.2) thereby optimizing the photosynthesis (Scheibe et al., 2005; Scheibe and Dietz, 2012). Additionally, chloroplastic ATP is consumed for conversion of glycerate to 3-phosphoglycerate (PGA) in the glycolate cycle. During the refixation of CO_2, twice as much NADPH and ATP consumed in the Calvin cycle. Thus, photo-respiration serves as an energy-dissipating mechanism which helps in protection of chloroplasts from photoinhibition (Wingler et al., 2000; Bauwe et al., 2010; Takahashi and Badger, 2011).

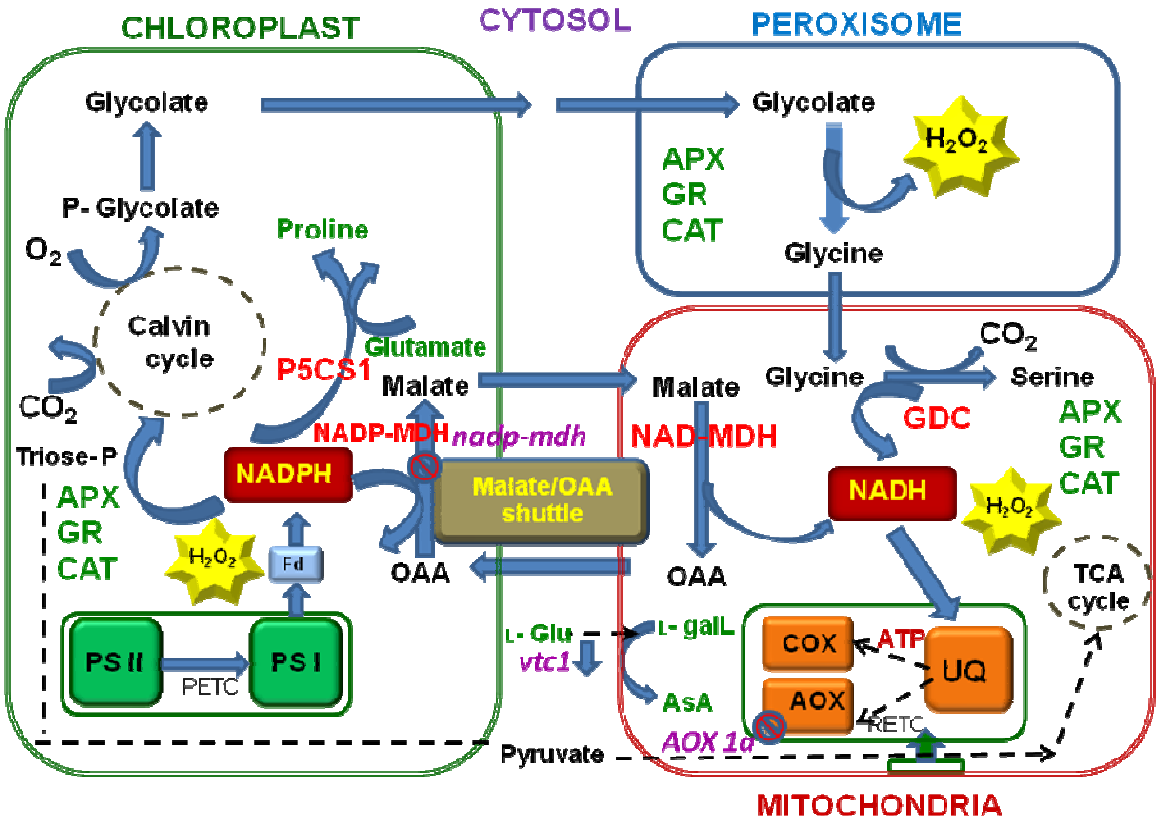

Figure 1.2. An integrated picture of the intra- and extra-chloroplastic protective mechanisms which prevent over-reduction and over energization of the chloroplasts as well as mitochondria. The roles of AsA, malate valve, photorespiratory pathway, AOX and proline are emphasized. The mutants with deficiency of these above components and localization are also indicated in italics. The abbreviations of components involved **NADP-MDH**: NADP-malate dehydrogenase, **COX:** cytochrome oxidase pathway, **AOX:** alternative oxidase pathway, **AsA**: ascorbate (modified from Hebbelmann et al., 2012).

Alternative oxidase

Apart from the above two components, the mitochondrial oxidative metabolism is quite important for utilizing excess of photosynthetic reducing power, and preventing oxidative damage of cellular components (Yoshida and Noguchi, 2010; Xu et al., 2011)**.** AOX is a dimer, located in the inner mitochondrial membrane and is in an active state, when the disulfide bonds are reduced. Encoded by a multi-gene family, five isoforms of AOX are known in *Arabidopsis* (Yoshida and Noguchi, 2010; Xu et al., 2011). Several reports state that inhibition of AOX led to a decrease in the photosynthetic rate and the over-reduction of the photosynthetic electron transport chain in leaves and in protoplasts (Padmasree and Raghavendra, 1999; Bartoli et al., 2005). It was also reported that the amount and activity of AOX dramatically increased in HL (Noguchi and Yoshida, 2008). Thus it can be assumed that AOX would function as a sink for excess reducing equivalents generated in the chloroplasts and serves as a protective mechanism in dissipation of excess reducing equivalents.

Modulation of antioxidants and antioxidant enzymes in response to different abiotic stress conditions

ROS unavoidable, being generated by photosynthetic electron transport system in both chloroplasts and mitochondria, besides peroxisomal metabolism. In order to prevent such oxidative damage by ROS, higher plants possess a complex antioxidative defense system, comprising of both antioxidant compounds and related enzymes. It is quite common that, at high light (HL) and high temperature conditions, the level of AsA content will be increased with consequent decrease in redox ratios of AsA (Foyer and Noctor, 2011; Zechmann et al., 2011). Similarly, at HL and high temperature conditions, the GSH contents increased with drop the redox ratio of GSH. The mutants with deficiency of AsA and GSH are known to be more susceptible to different abiotic stress conditions (Szalai et al., 2009;

Khan et al., 2011). At elevated CO_2 condition too, the AsA content and redox ratios of AsA decreased, while the total content and redox state of GSH was decreased (Gillespie et al., 2011).

Proline accumulates during conditions of abiotic and biotic stresses (Fabro et al., 2004; Yang et al., 2009). Accumulation of proline in higher plants is considered as an indication of oxidative stress. Different environmental stress conditions leads to induction of transcript levels of its related biosynthetic genes (Verbruggen and Hermans, 2008; Szabados and Savouré, 2010). Recent report suggests that proline also can be an efficient redox buffer (Moustakas et al., 2011).

Environmental stress conditions such as HL and high temperature enhanced the CAT activity (Vandenabeele et al., 2004; Lu et al., 2008), while elevated CO_2 decreased the activity (Aranjuelo et al., 2008). Willekens et al. (1997) observed an increased susceptibility of CAT-deficient plants to HL. These above reports signify that CAT is critical for maintaining the redox balance during the oxidative stress conditions. The activity and expression level of APX was enhanced at HL and high temperature (Karpinski et al., 1997; Storozhenko et al., 1998), while elevated CO_2 levels decreased the activity of APX (Gillespie et al., 2011) . Over-expression of tAPX in tobacco plants resulted in higher tolerance to photo-oxidative stress conditions (Yabuta et al., 2002; Kangasjärvi et al., 2008). These reports indicate the beneficial role of APX in protection of plant against oxidative stress conditions. The activity of GR increased under environmental stresses such as HL and high temperature (Ali et al., 2005; Oelze et al., 2012). Gillespie et al. (2011) reported that exposure to elevated CO_2 decreased the activity of GR. Over-expression of GR in *N. tabacum* and Populus plants leads to higher foliar AsA contents and improved tolerance to oxidative stress (Aono et al., 1993; Hernández et al., 2001). From these above findings, it was clear that GR will also play crucial role in protection of plant against oxidative stress.

Our present study is therefore, designed to study the role of antioxidant defense systems in mutants of *Arabidopsis* lacking or deficient of redox components such as AsA or malate valve or AOX and their response towards HL and elevated CO_2 conditions.

Arabidopsis: Mutants employed in the present study

Arabidopsis is one of the best model plants for plant biology research. The genome of *Arabidopsis* is relatively small and its genome is well characterized. The small size and rapid life cycle of *Arabidopsis* are additional advantages. Further, the availability of a wide spectrum of mutants and transgenics of *Arabidopsis*, as well as established protocols for isolation of protoplasts, transient expression of recombinant proteins offers a wide scope for experiments in physiology, biochemistry and molecular biology. The three *Arabidopsis* mutants employed in this study are: *vtc1, nadp-mdh* and *aox1a* mutants.

The *vtc1* mutant is an ascorbate deficient mutant with constitutively low AsA content as a result of deficiency in GDP-mannose pyrophosphorylase (GMPase) and impaired biosynthesis of AsA. Leaf AsA contents are 70 % lower than in the wild type (Conklin et al., 1996; Veljovic-Jovanovic et al., 2001). This mutant is stunted in appearance compared to the wild-type and exhibited retarded flowering and accelerated senescence (Veljovic-Jovanovic et al., 2001). There are reports on *vtc1* mutants suggesting that these mutants are more sensitive to environmental stress conditions such HL (Muller-Moulé et al, 2004), UV light (Gao and Zhang, 2008) and salinity (Huang et al., 2005) treatment.

The *nadp-mdh* mutants are the NADP-MDH knockout mutants of *Arabidopsis thaliana*. These mutants are lack the NADP-MDH transcript as indicated by northern blot analysis and RT-PCR, and were devoid of the NADP-MDH protein as demonstrated by western blot analysis. The phenotype of *nadp-mdh* plants under standard growth conditions on soil was indistinguishable from that of the WT (Hebbelmann et al., 2012). These *nadp-mdh* mutants upon treatment with either HL or low temperature exhibited an unaltered

phenotype compared with the WT. In *nadp-mdh* mutants, a novel combination of compensatory mechanisms in order to maintain redox homeostasis in the *nadp-mdh* plants under high-light conditions, particularly an increase in the NTRC/2-Cys peroxiredoxin (Prx) system in chloroplasts. There were indications of adjustments in extra-chloroplastic components of photorespiration and proline levels, which all could dissipate excess reducing equivalents, sustain photosynthesis, and prevent photoinhibition in *nadp-mdh* mutants.

The *aox1a* mutant is also a homozygous mutant of *Arabidopsis* which is deficient in leaf form of mitochondrial alternative oxidase (AOX1A) (Strodtkötter et al., 2009). These mutants exhibited no alteration of phenotypic appearance under standard growth conditions, but wilted and became necrotic when exposed to antimycin A. The antimycin A caused inhibition of photosynthesis, increased ROS, and ultimately resulted in amplified membrane leakage and necrosis in *aox1a* mutants. Zhang et al. (2010) reported that at HL intensities there occurs increased reduction of the photosynthetic electron transport chain and accumulation of reducing-equivalents in this mutant.

Earlier reports suggest that, the *vtc1* and *aox1a* mutants are highly susceptible to stress conditions such as HL conditions, while the *nadp-mdh* exhibited tolerance. This point provoked us to choose these mutants to further investigate the underlying roles of protective components such as antioxidants and antioxidative enzymes in response to HL and elevated CO_2 conditions.

The objectives and approach of the present work are described in the next chapter.

****

Chapter 2

Objectives and Approaches

Chapter 2

Objectives and Approaches

Specific objectives of the present study

The role of redox components of plants in response to different environmental stress conditions have been studied extensively (Scheibe et al., 2005). However, the magnitude and multiplicity of compensatory protective mechanisms, are getting increased attention only in recent years. Further, the modulation of these adaptive features, when there is a suppressed function of different redox components, such as ascorbate (AsA) or malate valve or alternative oxidase (AOX) or photorespiration, is yet to be examined in detail. In the context of above scenario, the objectives of present work are set as follows:

1. To study the role of AsA during the interactions between chloroplast and mitochondria in optimizing photosynthesis under photoinhibitory conditions.
2. To examine the response of *Arabidopsis* mutants deficient or lack AsA or NADP-MDH or AOX1a towards supra-optimal conditions.
3. To assess the importance of photorespiration and alternate oxidase pathway in *Arabidopsis* mutants lacking crucial enzyme of malate valve.
4. To characterize the effect of supraoptimal bicarbonate in *nadp-mdh* and *vtc1* mutants of *Arabidopsis*.

The rationale of our experiments are described below

Plant material: *Arabidopsis thaliana*

Arabidopsis thaliana is one of the most popular model systems for intensive research in several areas of plant biology. Further, the availability of a large number of mutants and transgenics of *Arabidopsis* offers unlimited and challenging scope for experiments in

physiology, biochemistry and molecular biology (Koornneef and Meinke, 2010; Stitt et al., 2010).

Protoplasts offer an attractive tool to study several aspects of plant cell biochemistry and physiology, such as photosynthesis (Riazunnisa et al., 2007), intracellular distribution of metabolites (Robinson and Walker, 1979), isolation of intact chloroplasts (Walker, 1988) and transport/accumulation of organic/inorganic compounds. *Arabidopsis* mesophyll protoplasts have been used extensively for molecular biology, transient gene expression, signal transduction, ion channels and protein-protein interactions (Sheen, 2001; An et al., 2003; Lemtiri-Chlieh and Berkowitz, 2004; Li et al., 2012).

Systems of study: mesophyll protoplasts and leaf discs

We have used the system of either mesophyll protoplasts or leaf discs, as per the requirement of the experiment. The system of mesophyll protoplasts offers certain advantages, such as free diffusion of O_2 or CO_2, taking in of the externally added compounds quickly and exert their effects on photosynthesis/respiration within 5-10 minutes, and closeness to the *in vivo* situation compared to isolated organelles, thus facilitating studies on interorganelle interaction. However, protoplasts also have certain disadvantages like limited stability at room temperature, fragile nature and the tendency to sediment.

Leaf discs on the other hand are easy to handle, and are close to *in vivo* conditions. However, the process of punching can injure the leaf tissue and hence the leaf discs have been kept in water/buffer for at least 1 h, so that the effects of mechanical stress are minimized. Additional disadvantage of leaf discs is the presence of physical barriers such as cell wall and intercellular spaces, and intercellular recycling of O_2 and CO_2, thus making precise measurements of photosynthesis and respiration difficult.

Use of modulators and metabolic inhibitors

Several metabolic inhibitors are available, which are used frequently to study the metabolic pathways and their regulation. While ensuring to use low concentrations of inhibitors, so as to exert specific action, we have used compounds either to raise the AsA content (L-galactono-β-lactone, L-galL) or to inhibit mitochondrial electron transport (antimycin A and salicylhydroxamic acid, SHAM) or photorespiration (aminoacetonitrile, AAN and glycine hydroxamate, GHA) or as external source of CO_2 (sodium bicarbonate, $NaHCO_3$).

Use of *vtc1 or nadp-mdh or aox1a* mutants of *Arabidopsis* in response to stress conditions

Evidences have emerged that the AsA, malate valve, photorespiration and AOX serves as crucial protective machinery in response to oxidative stress conditions (Igamberdiev et al., 2001; Scheibe, 2005; Foyer and Noctor, 2011; Xu et al., 2011). The mutants of Arabidopsis with altered levels of these different redox components, give us an excellent opportunity to study the adaptability of plants under stressful conditions. In the present study, we employed three mutants: (i) *vtc1* mutant - deficient in ascorbate, due to down-regulation of GDP-mannose pyrophosphorylase, (ii) *nadp-mdh* mutant - lacks chloroplastic NADP-malate dehydrogenase, a crucial enzyme of malate valve and (iii) *aox1a* mutant - deficient in leaf form of mitochondrial alternative oxidase of Arabidopsis.

Varied experimental techniques were used to monitor their photosynthetic performance, respiratory rates, ROS accumulation, the levels of key antioxidants and related antioxidant enzymes. The results and discussion are organized into four chapters, corresponding to four objectives mentioned at the beginning of this chapter.

******

Chapter 3

Materials and Methods

Chapter 3

Materials and Methods

Plant material

Seeds of wild type, *vtc1* (Conklin et al., 1999), *nadp-mdh* (Hebbelmann et al., 2012) and *aox1a* (Strodtkötter et al., 2009) mutants of *Arabidopsis thaliana* (ecotype Columbia) were sown on a 1:1:1 mixture of vermiculite, perlite and soilrite in plastic disposable pots and kept at 4 °C in dark for 3 days. The pots were then transferred to growth room, allowing the seeds to germinate. In growth room, the plants were grown under standard conditions with a photoperiod of 8 h light (125-150 µmol m^{-2} s^{-1}) and 16 h dark and temperature of 22-25 °C. Nutrient solution (suggested by Somerville and Ogren 1982; Details in Table 3.1) was supplied twice a week.

Leaves from 7 to 8 week-old plants (Figure 3.1) were harvested for preparing leaf discs or isolation of mesophyll cell protoplasts.

The initial supply of seeds of wild type and *vtc1* mutant of *Arabidopsis thaliana* were a kind gift from Dr. Nick Smirnoff, University of Exeter, Exeter, UK, and later obtained from the Arabidopsis Biological Resource Center (ABRC, Ohio State University, Columbus, Ohio). Arabidopsis *nadp-mdh* and *aox1a* knock out seeds were kind gift from Prof. Renate Scheibe, University of Osnabrueck, Germany.

Preparation and treatment of leaf discs

Discs (*ca*. 0.25 cm^2) were prepared from leaves with a sharp paper punch, from either side of the midrib, under water. These discs were pre-incubated in 5-cm-diameter Petri dishes containing 20 mM MES buffer (pH 7.0) and 1 mM $CaCl_2$. When indicated, test compounds were included. Also, small fans were used to blow air over the Petri dishes. The inhibitors

Table 3.1. The composition of nutrient solution used for growing *Arabidopsis* plants (adapted from Somerville and Ogren, 1982).

Macronutrients	**(mM)**	**Micronutrients**	**(µM)**
KNO_3	5.0	$FeSO_4 .7H_2O$	50 (in 50 mM Na_2EDTA)
KH_2PO_4	2.5	$MnSO_4 .4H_2O$	60
$MgSO_4$	2.0	$ZnSO_4 .4H_2O$	7
$Ca(NO_3)_2$	2.0	$CuSO_4 .5H_2O$	0.1
		H_3BO_4	49
		KI	4.5
		$Na_2MoO_4 .2H_2O$	1.0
		$CoCl_2$	0.1

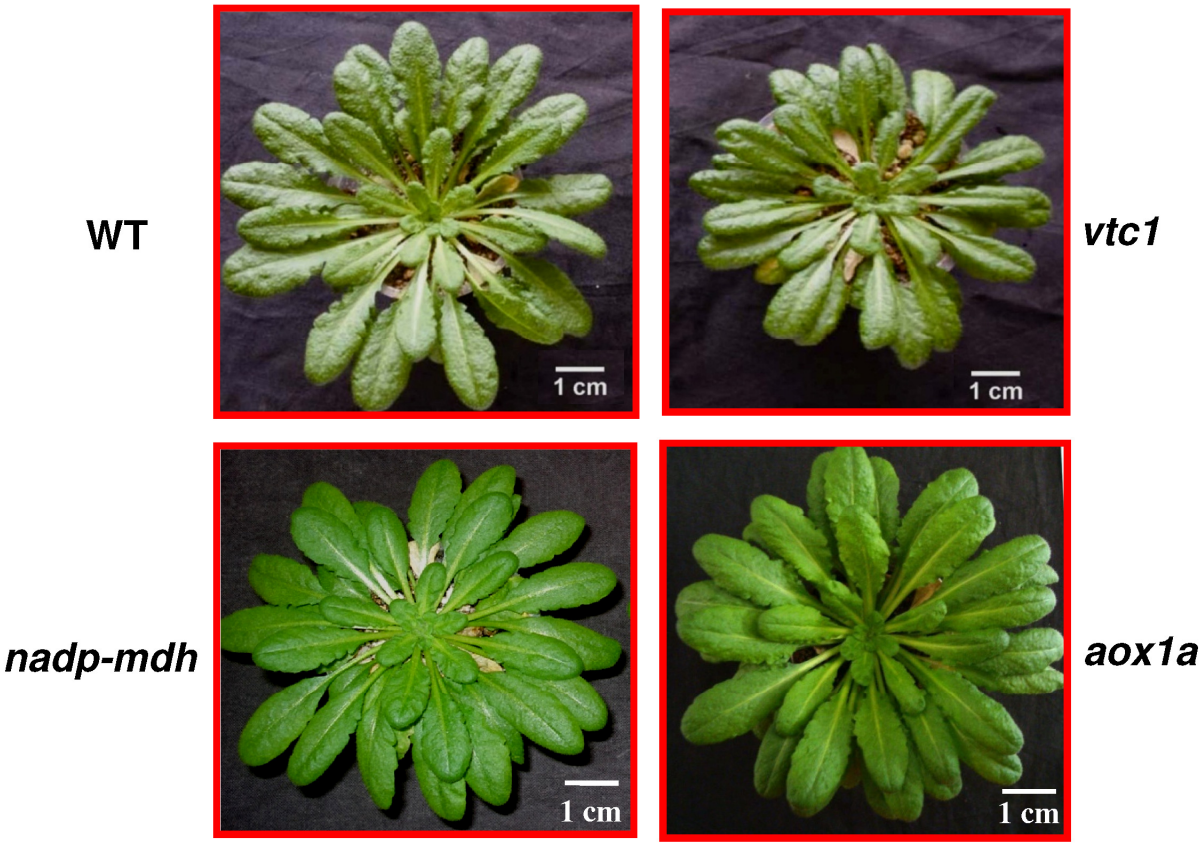

Figure 3.1. Phenotypic appearance of 8-week-old plants of wild type (cv. Columbia), *vtc1, nadp-mdh* and *aox1a* mutants of *Arabidopsis thaliana* grown in a controlled environment room, at a photoperiod of 8 light (120 µE m^{-2} s^{-1}) and 16 h dark at 22-25 ^{o}C .

were dissolved in ethanol, and the concentration of ethanol in the final volume of test solutions ranged from 0.1 % to 1 % (v/v). A similar amount of ethanol was added to controls in parallel experiments. Similarly, parallel batches of leaf discs were used for measuring photosynthesis or AsA/dehydroascorbate (DHA) levels, separately.

Isolation of mesophyll cell protoplasts

Mesophyll cell protoplasts from *A. thaliana* were isolated as per the protocol given in detail by Riazunnisa et al. (2007). About 10 leaves were excised from 8-week-old plants (Figure 3.1) with surgical blade and kept in a beaker of water covered with dark cloth. The mid rib was removed with the help of blade. The deribbed leaf was placed on a moistened glass slide with the lower epidermis up. The lower epidermis of Arabidopsis leaves was peeled off, using a curved microdissection forceps (No. 7). The leaf, devoid of epidermis, was cut into 1-cm-wide pieces. These pieces were left on a pre-plasmolysis buffer [0.65 M sorbitol, 1 mM $CaCl_2$, 5 mM 2-(N-morpholino)ethanesulfonic acid (MES)-KOH, pH 6.0] with the peeled lower surface touching the medium. After about 15 min, the pre-plasmolysis medium was removed with a Pasteur pipette (glass), and digestion medium [1 % (w/v) Cellulase Onozuka R-10, 0.4 % (w/v) Macerozyme R-10, 0.2 % (w/v) bovine serum albumin (BSA), 5 mM sodium ascorbate were freshly added, 0.65 M sorbitol, 1 mM $CaCl_2$, 0.25 mM ethylenediaminetetraacetate (EDTA) and 5 mM MES-KOH buffer, pH 5.5] was added. The leaf pieces were digested for 40 min, at 25 ^{o}C with slow orbital shaking (30 excursions per min).

The digestion medium was then gently removed with a Pasteur pipette. Washing medium [0.65 M sorbitol, 1 mM $CaCl_2$ in 5 mM MES-KOH, pH 6.0] was added to the Petri dish containing the digested leaf pieces. The Petri dish was tapped and swirled gently to release the protoplasts into the medium. All further operations were done at 4 ^{o}C. The

suspension was filtered through a nylon filter of 60-µm pore size (Saryu Textiles, Mumbai, India) and the filtrate was centrifuged at 100 g for 3 min. The supernatant was discarded and the pellet was washed with suspension medium [0.65 M sorbitol, 1 mM $CaCl_2$, 0.5 mM $MgCl_2$, and 10 mM N-2-hydroxyethylpiperazine-N'-2-ethanesulfonic acid (HEPES)-KOH, pH 7.0], followed by centrifugation at 100 g for 2 min (to remove broken protoplasts). The pellet was finally suspended in 0.5 ml of suspension medium, mixed well by gently swirling the test tube containing the protoplasts and kept on ice. The protoplasts (Fig. 1B) were kept on ice and handled gently throughout the experiments.

Estimation of chlorophyll

Chlorophyll was estimated in mesophyll protoplasts by extracting into 80 % (v/v) acetone (Arnon, 1949). An aliquot of 12.5 µl of protoplast suspension was added to 5 ml of 80 % (v/v) acetone and mixed on a cyclo-mixer. The absorbance of acetone extract was measured at 652 nm (A_{652} - to determine chlorophyll) and 710 nm (A_{710} - to correct for turbidity), using a spectrophotometer (Shimadzu UV-1700).

The chlorophyll concentration in the protoplast preparation was calculated using the following formula:

$$\text{Chl (mg ml}^{-1}\text{ of protoplast suspension)} = (A_{652} - A_{710}) \times 11.11$$

Monitoring photosynthesis and respiration

Leaf discs:

After a given treatment, the leaf discs (19 in number) were quickly blotted dry and transferred into the leaf disc oxygen electrode chamber (LD-2, Hansatech Instruments Ltd., King's Lynn, UK). The components in the chamber were arranged as per the instructions of the manufacturer. The topmost capillary matting was moistened with 200 µl of 1 M bicarbonate buffer (pH 9.0), which results in a gaseous atmosphere of 5 % (v/v) CO_2 in the

chamber (Walker 1988). The leaf discs were arranged on this matting symmetrically in 3 successive rings of 1, 6 and 12. Oxygen in the chamber was calibrated for every sample as per the instructions of the manufacturer. Photosynthetic oxygen evolution or dark oxygen uptake was measured at 25 ^{o}C by a computerized leaf disc oxygen electrode system (LD-2, Hansatech Instruments Ltd., King's Lynn, UK). Light, at the required intensity was provided by an array of light emitting diodes (Hansatech Instruments Ltd., King's Lynn, UK).

Leaf discs of Arabidopsis were floated on 20 mM MES buffer (pH 7.0) containing 1 mM $CaCl_2$ in 9 cm diameter Petri dishes and incubated in either dark or moderate light (300 µmol m^{-2} s^{-1}) or high light (1800 µmol m^{-2} s^{-1}) at room temperature, for 2 h in the presence or absence of test compounds. The illumination was provided by halogen lamps, 24V/150 W (Philips Comptalux). An 8 cm thick circulating water jacket was used between the light source and the sample to prevent heating and of the sample. Also small fans were used to blow air over the leaf discs.

Protoplasts: The photosynthetic O_2 evolution and respiratory O_2 uptake in protoplasts was monitored using liquid phase Clark-type O_2 electrode (DW2) supplied by Hansatech Ltd., King's Lynn, UK. Protoplasts equivalent to 10 µg Chl, 1 mM $NaHCO_3$ and test compounds were added to the reaction medium [0.65 M sorbitol, 1 mM $CaCl_2$, 1 mM $MgCl_2$, and 10 mM N-2-hydroxyethylpiperazine-N'-2-ethanesulfonic acid (HEPES)-KOH, pH 7.5] with protoplasts equivalent to 10 µg in a total volume of 1 ml. Water at a constant temperature of 25 ^{o}C was circulated through the outer jacket of the reaction chamber. Illumination for protoplasts (700 µmol photons m^{-2} s^{-1}) was provided by a 35-mm-slide projector, equipped with a 24 V/150 W halogen lamp (Philips Focusline).

The capacities of the cyanide-sensitive cytochrome oxidase (COX) and cyanide-resistant alternate oxidase (AOX) pathways were determined by monitoring respiratory O_2 uptake in mesophyll cell protoplasts, in presence of an uncoupler 1 µM carbonyl cyanide

m-chlorophenylhydrazone (CCCP). The capacities of these two pathways were calculated as described by Robson and Vanlerberghe (2002), by using antimycin A (COX pathway inhibitor) and/or salicyl hydroxamic acid (SHAM, AOX pathway inhibitor). The capacity of COX pathway is defined as O_2 uptake in the presence of CCCP and SHAM that was sensitive to antimycin A. The capacity of the AOX pathway is defined as the O_2 uptake in the presence of antimycin A that was sensitive to SHAM. The concentrations of mitochondrial inhibitors, which cause 50 % inhibition of total respiration, were chosen as recommended by Robson and Vanlerberghe (2002).

Lowering of O_2

Prior to monitoring photosynthesis, the reaction medium was gently bubbled with N_2 gas to lower the O_2 concentration. The normal O_2 concentration in the medium was *ca.* 410 nmol ml^{-1}, while after bubbling with nitrogen the O_2 concentration decreased to *ca.* 85 nmol ml^{-1}. Required quantity of protoplast suspension was then added, without opening the chamber.

Detection of H_2O_2

H_2O_2 detection by 3,3-diaminobenzidine (DAB) staining was carried out according to Yoshida et al. (2008), with slight modifications. Excised leaves were fed through petiole transpiration, aqueous solution of 1 mg ml^{-1} DAB (pH 3.8) for 1 h in low light (50 µE m^{-2} s^{-1}). Leaves were incubated under either dark or moderate light (300 µE m^{-2} s^{-1}) or high light (1200 µE m^{-2} s^{-1}), for 1 h and 2 h. Leaves were then fixed for 15 min with a mixture of ethanol: lactic acid: glycerol (3:1:1, v:v:v), washed with 75, 50, and 25 % methanol, equilibrated with water, and H_2O_2 was visualized as a reddish-brown color.

Estimation of antioxidants

Ascorbate (AsA)

AsA content was measured according to Foyer et al. (1983). Nineteen leaf discs (ca. 84 mg) of *A. thaliana* after respective treatments and incubation, frozen in liquid N_2, were ground using a mortar and pestle with 3 ml 2.5 M $HClO_4$. The extract was adjusted to pH 6.0 with 5 M K_2CO_3 and centrifuged at 10000 g for 6 min at 4 °C. In case of protoplasts, aliquot (equivalent to 200 µg of Chl) in a total volume of 600 µl in the presence or absence of test compounds after exposure to 5 min dark and 10 min light (700 µE m^{-2} s^{-1}) were withdrawn and mixed immediately with ice-cold 2.5 M $HClO_4$ (final concentration 0.5 M) and frozen in liquid nitrogen. The samples were thawed and centrifuged at 4 ^{o}C for 10 min at 10,000 *g* and the supernatant was collected for analysis. The pH of the supernatant was neutralized by stepwise addition of 1.25 M potassium carbonate (30-40 µl). The supernatant was centrifuged at 10,000 *g* for 6 min at 4 °C.

An aliquot of 100 µl of supernatant sample of leaf extract or mesophyll cell protoplast was added to 900 µl of a 0.1 mM sodium phosphate buffer (pH 6.0), and $A_{265\ nm}$ was recorded. To this mixture, 2.5 U of AsA oxidase (EC 1.10.3.3) from *Cucurbita sp.* (Sigma-Aldrich, USA) was added, and $A_{265\ nm}$ was recorded after 5 min. The difference between the absorbance of the extract, before and after the addition of AsA oxidase, indicates the level of reduced AsA. For the determination of total AsA, the extract was incubated with 10 mM reduced glutathione (GSH) and 0.1 M Tricine-KOH buffer (pH 8.5) for 15 min at 25 °C in a total volume of 250 µl. An aliquot of GSH-treated sample was used to estimate AsA, again as described above. The difference between the total AsA and this AsA gives the amount of DHA. The absorbance at 265 nm into the exact amount of AsA was converted using the extinction coefficient of AsA as 14.1 mM^{-1} cm^{-1}.

Glutathione (GSH)

Nineteen leaf discs (ca. 84 mg) of *A. thaliana*, after respective treatments were frozen in liquid N_2, were ground using a mortar and pestle in 1 ml of 0.2 N HCl and allowed to thaw. The extract was then centrifuged at 14,000 rpm for 10 min at 4 ºC. The supernatant was neutralized by adding 0.2 N NaOH. In experiments, using mesophyll protoplasts, suspensions equivalent to 200 µg of Chl in the presence or absence of test compounds after exposure to 5 min dark and 10 min light (700 µE m^{-2} s^{-1}) were ground with a teflon pestle in a 1.5 ml eppendorf tube containing 50 mM sodium phosphate buffer (pH 7.0). The reaction was stopped by adding 7 % sulfosalicylic acid. The samples were centrifuged at 4,500 g for 10 min and the supernatant was neutralized by the addition of 20 µl of 7.5 M triethanolamine (TEM). This supernatant was used for the analysis of GSH and GSSG.

Total, oxidized, reduced GSH were determined spectrophotometrically described by Griffith (1980) using the absorbance at 412 nm. The assay mixture (2 ml) contained 100 mM phosphate buffer (pH 7.5), 2 mM ethylene diamino tetra acetic acid (EDTA), 6.3 mM 5-5^1-dithiobis-2-nitrobenzoic acid (DTNB), 5 mM NADPH, 1 unit of GR (from yeast, Boehringer Mannheim, Germany) and the neutralized protoplast extract (100 µl). The $A_{412\ nm}$ values are calculated and expressed as GSH (reduced form of glutathione) equivalents, with the help of a GSH standard curve. For the estimation of GSSG (oxidized form of GSH), 0.01 ml of 2-vinyl pyridine (2 V-P) was added to 0.5 ml of neutralized extract, so as to mask GSH and GSSG was extrapolated from a standard plot for GSSG. The solution was stirred for 1 min and incubated for 1 h at 25 ^oC. Neutralized extraction medium served as a blank. Total GSH was determined by reference to a standard curve of GSH and reduced GSH was determined as the difference between the total GSH and the GSSG.

Assays of antioxidant enzymes

The leaf discs (approx. 100 mg fresh weight) after respective treatment were ground to powder in liquid nitrogen. In case of mesophyll cell protoplasts, aliquots, equivalent to 200 µg Chl, were ground to powder in liquid nitrogen. The powdered samples of leaf discs or protoplasts were homogenized in 50 mM phosphate buffer pH 7.0 containing 1 mM of phenyl methane sulfonyl fluoride (PMSF) and followed by a brief centrifugation step at 1000 g for 1 min.

Before enzymatic assays, the homogenate was centrifuged at 10,000 g for 10 min and the supernatant was used for the assays of CAT, APX and GR. Protein concentration in the enzyme extracts was determined by the method of Lowry et al. (1951) using defatted bovine serum albumin (BSA), as a standard.

Ascorbate peroxidase (APX, E.C. 1.11.1.11)

Ascorbate peroxidase activity was examined by the method of Nakano and Asada (1981). The reaction mixture for measuring APX activity contained 50 mM sodium phosphate buffer (pH 7.0), 0.2 mM EDTA, 0.5 mM AsA, 20 mM H_2O_2 and enzyme extract equivalent to 50 µg of protein. The activity was recorded as decrease in absorbance at 290 nm for 1 min and the amount of AsA oxidized was calculated from the extinction coefficient of 2.8 mM^{-1} cm^{-1}.

Catalase (CAT, E.C. 1.11.1.6)

Catalase activity was measured spectrophotometrically by following the oxidation of H_2O_2 at 240 nm according to the method of Patterson et al. (1984). The reaction mixture contained 50 mM sodium phosphate buffer (pH 7.0), 20 mM H_2O_2 and enzyme extract equivalent to 25 µg protein in a final volume of 3 ml. Extinction coefficient for H_2O_2 at 240 nm is 43.6 mM^{-1} cm^{-1}.

Glutathione reductase (GR, E.C. 1.6.4.2)

The activity of GR was determined by modifying the method of Jiang and Zhang (2001). The reaction mixture contained 25 mM sodium phosphate buffer pH 7.5, 10 mM oxidized glutathione (GSSG), 3 mM $MgCl_2$ and 1 mM NADPH in a total volume of 2 ml. The reaction was started by addition of enzyme extract containing 50 µg protein and GR activity was monitored as NADPH oxidation (Extinction coefficient = 6.2 mM^{-1} cm^{-1}) by recording the decrease in $A_{340\ nm}$.

Western blotting

The leaf discs (approx. 100 mg fresh weight) after respective treatment were ground to powder in liquid nitrogen. Alternatively, aliquots of the mesophyll cell protoplasts (equivalent to 200 µg Chl) were ground to powder in liquid nitrogen. The powdered samples of leaf discs or protoplasts were homogenized in 125 mM Tris–HCl (pH 6.8) containing 5 % (w/v) sodium dodecyl sulfate (SDS) and 1 mM PMSF followed by a brief centrifugation step at 1000 g for 1 min and supernatant was collected. Protein estimation was accomplished by the method of Lowry et al. (1951).

SDS-PAGE was performed as per the principles of Laemmli (1970) using mini gels (8 x 8 cm). The resolving gel (6 cm long and 8 cm wide) was polymerized using 375 mM Tris-HCl buffer pH 8.8, 10 % acrylamide and 0.1 % (w/v) SDS. The stacking gel (2 cm long and 8 cm wide) was made of 125 mM Tris-HCl (pH 6.7), 4 % acrylamide, 0.1 % (w/v) SDS. The electrode buffer contained 25 mM Tris-HCl, 192 mM glycine pH 8.3 and 0.1 % (w/v) SDS. Proteins were dissolved in sample buffer (250 mM Tris-HCl pH 6.8, 8 % (w/v) SDS, 50 % (v/v) glycerol, 10 % (v/v) 2-mercaptoethanol, 0.04 % (w/v) bromophenol blue) and boiled at 100 ^{o}C for 2 min and stored at –20 ^{o}C, until loading onto the gel. n each well, 15 µg protein sample was loaded. Electrophoresis was performed initially at 50 V (until the dye

front migrated into the resolving gel) and then at 100 V. Power was supplied through Atto-Digi-Power (SJ-1081).

The proteins were then transferred electrophoretically from the gel onto polyvinylidene difluoride (PVDF) membranes (Towbin et al 1979). The PVDF membrane was carefully laid on the gel without any air bubbles between the two. The gel and the PVDF membrane were sandwiched between two layers of Whatmann No. 1 chromatography papers. A single layer of sponge was placed on either side. The entire sandwich was soaked in transfer buffer (25 mM Tris-HCl pH 8.3, 192 mM glycine and 20 % (v/v) methanol) and placed in the cassette of the western blot unit (Electro-eluter, Model 422, BIO-RAD, USA) and connected to a power pack (Atto Digi-Power, model SJ-1081). A power supply of 30 V was given overnight (8-10 h) at 4 ^{o}C. The transfer of proteins was confirmed by Ponceau's staining (0.2 % (w/v) Ponceau's stain in 3 % (w/v) trichloroacetic acid). Ponceau's stain was removed by repeated washing with distilled water.

The PVDF membrane was blocked, to saturate the non-specific binding sites, with 5 % (w/v) BSA in Tris-Buffered saline (TBS) containing 25 mM Tris- HCl pH 7.5 and 150 mM NaCl. The blocking was allowed for 1 h at room temperature with constant shaking. The blocked membrane was washed for 45 min (3 washes, 15 min each) with washing buffer (25 mM Tris-HCl pH 7.5, 150 mM NaCl, and freshly added 0.2 % Tween 20). Now the PVDF membrane was treated for 1 h with respective anti-rabbit primary antibody (anti-catalase antibody - 1: 1,000; anti-APX antibody - 1: 2,000 and anti-GR antibody - 1: 2,000) (Agrisera AB, Sweden) followed by 1: 2,000 dilution of anti-rabbit IgG alkaline phosphatase conjugate for 1 h and washed. All the above treatments were done with the help of a shaker.

The washed blot was developed with 50 µl of a mixed stock solution containing *p*-nitroblue tetrazolium chloride (NBT) and 5-bromo 4-chloro 3- indolyl phosphate (BCIP) (NBT/BCIP stock solution, Sigma-Aldrich, St. Louis, USA) in 10 ml of 0.1 M Tris-HCl

pH 9.5, 0.1 M NaCl, 0.05 M $MgCl_2$. The time taken for development of protein bands was 10 to 15 min.

Total RNA isolation and reverse transcriptase PCR (RT-PCR) analysis

RNA extraction

The extraction of RNA was done, using guanidine thiocyanate acid phenol-based method as described by Chomczynski and Sacchi (1986) using TRI-Reagent® (Sigma-Aldrich, USA). The leaf discs (approx. 100 mg fresh weight) after respective treatment were ground to powder in liquid nitrogen. In case of the mesophyll cell protoplasts, aliquots equivalent to 200 µg Chl were ground to powder in liquid nitrogen. These powdered samples were homogenized in a 1.0 ml of TRI-Reagent®, mixed well and harvested into eppendorf tubes. The samples were incubated at room temperature for 5 min and then centrifuged at 12000 *g* for 10 min at 4 °C to remove the cell debris.

The clear supernatant was carefully transferred to a fresh 2 ml eppendorf tube and 300 µl of chloroform was added. The tubes were capped securely and vortexed for 15 sec and incubated at 25-30 °C for 5 min. The samples were centrifuged at 12000 *g* for 15 min at 4 °C. After centrifugation, the mixture separated into a lower red, phenol-chloroform phase, an interphase, and a colorless upper aqueous phase. The upper aqueous phase was carefully transferred to a fresh 2 ml eppendorf tube without disturbing the middle phase. To this supernatant, equal volumes of isopropyl alcohol (500 µl of supernatant + 500 µl of isopropyl alcohol) was added, mixed well and incubated at 30 °C for 10 min. The samples were then centrifuged at 12000 *g* for 10 min at 4 °C and the pellet was stored and the supernatant was discarded.

The pellet (RNA) was washed with 500 µl of 70 % alcohol (flick the tube to wash) and then centrifuged at 12000 *g* for 5 min at 4 °C to re-pellet the RNA at the bottom of the tube and the pellet was air dried for 10-15 min at room temperature. The air dried pellet was

re-suspended in 30-50 µl of RNase free diethyl pyrocarbonate (DEPC) treated water (DEPC-H_2O). An aliquot was put into the spectrophotometer to determine RNA concentration and quality at A_{260} and A_{280}. For optimal spectrophotometric measurements, RNA aliquots were 1: 80 diluted with DEPC-H_2O. The RNA quantification was done using the following formula:

RNA concentration (µg ml-1) = 40 x A260 x dilution factor, where RNA extinction coefficient = 40 (1 OD at 260 equals 40 µg /ml RNA). The A_{260}/A_{280} ratio gives the purity of the RNA (ratio should be between 1.8 -2.1).

cDNA synthesis

The procedure followed for cDNA synthesis was according to manufacturer's instructions (RevertAid cDNA synthesis kit, Fermentas). The oligo(dT)12-18 primer was added to 1 µg of total RNA and the final volume was adjusted to 20 µl with RNase free water. The sample was mixed well and incubated in a thermal cycler at 65 °C for 5 min, snap frozen in ice for 2 min and spin briefly. The cDNA was synthesized using 200 units RevertAid M-MuLV Reverse Transcriptase (Fermentas) in a buffer (in a total volume of 8 µl comprises of 4 µl reaction buffer (5x), 1 µl of RiboLock RNase inhibitor and 1 µl of 10 mM dNTP). The reaction was performed at 42 °C for 50-60 min in a water bath and was stopped at 70 °C for 10 min. This cDNA synthesized was used as template for RT-PCR analysis.

RT-PCR analysis

Non-competitive reverse transcription-PCR (RT-PCR) was performed as described by Ahn (2002). Gene specific primers (Table 3.2) were designed on the basis of the published sequence (http://www.ncbi.nlm.nih.gov) using Primer3 software (Rozen and Skaletsky, 2000; http://fokker.wi.mit.edu/primer3/input.htm). cDNA samples were standardized by PCR for actin content. The PCR conditions were optimized empirically by testing various annealing temperatures.

Table 3.2. The sequence of the primers used for RT-PCR amplification of genes encoding for antioxidant enzymes (*CAT2*, *tAPX, sAPX, cAPX* and *GR2*) localized in chloroplast and gene involved in proline synthesis (Δ*P5CS1*) and the house keeping gene (*Actin 8*).

Gene function	**Gene locus**	**Sequence**
Catalase (***CAT2***)	AT4G35090	5^1-CGAGGTATGACCAGGTTCGT-3^1 (sense) 5^1-AGGGCATCAATCCATCTCTG-3^1 (antisense)
Thylakoidal APX (***tAPX***)	AT1G77490	5^1-TGGAGAAGCAGGAGGACAGT-3^1 (sense) 5^1-GCAGCCACATCTTCAGCATA-3^1 (antisense)
Stromal APX (***sAPX***)	AT4G08390	5^1-CCTCAGAAAAATGGCAGAG-3^1 (sense) 5^1-GAGGAGGAAGCGGAGAGAGT-3^1(antisense)
Cytosolic APX (***cAPX***)	AT1G07890	5^1-GCATGGACATCAAACCCTCT-3^1 (sense) 5^1-AGCAAACCCAAGCTCAG-3^1 (antisense)
Chloroplastic GR (***GR2***)	AT3G54660	5^1-TTTTGCGAACACTGCTTTTG-3^1 (sense) 5^1-AGCCTGAGGTGAAGACCAGA-3^1 (antisense)
Δpyrroline-5-carboxylate synthetase (Δ***P5CS1***)	AT2G39800	5^1-TACGACGGTGCTTCACTGAG-3^1 (sense) 5^1-CACCTCAAATCCATCCGAGT-3^1 (antisense)
Actin8	AT1G49240	5^1-CAGGGATCCACGAGACAACT-3^1 (sense) 5^1-CTGGAAAGTGCTGAGGGAAG-3^1 (antisense)

The mRNA transcripts of catalase (*CAT2),* thylakoidal APX *(tAPX),* stromal APX *(sAPX),* cytosolic APX *(cAPX),* chloroplastic GR *(GR2)* and Δpyrroline-5-carboxylate synthetase *(ΔP5CS1)* genes were examined. The primer sequences of the genes used for RT-PCR are given as a Table 3.2.

The PCR cycling conditions comprised

1. 94 °C for 3 min initial denaturation
2. 94 °C for 1 min denaturation
3. 60 °C for 45 sec annealing
4. 72 °C for 20 sec extension, 35 cycles from step 2- 4
5. 72 °C for 10 min final elongation

As an internal (constitutive) control, PCR was performed simultaneously using *Actin8* primers and amplification products were resolved by electrophoresis.

Agarose gel electrophoresis

Electrophoresis was carried on 1 % (w/v) agarose gels. The gel was polymerized in 1x TBE buffer (89 mM Tris base, 89 mM Boric acid, 2 mM EDTA, pH 8.0). The required quantity of agarose (500 mg) was suspended in appropriate volume of 1 x TBE (50 ml) and boiled for solubilization. The solution was allowed to cool till 60-65 °C and ethidium bromide (0.5 µg/ml) was added. The gel was poured into a horizontal gel electrophoresis system, into which the well comb was placed and left to polymerize at room temperature. The PCR products were loaded with 4 µl bromophenol blue (BPB) dye (loading dye) before being loaded into the wells of the gel. Then the samples (about 12 µl) were directly loaded on to gel. DNA ladder (Fermentas) was used as molecular weight marker, which on standard loading of 5 µl yields 14 regularly spaced bands from 50 bp to 1000 bp. The size of each band is an exact multiple of 50 bp. Electrophoresis was carried out in the same buffer (1x TBE) at a voltage of 50 V, until the dye reached 3/4th of the length of the gel. All the

ethidium bromide gels were visualized using UV-transilluminator and analyzed using UV-gel documentation system. The PCR amplified an approximately 0.5 kb fragment of the gene of interest.

Band intensities after electrophoresis were quantified using Scion software and normalized to band intensities of *ACTIN8* which is used as a house keeping gene.

Replications and statistical analysis

The data presented are the average values (± SE) of results from three to four experiments conducted on different days. The data were subjected to further statistical analysis by students' *t*-test and one way ANOVA (Student-Newman-Keuls method) using SigmaPlot Version 11.0.

Chemicals and materials

Cellulase (Onozuka R-10) and macerozyme R-10 (pectinase) were procured from Yakult Honsha Co. Ltd., Tokyo, Japan. Antimycin A, SHAM, AAN, GHA, L-GalL, reduced and oxidized glutathione, NADPH, MES, HEPES, sodium ascorbate, and all the enzymes used for the spectrophotometric assays were procured from Sigma-Aldrich Corporation, USA. PVDF membranes (Immobilon-P from Millipore). Nylon filter (60 µm pore size) was purchased from Sarayu Textiles, Mumbai. Ascorbate oxidase was procured from Roche Applied Science, Mannheim, Germany. All other chemicals and materials were of analytical grade and were purchased from the following companies: Sisco Research Laboratories, Loba Chemie, Himedia Laboratories and Qualigens, all from Mumbai. The antibodies were procured from Agrisera (Sweden). All the primers were synthesized by Bioserve (USA).

****

Chapter 4

Ascorbic acid is a key participant for optimization of photosynthesis and protection against photoinhibition

Chapter 4

Ascorbic acid is a key participant for optimization of photosynthesis and protection against photoinhibition

INTRODUCTION

In plant cells, a delicate metabolic equilibrium exists between the key compartments, including not only mitochondria and chloroplasts but also the peroxisomes and cytosol. Disturbance of any of these compartments perturbs the metabolism of whole cell (Raghavendra and Padmasree, 2003; Noguchi and Yoshida, 2008; Yoshida and Noguchi, 2010). A major factor for metabolic stability is the exchange of several metabolites between the different cell organelles. Besides the metabolites there are also other possible signals between mitochondria, chloroplasts, peroxisomes and cytosol, including L-ascorbate (AsA), nitric oxide (NO) and the cytosolic pH. Evidences suggest that the signalling network between chloroplasts and mitochondria involves ROS and antioxidants (Foyer and Noctor, 2003; Noctor et al., 2007).

AsA is the most abundant water-soluble antioxidant present in plant cells. It is ubiquitous and found in all sub-cellular organelles, including the apoplast (Smirnoff, 2000; Pignocchi and Foyer, 2003). For example, the concentration of AsA is in the range of 20 mM or more in chloroplasts (Smirnoff and Wheeler, 2000). The recycling of AsA regenerated via the ascorbate-glutathione cycle, helps to detoxify H_2O_2 produced during Mehler reaction and thus AsA is important for photoprotection (Halliwell and Foyer, 1976; Foyer and Noctor, 2000). Further, AsA appears to have multiple roles in metabolism, electron transport, control of the cell cycle, and even the responses of plants to biotic/abiotic stress (Ishikawa and Shigeoka, 2008).

The *vtc1* mutant is deficient in GDP-mannose pyrophosphorylase and has very low levels of AsA. The *vtc1* mutants of *Arabidopsis thaliana* are quite sensitive to various stress conditions like high light (HL), ozone, SO_2, UV-B radiation and even salt stress (Müller-Moulé et al., 2003, 2004; Huang et al., 2005). Further, the deficiency of AsA and L-GalL dehydrogenase (L-GalLDH) has been observed to affect the growth and development of not only *Arabidopsis* but also tomato (Veljovic-Jovanovic et al., 2001; Alhagdow et al., 2007). Mitochondria play an important role in the synthesis of AsA. The final step of the AsA biosynthesis occurs in the inner mitochondrial membrane. In this step, L-GalL dehydrogenase oxidizes L-GalL to AsA, utilizing cytochrome c as its electron acceptor (Smirnoff and Wheeler, 2000; Ishikawa and Shigeoka, 2008; Linster and Clarke, 2009). L-GalLDH uses L-GalL as an electron donor to reduce cyt c and appears to be associated with complex III/IV of mitochondrial electron transport chain (Bartoli et al., 2000). AsA biosynthesis is stimulated in light which appears to be through direct control by photosynthesis, but not of gene expression (Smirnoff, 2000; Gatzek et al., 2002; Yabuta et al., 2007). Although the role of AsA during the mitochondria-chloroplasts interactions is stressed (Foyer and Noctor, 2003; Nunes-Nesi et al., 2008), the details of modulation by AsA are yet to be examined in detail.

The AsA-deficient plants exhibit an enhanced photoinhibition and oxidative damage (Müller-Moulé et al., 2003, 2004). Interference with mitochondrial oxidative electron transport can also lead to pronounced photoinhibition (Raghavendra and Padmasree, 2003). However, it is not clear if AsA can provide a link during the interactions between photosynthesis and mitochondrial electron transport. The present work is designed to assess the role of AsA during the interactions between chloroplasts and mitochondria in leaves of *A. thaliana*. The consequences of decrease in AsA (by using AsA-deficient *vtc1* mutant) or enhancement by feeding leaf discs with L-GalL (precursor of AsA) on photosynthesis,

respiration and their interactions were studied. The levels as well as the redox state of AsA were determined with or without pretreatment with two mitochondrial inhibitors. The results suggest that AsA interacts with both chloroplasts and mitochondria, particularly during the protection of photosynthesis at HL and protection against photoinhibition.

RESULTS

Photosynthesis and respiration in AsA deficient *vtc1* mutant

AsA deficient (*vtc1*) mutants contained about one-third of the AsA found in WT (Figure 4.3A). Photosynthetic oxygen evolution by both *vtc1* mutant and WT increased with light intensity (Figure 4.1A, B). The rates of photosynthesis in mutants, at light intensities and above 300 μmol m^{-2} s^{-1} were less than those of WT. Whereas at light intensities of <150 μmol m^{-2} s^{-1} (or less) *vtc1* mutants had marginally higher photosynthetic rates than those of WT, whereas the photosynthetic rates of WT were seem to be higher at light intensities of 300 μmol m^{-2} s^{-1} or higher (Figure 4.1A, B).

The rate of respiration in leaf discs of mutant plants was less than that in the WT (Figure 4.2A). However, the extent of inhibition by mitochondrial inhibitors (antimycin A or SHAM) was more in the *vtc1* mutants than that in the WT. The inhibition of respiration by SHAM was pronounced in mutants. As it is difficult to estimate the cytochrome and alternative pathway capacities in leaf discs, mesophyll cell protoplasts were chosen and experiments were conducted using mesophyll protoplasts to monitor respiration in presence of an uncoupler (carbonyl cyanide *m*-chlorophenylhydrazone, CCCP). The respiration in mesophyll cell protoplasts of mutant plants was lower than that in the wild-type (Figure 4.2B). The capacity of COX pathway in WT and *vtc1* mutants was 43 and 26 % of total respiration, whereas the capacity of AOX pathway in WT and *vtc1* mutants was 34 and 39 % of total respiration, respectively.

The content and redox state of AsA in WT and *vtc1* mutants: Response to mitochondrial inhibitors and L-GalL

The levels of AsA in leaf discs of both WT and *vtc1* mutant increased on illumination and under HL. In contrast, the ratios of reduced to total AsA were altered marginally by light. However, the ratios of reduced to total AsA fell steeply by >60 %, in presence of antimycin A or SHAM (Figure 4.3C). The levels of total AsA in the *vtc1* mutant were much less than those in the wild-type plants (Figure 4.3A, B). The total AsA levels in mutants too increased slightly in presence of antimycin A or SHAM, but the ratios of reduced to total AsA fell sharply by >80 % (Figure 4.3C, D). The decrease in ratio of reduced/total AsA at HL was more pronounced with SHAM than that with antimycin A in mutant plants.

Feeding with L-GalL elevated the levels of AsA in both wild-type and mutant plants (Figure 4.3B). A prominent effect of L-GalL was the maintenance of high reduced to total AsA ratios even in presence of antimycin A or SHAM, compared to its absence (Figure 4.3D). Even in presence of L-GalL, illumination with normal or HL increased the total AsA level and reduced the ratios of reduced/total AsA. The modulation by mitochondrial inhibitors (Antimycin A, or SHAM) on the total AsA levels and the ratios of reduced/total AsA at HL was more pronounced in *vtc1* than that in WT.

Photosynthesis and photoinhibition in leaf discs of wild-type and *vtc1* mutants: Effect of mitochondrial inhibitors and L-GalL

Treatment with mitochondrial inhibitors decreased photosynthesis in both WT and AsA deficient mutants especially in normal and HL. Such decrease was pronounced with SHAM at normal and HL (Figure 4.4A). The inhibition of photosynthesis by mitochondrial inhibitors was marginal at normal light in both WT and *vtc1* mutant (Figure 4.4A). Further, the decrease in photosynthesis and the extent of photoinhibition at HL were more in mutant than that in WT (Figure 4.4A). The *vtc1* mutants were highly sensitive to SHAM at HL

intensity. Pretreatment with L-GalL resulted in a significant protection of photosynthesis, particularly at HL (Figure 4.4B). The protection by L-GalL of photosynthesis and sensitivity to mitochondrial inhibitors was quite pronounced in mutants.

The high sensitivity of mutant plants to mitochondrial inhibitors at HL intensity and the marked protection by L-GalL were very clear, when the percent of photoinhibition was calculated (Table 4.1). In a typical experiment, the percent of photoinhibition in mutant (64 %) was higher than that in WT (48 %). The treatment with antimycin A or SHAM further increased the percent of photoinhibition in both WT and mutants. Highest photoinhibition of 83 % occurred in mutant plants in presence of SHAM. The treatment with L-GalL decreased the photoinhibition, even in presence of antimycin A or SHAM. Again maximum protection by L-GalL was recorded in *vtc1* mutant in presence of SHAM.

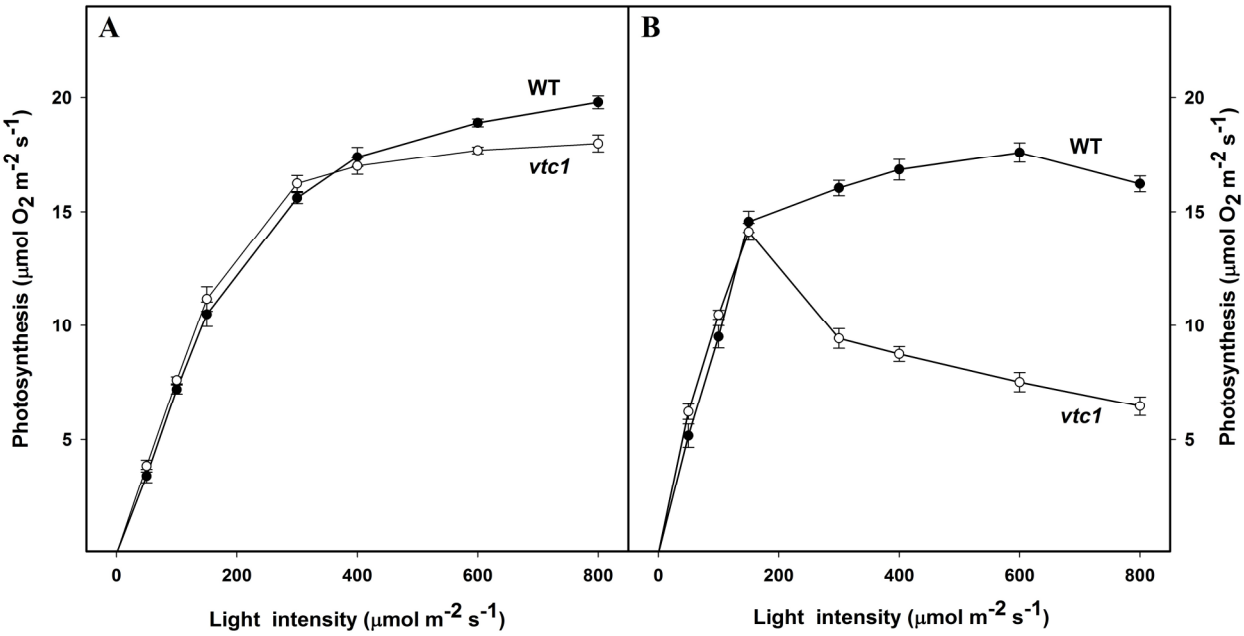

Figure 4.1. Photosynthetic oxygen evolution by leaf discs from WT and *vtc1* mutants of *Arabidopsis thaliana* in response to increasing intensity of light in the absence (A) or in presence (B) of preillumination. The leaf discs were preilluminated at 2 h light (300 μmol m^{-2} s^{-1}) after 8 h dark incubation. Data represent mean values (± SE) from at least four independent experiments.

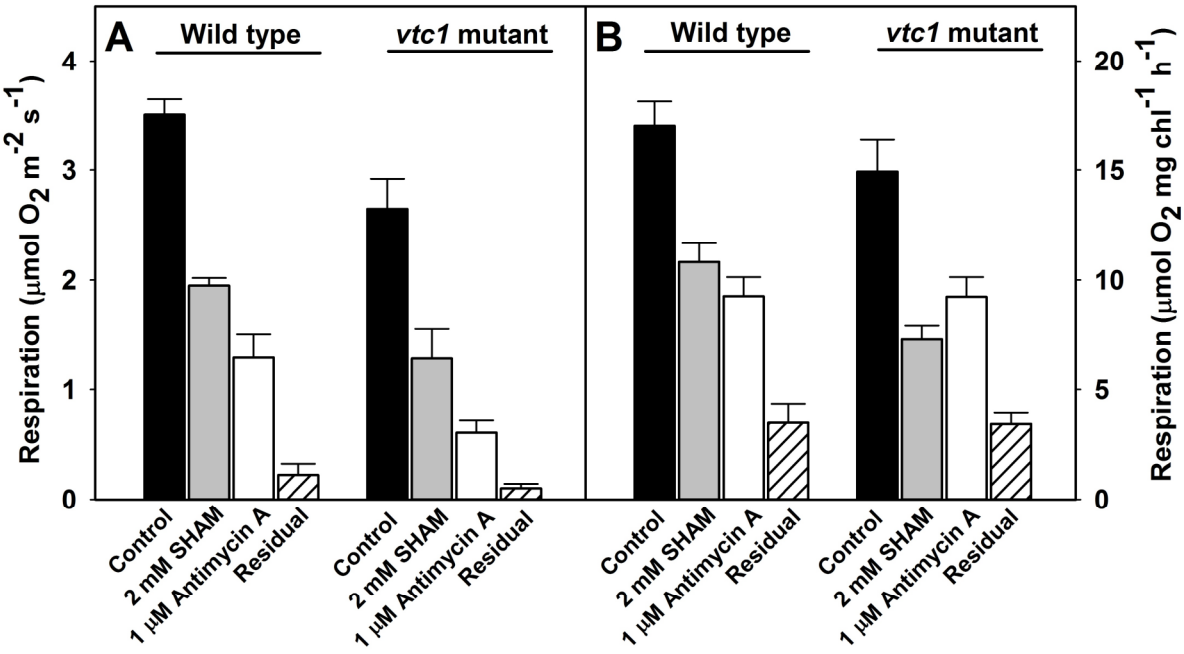

Figure 4.2. The respiratory O_2 uptake in leaf discs (A) or mesophyll cell protoplasts (B) of WT and *vtc1* mutant of *Arabidopsis thaliana* on exposure to mitochondrial inhibitors (1 μM antimycin A or 2 mM SHAM). Data represent mean values (± SE) from at least four independent experiments.

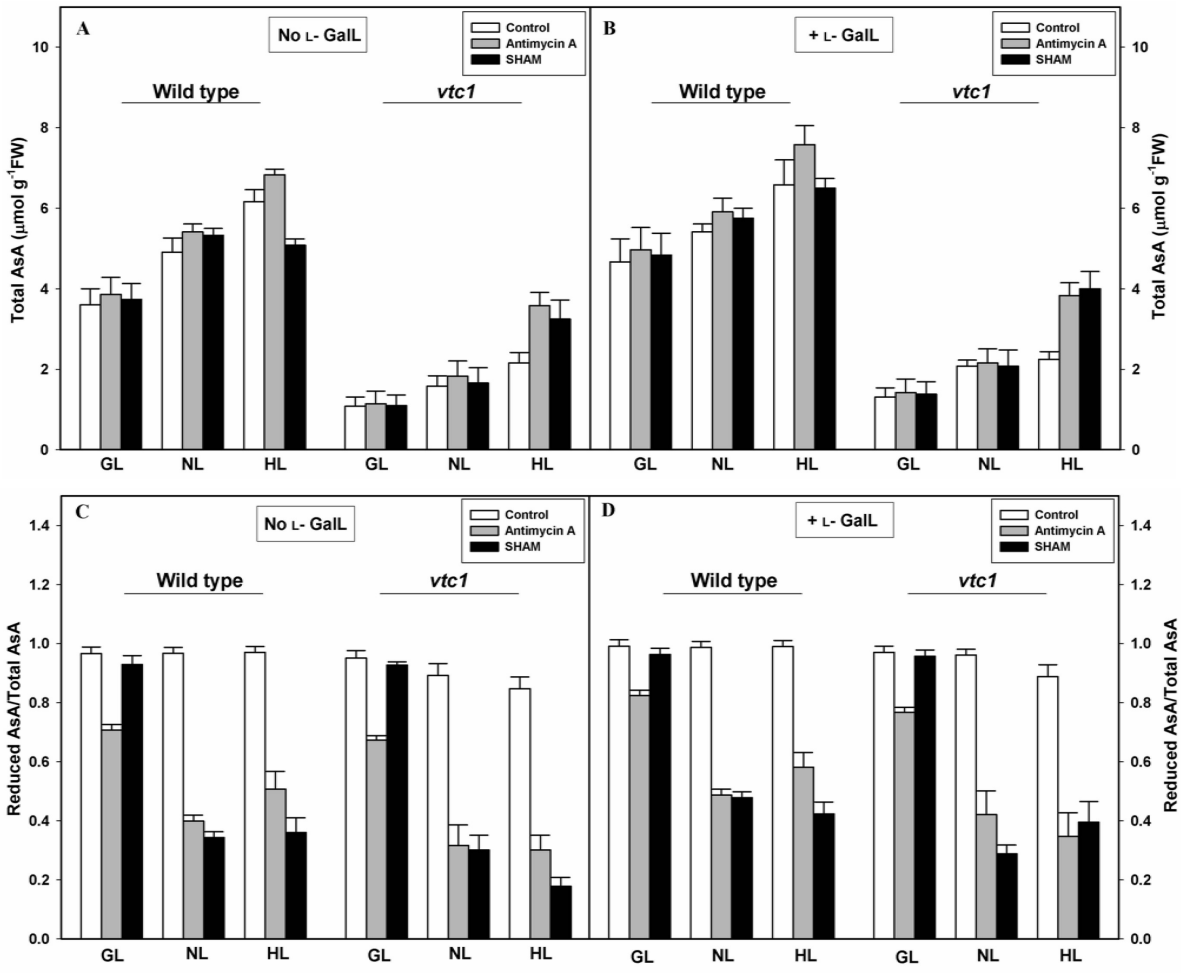

Figure 4.3. The levels and redox state of AsA in leaf discs of wild type (A and C) and *vtc1* mutant (B and D) of *Arabidopsis thaliana* pretreated without or with 25 mM L-GalL and then exposed to mitochondrial inhibitors (1 µM antimycin A or 2 mM SHAM). The leaf discs were exposed to either growth light (GL, 150 µmol m^{-2} s^{-1}) or normal (NL, 300 µmol m^{-2} s^{-1}) or high light (HL, 1800 µmol m^{-2} s^{-1}) for 2 h. Data are averages (± SE) in vertical bars of at least three experiments conducted on different days.

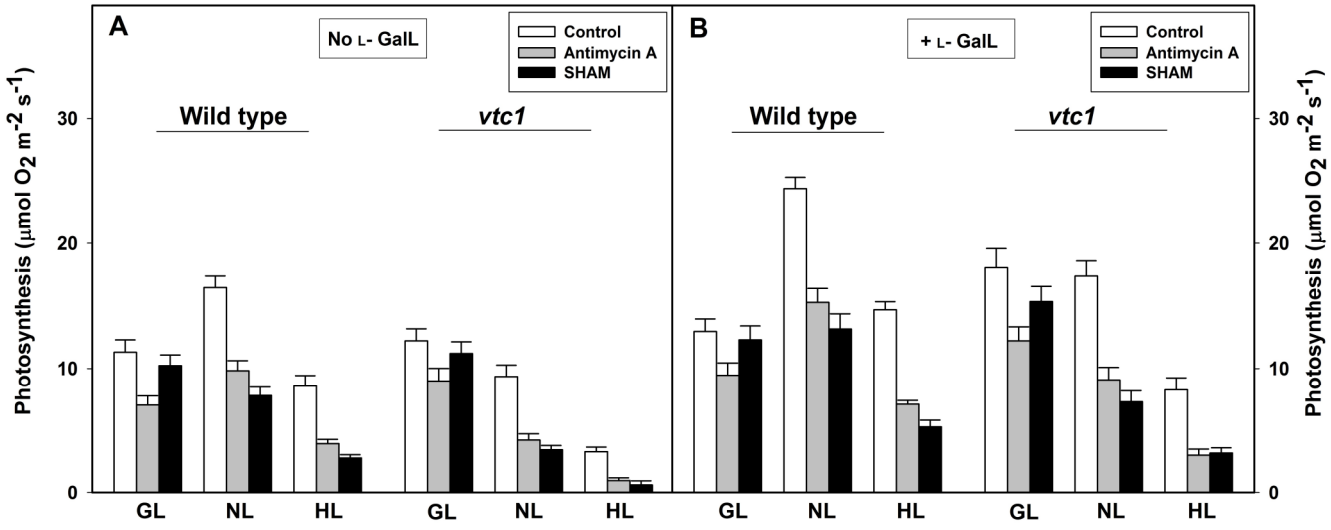

Figure 4.4. The photosynthetic rates in leaf discs of wild type (A) and *vtc1* mutant (B) of *Arabidopsis thaliana*, upon treatment with mitochondrial inhibitors (1 µM antimycin A or 2 mM SHAM) upon pretreatment without and with 25 mM L-GalL. The leaf discs were exposed to either growth light (GL, 150 µmol m^{-2} s^{-1}) or normal (NL, 300 µmol m^{-2} s^{-1}) or high light (HL, 1800 µmol m^{-2} s^{-1}) for 2 h. Photosynthetic rates were then determined at 300 µmol m^{-2} s^{-1}. Data are averages (± SE) in vertical bars of at least three experiments conducted on different days.

Table 4.1 The extent of photoinhibition of photosynthesis in wild type and *vtc1* mutants of *Arabidopsis* without or with treatment with 25 mM L-GalL and/or exposure to mitochondrial inhibitors. Data recalculated from Figure 4.4.

		Photoinhibition (%)*		
Treatment	Plant type	None	Antimycin A (1 μM)	SHAM (2 mM)
No L-GalL	Wild type	48	59	63
	vtc1	64	77	83
25 mM L-GalL	Wild type	40	54	59
	vtc1	52	66	55

* Inhibition of photosynthesis at HL, calculated as % of that at NL.

DISCUSSION

The sensitivity of photosynthesis to supraoptimal light (i.e. photoinhibition) was dependent on both mitochondrial metabolism and AsA levels in leaf discs. This article therefore complements and confirms the suggestion that AsA is a key component during the interaction of photosynthesis with mitochondrial metabolism (Nunes-Nesi et al., 2008).

AsA deficiency increased the sensitivity of photosynthesis and photoinhibition to SHAM and antimycin A

The hypersensitivity of AsA-deficient plants to photoinhibition and oxidative damage was known (Müller-Moulé et al., 2003, 2004). The present results highlight the enhanced sensitivity of photosynthesis, particularly at HL, to AOX pathway. The inhibition of photosynthesis at HL in *vtc1* mutant was aggravated by SHAM (an inhibitor of AOX pathway) and antimycin A (inhibitor of COX pathway). The effect of SHAM being more pronounced than that by antimycin A (Figure 4.4A). Bartoli et al. (2006) reported that AOX pathway might help in photoprotection of *Arabidopsis* leaves. Even at low light, inhibition of AOX pathway caused a decrease in photosynthesis and over-reduction of cyclic electron flow (Yoshida et al., 2006). Our results therefore point out that the importance of mitochondrial electron transport chain (particularly AOX pathway) is related to AsA content of leaves.

The use of SHAM to determine the activity of AOX pathway is often criticized as SHAM may affect peroxidase and thus interfere with measurements (Moller et al., 1988). However, SHAM is used extensively to study AOX pathway, with proper precautions. At low concentrations, as used in present work, the mitochondrial inhibitors had no direct effect on either light activation of enzymes or photochemical electron transport in mesophyll protoplasts (Padmasree and Raghavendra, 1999, 2001).

Elevation of AsA decreased the sensitivity of photosynthesis and photoinhibition to SHAM and antimycin A

Stressed wheat leaves, fed with L-GalL, increased their AsA and enhanced photochemical and non-photochemical quenching of chlorophyll fluorescence (Tambussi et al., 2000). However, L-GalL could arrest the decrease in PSII electron transport only partially, suggesting that other factors also contributed to loss of PSII activity in drought-stressed plants. Similarly, L-GalL treatment enhanced the photosynthetic rates in leaf discs of mitochondrial malate dehydrogenase deficient transgenic tomato plants (Nunes-Nesi et al., 2005). The efficacy of L-GalL to increase was dependent on the activity of L-GalL dehydrogenase, in *Arabidopsis* leaves (Bartoli et al., 2006).

The marked relief in the inhibition of photosynthesis by mitochondrial inhibitors in leaf discs fed with L-GalL (Figure 4.4B) indicated that AsA alleviated the dependence of photosynthesis on mitochondrial metabolism. The protection of photosynthesis by L-GalL at HL was more pronounced in *vtc1* mutants than that in WT (Figure 4.4B). Thus elevation of AsA decreased the dependence of photosynthesis on AOX pathway in not only WT but also mutants. While acknowledging the importance of COX, we suggest that the extreme sensitivity to HL or SHAM of *vtc1* mutants could be due to their altered activity of AOX pathway.

Evidence for increased capacity of AOX pathway in *vtc1* mutants

An increased AOX pathway capacity has been observed under stress conditions, where the ROS levels are high (Yoshida et al., 2007; Bartoli et al., 2005). Increased capacity of AOX pathway in *vtc1* mutants can therefore be the reason for its high sensitivity of photosynthesis and photoinhibition to SHAM. An analysis of respiration in mesophyll protoplasts revealed that the capacity of AOX pathway in mutants was higher than that in WT. The increase in AOX pathway capacity in *vtc1* mutant is possibly due to increased

oxidative stress in mesophyll cell protoplasts of AsA deficient *vtc1* mutants of *Arabidopsis thaliana*, particularly under a combination of HL and presence of mitochondrial inhibitors.

Both mitochondria and chloroplasts modulate the levels and the redox state of AsA

A stimulation of AsA biosynthesis by antimycin A in isolated mitochondria from potato tubers suggests that L-GalLDH could facilitate electron flow through cytochrome c to complex IV, even when complex III is inhibited by antimycin A (Bartoli et al., 2000). In the present study too, in the *vtc1* mutants, the total AsA levels stimulated in presence of antimycin A or SHAM (Figure 4.3A, B), in the absence or presence of L-GalL. The synthesis of AsA is dependent on not only L-GalLDH, but also complex I (Millar et al., 2003; Bartoli et al., 2006; Pineau et al., 2008). Since, the inhibition of electron transport by antimycin A or SHAM increases ROS production (Maxwell et al., 1999), the protective role of AsA becomes quite relevant in such circumstances, as light can stimulate and sustain enhanced AsA levels in leaves (Figure 4.3A, B). Thus, the increase in total AsA appears to be an attempt by the cell to counter the oxidative stress as a consequence of inhibition of mitochondrial electron transport.

Bartoli et al. (2006) reported that light stimulated AsA synthesis was due to the interrelations of chloroplast and mitochondria. Yabuta et al. (2007) observed that the upregulation of AsA biosynthesis was mediated primarily by photosynthetic electron transport. From our findings, it was quite clear that elevated levels of AsA did not always protect photosynthesis against photoinhibition and a high ratio of reduced AsA/total AsA (Figure 4.3D) appeared to be quite important. We therefore suggest that the redox status of AsA could be crucial in mediating the cross-talk between mitochondria and chloroplasts.

Similar roles of AsA and AOX pathway preventing over accumulation of ROS

The interrelationship between mitochondria, chloroplasts and AsA is not surprising. One may argue that such 'cross talk' is unavoidable, since AsA is synthesized in mitochondria, while

accumulating mostly in chloroplasts (Nunes-Nesi et al., 2008). It is possible that the change in AsA is a consequence of photoinhibition. AsA may have additional roles and can be also supplemented with other factors. For e.g. AsA promoted cyclic electron flow around PSI when the electron transport through PSI + PSII is impaired (Mano et al., 2004). The deficiency of AsA had an aggravating effect, when plants are deficient in both AsA and zeaxanthin (Müller-Moule et al., 2003). Further experiments are necessary to understand the multifaceted interactions of mitochondria and chloroplasts through not only AsA but also other signals, including metabolites.

The AsA–glutathione and AOX pathway seem to have similar role, i.e. prevent over accumulation of ROS by either scavenging or restricting ROS production. When AsA level was raised by feeding L-GalL, photosynthesis by leaf discs of *Arabidopsis thaliana* was less sensitive to SHAM (an inhibitor of AOX pathway) was lowered (Figure 4.4B). In contrast, photosynthesis and photoinhibition in AsA deficient mutants of *Arabidopsis thaliana* were more sensitive to SHAM, than that of WT (Figure 4.4A). Increased capacity and levels of AOX upon illumination of leaves signifies the role of AOX in photoprotection (Guy and Vanlerberghe, 2005). A change in expression of AOX levels also led to changes in the activities of AsA and levels of L-GalL-dehydrogenase in *Arabidopsis* leaves (Bartoli et al., 2006). We propose that AsA and AOX pathway may complement each other in minimizing ROS. In a complex I deficient tobacco mutant, as the levels of ROS rose, there was a marked increase in not only AsA but also AOX pathway, along with the other scavenging systems (Vidal et al., 2007).

CONCLUSIONS

1. The modulation of AsA levels lead to marked changes in the patterns of photosynthesis and photoinhibition and their sensitivity to mitochondrial inhibitors: antimycin A or SHAM, particularly at HL.

2. The levels and redox state of AsA were modulated by not only mitochondrial metabolism but also light. While suggesting that AsA is a key player during the interactions between chloroplasts and mitochondria, our observations draw attention to interesting relationship of AsA with AOX pathway.
3. We propose that AsA and AOX pathway could both help in preventing the over accumulation of ROS and thus may complement each other in protecting photosynthesis against photoinhibition.
4. While the importance of COX pathway in optimizing photosynthesis and protecting against photoinhibition cannot be ignored, further work is warranted to establish the complementary roles of AsA and AOX pathway.

****

Chapter 5

Effect of high light on leaves of three *Arabidopsis* mutants lacking redox related components (*nadp-mdh, vtc1* and *aox1a*)

Chapter 5

Effects of high light on leaves of three *Arabidopsis* mutants lacking redox related components (*nadp-mdh, vtc1* and *aox1a*)

INTRODUCTION

In natural environments, plants are exposed to varying intensities of light. Optimal levels of light are essential for plant growth and differentiation. If the incident light levels exceed the photosynthetic capacity, it results in the generation of reactive oxygen species (ROS) in chloroplasts (Li et al., 2009; Galvez-Valdivieso and Mullineaux, 2010; Murchie and Niyogi, 2011). The ROS at limited levels may act as signal molecules to regulate developmental aspects, and even trigger defense responses. However, ROS in excess can cause extensive damage of membrane components, proteins, lipids, and even DNA, -all of them termed together as the phenomenon of photo-oxidative stress (Mittler et al., 2004; Halliwell, 2006).

Plants have developed several strategies to protect against photo-oxidative stress. The diverse photo-protection mechanisms include light avoidance associated with the movement of leaves and chloroplasts; screening of photo-radiation; antioxidant systems to scavenge ROS; dissipation of absorbed light energy as thermal energy (qE); Mehler's reaction and cyclic electron flow (CEF) around photosystem I (PSI) (Takahashi and Badger, 2011; Pospíšil, 2012). Plants also possess a set of additional energy dissipating mechanisms, through mitochondrial oxidative electron transport system, photorespiration and malate valve, as these export the excess reducing equivalents out of chloroplasts (Scheibe et al., 2005; Nunes-Nesi et al., 2008; Foyer and Noctor, 2009; Bauwe et al., 2010; Wilhelm and Selmar, 2011).

The present study is an attempt to study the responses towards supra-optimal light of three mutants of *Arabidopsis,* which lack crucial redox components. The mutants employed

in this study are, *nadp-mdh* (lacks chloroplastic NADP-malate dehydrogenase, a crucial enzyme of malate valve); *vtc1* (an ascorbate deficient mutant) and *aox1a* mutant (lacks a leaf form of mitochondrial alternate oxidase). The responses of these three mutants to high light intensity (HL, 1200 μE m^{-2} s^{-1}), in comparison with dark or moderate light (ML, 300 μE m^{-2} s^{-1}) are described below. The data of wild type are also included. All the experiments were performed with leaf discs.

RESULTS

Photosynthesis

The rates of photosynthesis in WT as well as mutants increased upto a light intensity of 600 μE m^{-2} s^{-1}. At HL intensities, there was a decrease in photosynthesis of *vtc1* and *aox1a* mutants (Figure 5.1). This decrease in photosynthesis was more pronounced in *aox1a* mutant, with maximum inhibition of photosynthesis (75 %) at HL compared to ML. In strong contrast, the *nadp-mdh* mutants exhibited the sustained photosynthetic rates even at HL.

ROS accumulation

Exposure of leaves to HL enhanced ROS accumulation in *vtc1* and *aox1a* mutants, whereas the levels of ROS in *nadp-mdh* mutants were still low at 1 h and 2 h of ML and HL treatment (Figure 5.2). Quite interestingly, the accumulated levels of ROS in *nadp-mdh* mutants were low, even when treated with 10 μM of H_2O_2, compared to high ROS in *vtc1* and *aox1a* mutants (Figure 5.2).

Antioxidant contents

Ascorbate (AsA): The total AsA was stimulated at HL in *nadp-mdh, vtc1* and *aox1a* mutants, such increase was more pronounced in *aox1a* mutants (60 %) particularly at HL conditions (Figure 5.3A). The redox ratios (reduced/total AsA) dropped considerably in *aox1a* (from

0.91 to 0.67) and *vtc1* mutants (from 0.81 to 0.39) at HL, whereas the redox ratio unaffected in *nadp-mdh* mutant (from 0.86 to 0.90) at HL (Figure 5.3B).

Glutathione (GSH): The total GSH content was stimulated at HL in *nadp-mdh* and *vtc1*, and such increase was more pronounced in *nadp-mdh* (40 %) particularly at HL intensities. The total GSH remained unchanged in *aox1a* mutant (Figure 5.4A). The redox ratios (reduced/total GSH) dropped considerably at HL intensities in *vtc1* (from 0.75 to 0.56) and *aox1a* mutant (from 0.97 to 0.72), whereas *nadp-mdh* mutant (from 0.89 to 0.87) exhibited no change in the redox ratios of GSH at HL conditions (Figure 5.4B).

Antioxidant enzyme activities

The activity of ascorbate peroxidase (APX) was high at HL in all three mutants. The increase in activity was more pronounced in *vtc1* (>2-fold) and *aox1a* (>2-fold), whereas *nadp-mdh* mutant exhibited a marginal increase in APX activities at HL intensities (Table 5.1). The activity of glutathione peroxidase (GR) enhanced at HL in all the three mutants, which was pronounced in *vtc1* (>6-fold) and *aox1a* (>4-fold) mutants compared to that of WT, whereas *nadp-mdh* mutant exhibited only about <2-fold increase in GR activity at HL intensities (Table 5.1). The activity of catalase (CAT) also increased significantly at HL in all three mutants. The rise was similar (>5-fold) in *nadp-mdh*, *vtc1* and *aox1a* mutants (Table 5.1).

Protein levels of antioxidant enzymes

Treatment with HL, enhanced the levels of CAT protein in all the three plants, with the response being more pronounced in *aox1a* (>2-fold) and *vtc1* mutants (>2-fold) compared to WT. In contrast, the level of CAT proteins in *nadp-mdh* enhanced by >1-fold at HL (Figure 5.5). The protein levels of four isoforms of APX (tAPX, sAPX, pAPX and cAPX) increased at HL in *vtc1* and *aox1a* mutants compared to WT. The expression of cAPX was more pronounced compared to other isoforms of APX (Figure 5.5), whereas the accumulation

of chloroplastic isoforms of APX was low in *vtc1* mutant. In *nadp-mdh* mutants, the four APX isoforms were unaffected. The GR protein levels were higher under HL in *vtc1* and *aox1a* mutants than those in WT and this increase was high in *aox1a* mutants. In *nadp-mdh* mutants, the levels of GR protein declined at HL (Figure 5.5).

mRNA transcripts of antioxidant enzymes

Exposure to HL up-regulated the expression of transcripts of *CAT2* (chloroplastic form) in *vtc1* and *aox1a* mutants (>2-fold) compared to WT, while *CAT2* was down-regulated in *nadp-mdh* mutants (Figure 5.6). The expression of transcripts of four isoforms of *APX* was up-regulated at HL in *vtc1* and *aox1a* mutants (>1-fold) compared to WT, the expression of *cAPX* was more pronounced compared to other isoforms of *APX* (Figure 5.6), whereas in *vtc1* there was very low expression of mRNA transcript levels of chloroplastic isoforms of *APX* was noticed, while the four isoforms *APX* were down-regulated in *nadp-mdh* mutants. Expression of transcripts of *GR2* (chloroplastic form) were up-regulated at HL in *vtc1* (>2-fold) and *aox1a* (>1-fold) compared to WT, whereas the *GR2* transcript levels of *nadp-mdh* were down-regulated at HL (Figure 5.6).

Free proline content and transcript level of chloroplastic Δpyrroline-5-carboxylate synthetase *(ΔP5CS1)*

The free proline content increased at HL in *nadp-mdh, vtc1* and *aox1a* mutant compared to WT, and this increase was quite pronounced in *nadp-mdh* mutant (>3-fold) particularly at HL (Table 5.2). Exposure to HL up-regulated the expression of *ΔP5CS1* transcript levels in *nadp-mdh, vtc1* and *aox1a* mutants. Again, such upregulation was maximum in *nadp-mdh* mutants (>3-fold) particularly at HL (Figure 5.7).

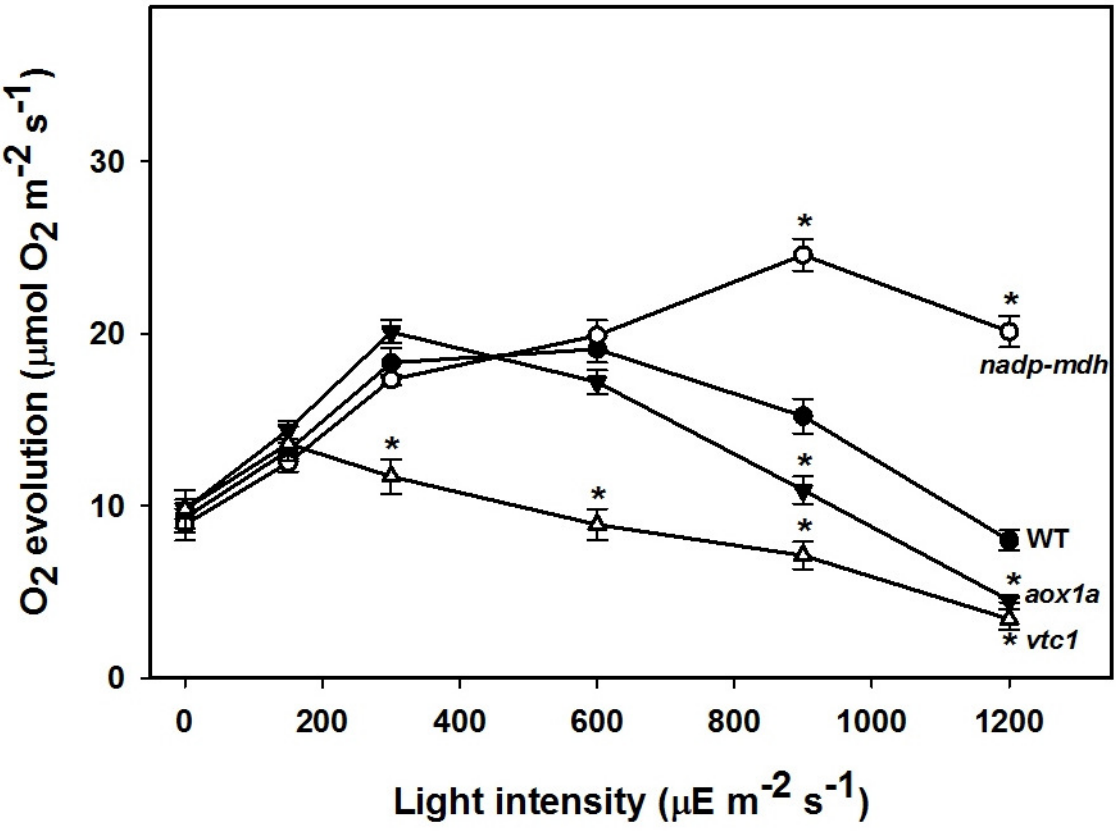

Figure 5.1. Photosynthetic rates measured in leaf discs of wild type, *nadp-mdh* and *aox1* mutants of *Arabidopsis thaliana* after treatment with increasing intensity of light for 2 h. Photosynthetic O_2 evolution was measured at end of 2 h, at a light intensity of 300 μE m^{-2} s^{-1}. Data represent mean values (± SE) from at least four independent experiments. Asterisks indicate statistically significant differences ($P< 0.05$) between the WT, *nadp-mdh, vtc1* and *aox1a* mutants at its respective light intensities, as determined by one way ANOVA (Student-Newman-Keuls method).

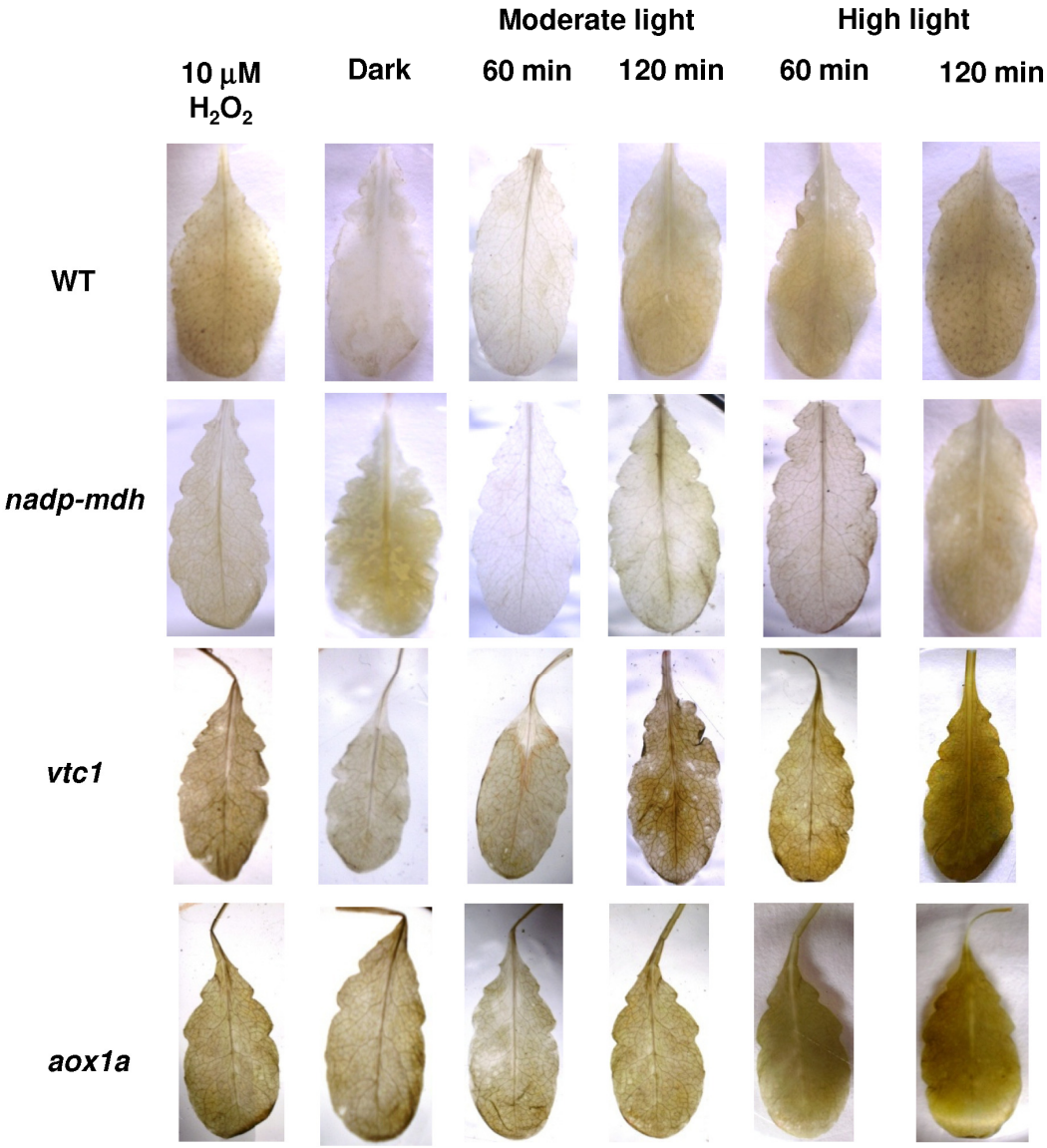

Figure 5.2. Accumulation of H_2O_2 as visualized by DAB (1 mg/mL), in response to dark, moderate light (300 µE m^{-2} s^{-1}) and high light (1200 µE m^{-2} s^{-1}) for either 60 or 120 min, in leaves of WT, *nadp-mdh, vtc1* and *aox1a* mutants of *Arabidopsis thaliana*. Leaves treated with 10 µM H_2O_2 were used as a control.

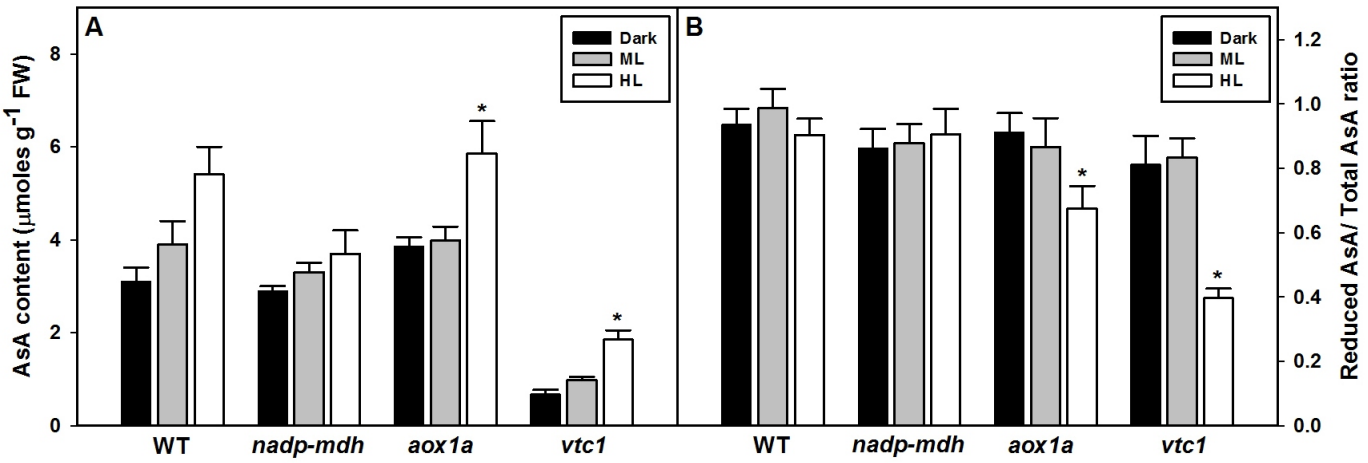

Figure 5.3. Ascorbate content (A) and redox ratios (B) in the leaf discs of wild type, *nadp-mdh, vtc1* and *aox1a* mutants of *Arabidopsis thaliana,* after treatment with dark, moderate light (300 μE m^{-2} s^{-1}) and high light (1200 μE m^{-2} s^{-1}) for 2 h. Data represent mean values (± SE) from at least four independent experiments. Asterisks indicate statistically significant differences (P< 0.05) between the different light intensities, as determined by one way ANOVA (Student-Newman-Keuls method).

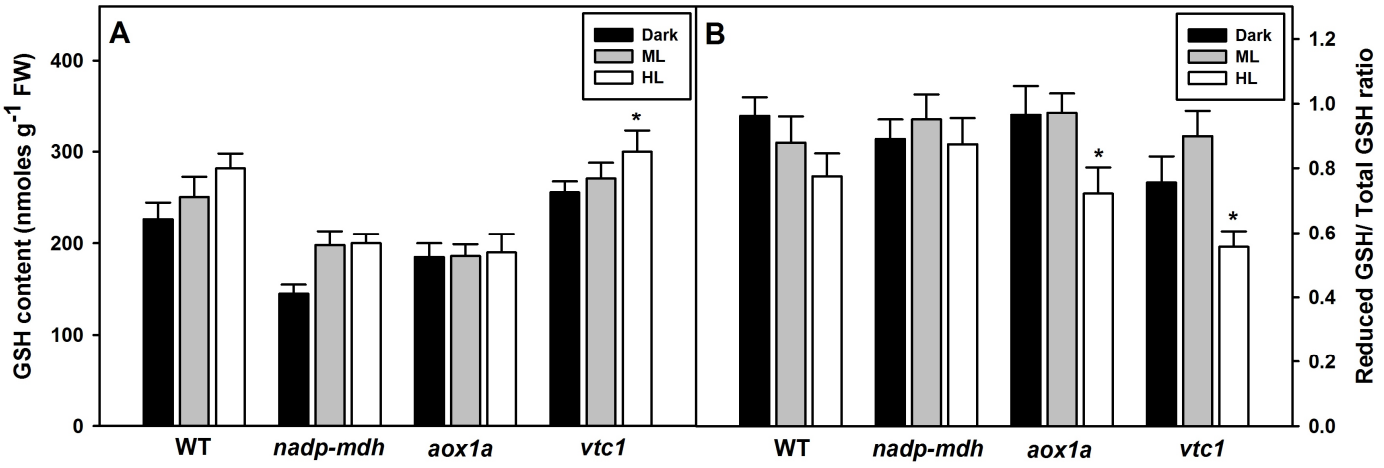

Figure 5.4. Glutathione content (A) and its redox ratios (B) in the leaf discs of wild type, *nadp-mdh, vtc1* and *aox1a* mutants of *Arabidopsis thaliana,* after treatment with dark, moderate light (300 µE m^{-2} s^{-1}) and high light (1200 µE m^{-2} s^{-1}) for 2 h. Data represent mean values (± SE) from at least four independent experiments. Asterisks indicate statistically significant differences ($P< 0.05$) between the different light intensities, as determined by one way ANOVA (Student-Newman-Keuls method).

Table 5.1. Activities of ascorbate peroxidase (APX), glutathione reductase (GR) and catalase (CAT) in leaf discs of wild type, *nadp-mdh*, *vtc1* and *aox1a* mutants of *Arabidopsis thaliana* after treatment with dark, moderate light (300 µE m^{-2} s^{-1}) and high light (1200 µE m^{-2} s^{-1}) for 2 h. Data represent mean values (± SE) from at least four independent experiments.

Treatment	**Wild type**	**%**	***nadp-mdh***	**%**	***aox 1a***	**%**	***vtc1***	**%**
				APX activity				
				(µmol oxidised mg^{-1} protein min^{-1})				
Dark	2.0 ± 0.3	100	1.7 ± 0.1	100	4.1 ± 0.5	100	0.7 ± 0.03	100
ML	3.3 ± 0.1	165	1.9 ± 0.3	112	5.2 ± 0.7	127	0.9 ± 0.06	129
HL	3.9 ± 0.1*	195	2.3 ± 0.2	135	9.6 ± 0.8*	234	1.4 ± 0.05	200
				GR activity				
				(µmol mg^{-1} protein min^{-1})				
Dark	0.06 ± 0.001	100	0.04 ± 0.006	100	0.06 ± 0.003	100	0.05 ± 0.003	100
ML	0.09 ± 0.012	150	0.06 ± 0.009	150	0.08 ± 0.007	133	0.07 ± 0.009	140
HL	0.14 ± 0.006*	233	0.07 ± 0.004	175	0.24 ± 0.011*	400	0.31 ± 0.016*	620
				CAT activity				
				(µmol oxidised mg^{-1} protein min^{-1})				
Dark	34 ± 3	100	48 ± 5	100	30 ± 2	100	41 ± 5	100
ML	56 ± 4	165	76 ± 9	158	62 ± 1	207	69 ± 6	168
HL	99 ± 8*	291	228 ± 17*	475	120 ± 9*	400	190 ± 11*	463

*Asterisks indicate statistically significant differences ($P < 0.05$) between the different light intensities, as determined by one way ANOVA (Student-Newman-Keuls method).

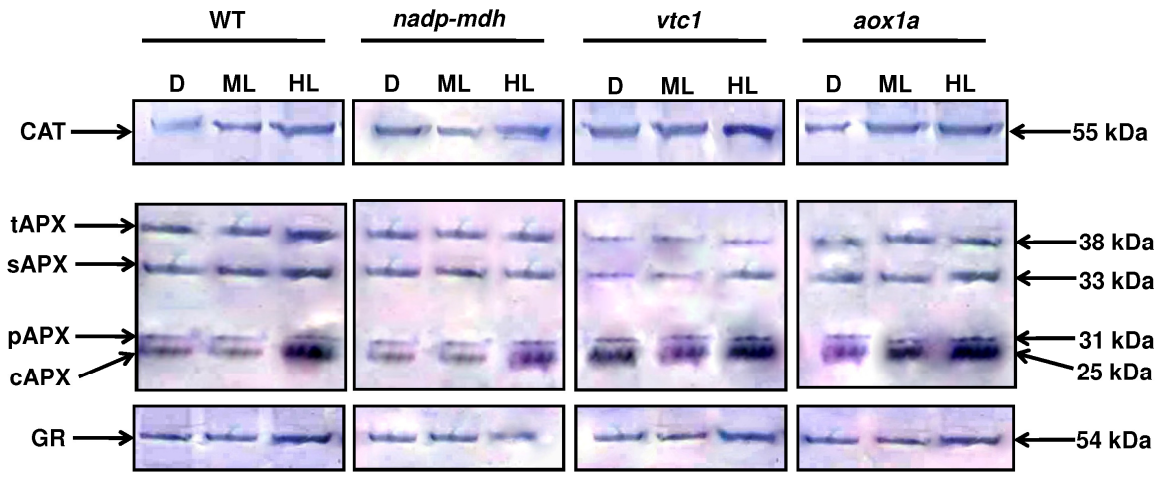

Figure 5.5. Protein levels of CAT, stromal APX, thylakoidal APX, cytosolic APX and GR in leaf discs of wild-type, *nadp-mdh, vtc1* and *aox1a* mutants of *Arabidopsis thaliana* after treatment with dark, moderate light (ML, 300 µE m^{-2} s^{-1}) and high light (HL, 1200 µE m^{-2} s^{-1}) for 2 h. Each well contains 15 µg of protein sample.

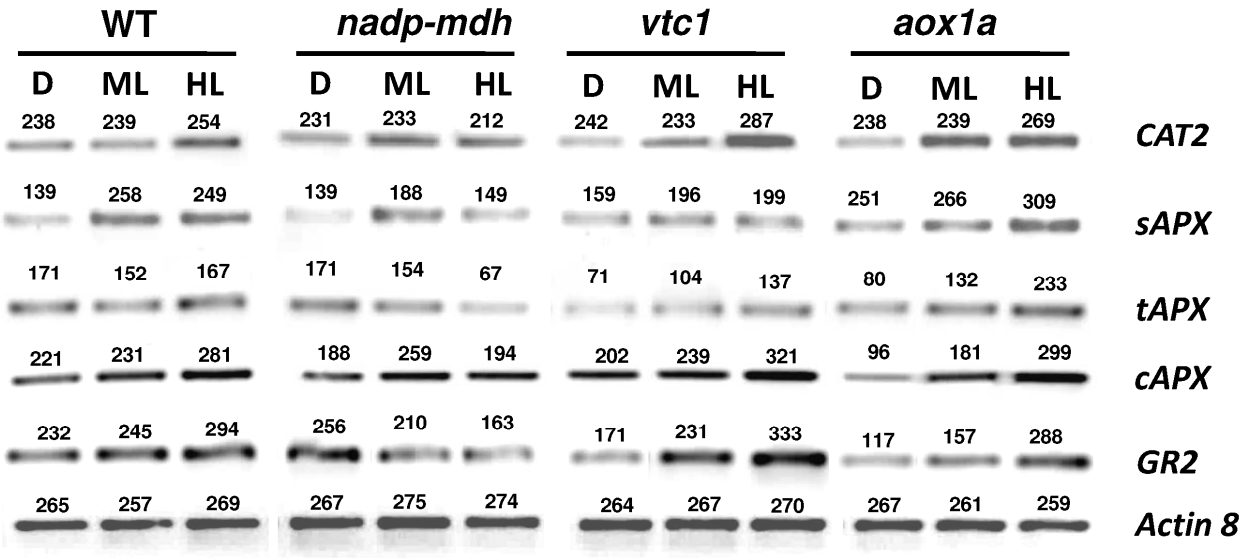

Figure 5.6. Expression of the mRNA transcript levels of *CAT2, sAPX, tAPX, cAPX* and *GR2* in leaf discs of wild-type, *nadp-mdh, vtc1* and *aox1a* mutants of *Arabidopsis thaliana* after treatment with dark, moderate light (ML, 300 µE m^{-2} s^{-1}) and high light (HL, 1200 µE m^{-2} s^{-1}) for 2 h. *ACTIN 8* was used as a loading control. Relative band intensities are indicated by the numbers on top of each band.

Table 5.2. The levels of free proline in leaf discs of wild type, *nadp-mdh*, *vtc1* and *aox1a* mutants of *Arabidopsis thaliana* after treatment with dark, moderate light (300 µE m^{-2} s^{-1}) and high light (1200 µE m^{-2} s^{-1}) for 2 h. Data represent mean values (± SE) from at least four independent experiments.

Treatment	**Free Proline content (µg g^{-1} FW)**							
	WT	%	*nadp-mdh*	%	*vtc1*	%	*AOX 1a*	%
Dark	199 ± 14	100	227 ± 19	100	143 ± 09	100	160 ± 22	100
ML	192 ± 13	96	261 ± 19	115	178 ± 12	124	180 ± 13	113
HL	339 ± 19*	170	571 ± 18*	251	209 ± 18	146	258 ± 18*	161

*Asterisks indicate statistically significant differences ($P < 0.05$) between the different light intensities, as determined by one way ANOVA (Student-Newman-Keuls method).

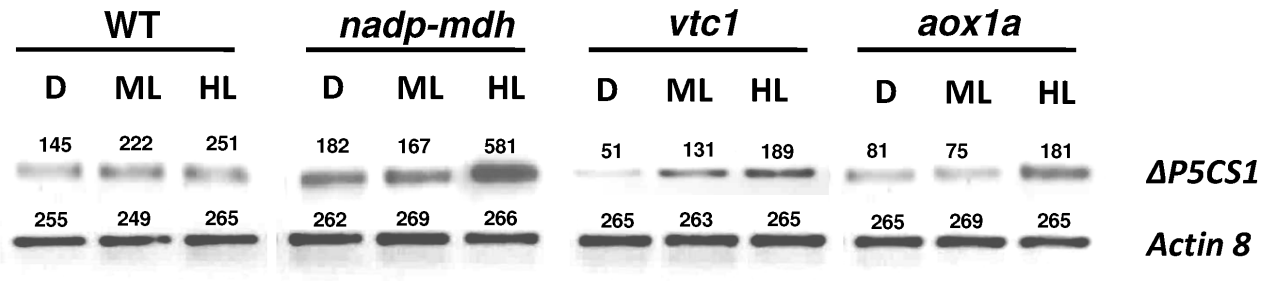

Figure 5.7. Expression of Δ*P5CS1* gene transcript in the leaf discs of wild type, *nadp-mdh*, *vtc1* and *aox1a* mutants of *Arabidopsis thaliana* after treatment with dark, moderate light (300 µE m^{-2} s^{-1}) and high light (1200 µE m^{-2} s^{-1}) for 2 h.

DISCUSSION

The malate valve, AOX pathway and antioxidant defense systems: all play a major role in protection of chloroplasts under stress conditions by dissipating excess reducing equivalents from chloroplasts and thereby minimizing the excess ROS generation. The present chapter deals with the comparative responses of *nadp-mdh* or *vtc1* or *aox1a* mutants to supraoptimal light. In our experiments, exposure to HL led to marked inhibition of photosynthesis, and enhanced response of antioxidant defense systems in *vtc1* or *aox1a* mutants, while *nadp-mdh* mutants exhibited sustained photosynthesis and least response of antioxidant defense systems. Our results emphasize that, *vtc1* or *aox1a* mutants are unable to adapt and are highly susceptible to photo-oxidative stress, while the *nadp-mdh* mutants are tolerant, due to acclimatization.

Sustained response of photosynthesis to supraoptimal light in *nadp-mdh* and susceptibility of *vtc1 or aox1a* mutants

The sensitivity of photosynthesis to photoinhibition in *vtc1* or *aox1a* mutants and is explained to be due to lack of protective antioxidant components (Müller-Moulé et al., 2004; Zhang et al., 2010). Our results on photosynthesis also demonstrate that, *vtc1* or *aox1a* mutants experienced high photo-oxidative stress, indicated by the reduced photosynthetic performance at HL. Drastic inhibition of photosynthetic rates in *vtc1* or *aox1a* mutants at HL (Figure 5.1) emphasizes the importance of AsA or AOX in optimizing photosynthesis and protecting against HL (Zhang et al., 2010; Talla et al., 2011).

Laisk et al. (2007) reported that the potato plants with minimal amounts of NADP-MDH were able to keep up their rates of photosynthesis and CO_2 assimilation, probably by employing the suitable energy-dissipating cycles at PSI and PSII. In the present study also, the *nadp-mdh* mutants sustained their photosynthetic rates even at HL signifying their tolerance to photo-oxidative stress (Figure 5.1). A recent report on photosynthesis in

nadp-mdh mutants described the possible existence of efficient compensatory mechanisms in *nadp-mdh* mutants to protect its chloroplasts from excess reductants and subsequent oxidative stress (Hebbelmann et al., 2012).

Low accumulation of ROS in *nadp-mdh* and enhanced accumulation of ROS in *vtc1*, *aox1a* mutants

The leaves of *vtc1* or *aox1a* mutants on exposure to HL intensities pre-treated with 3,3-diaminobenzidine (DAB, 1 mg/ml at pH 3.8) led to the enhanced accumulation of ROS, visualized by brown color (Figure 5.2). Our findings correlate with the earlier reports, that the *vtc1* and *aox1a* mutants are highly sensitive to photo-oxidative stress (Maruta et al., 2010; Zhang et al., 2010). The low levels of ROS in *nadp-mdh* mutants even at HL condition (Figure 5.2) suggests that this mutant was not proned to photo-oxidative stress. This point is in agreement with the findings of Hebbelmann et al. (2012) that the *nadp-mdh* mutant accumulated low levels of ROS even under HL.

Stimulation of AsA and GSH content in all three mutants and redox ratios dropped in *vtc1* or *aox1a* mutants/ undisturbed in *nadp-mdh* mutants at supraoptimal light

AsA and glutathione (GSH) are the redox buffers which play a crucial role in protection of plants under photo-oxidative stress conditions, through the Beck–Halliwell–Asada pathway (Mullineaux and Rausch, 2005). There are convincing reports that, the pool sizes of antioxidants increase at HL, along with that enhanced capacity of AOX (Bartoli et al., 2006; Talla et al., 2011). In the present study, on exposure to HL the *aox1a* and *vtc1* mutants exhibited slight stimulation in total AsA and total GSH levels followed by a drop in redox ratios of AsA and GSH (Figure 5.3 and 5.4).

Exposure of *nadp-mdh* mutants to HL, led to slight stimulation in the total AsA or total GSH levels but the redox ratios of AsA and GSH were not affected (Figure 5.3 and 5.4).

An earlier report also observed that the AsA/GSH based ROS scavenging systems were unaffected in *nadp-mdh* mutants even at HL (Hebbelmann et al., 2012).

Antioxidant enzymes: activities, protein and transcript levels

On exposure to HL stress, the activities as well as the expression of superoxide dismutase (SOD), CAT, APX, GR, dehydroascorbate reductase (DHAR), and monodehydroascorbate reductase (MDHAR) increase (Chen et al., 2011; Zhang et al., 2011). In conformity with earlier observations, in the present study the activities of APX, GR and CAT enzymes increased at HL. This increase was more prominent in *aox1a* and *vtc1* mutants (Table 5.1) signifying the importance of antioxidant defense systems and AOX in minimizing the ROS, while no significant change in the activities of APX, GR or CAT in *nadp-mdh* mutants indicates that the antioxidant defense mechanisms have a least role to play in maintenance of redox balance.

The HL conditions usually induced an increased accumulation of APX, GR and CAT protein levels (Mullineaux et al., 2000; Oelze et al., 2011). In our case too, the *aox1a* and *vtc1* mutants accumulated high levels of APX (especially cAPX), GR and CAT proteins (Figure 5.5) highlighting the sensitivity of these mutants towards photo-oxidative stress. While the unaltered protein levels of antioxidant enzymes in *nadp-mdh* mutants signifies the least role of antioxidant systems in protection.

Exposure to HL led to the upregulation in expression of APX, GR and catalase gene transcripts (Chang et al., 2004; Hernández et al., 2006). It is reported that *cAPX* induction is high upon treatment with MV or high-light stress in several plants, including Arabidopsis (Yoshimura et al., 2000; Li et al., 2009). It seems likely that the induction in *cAPX* expression during an early stage of oxidative stress is important in removing H_2O_2 and minimizing photooxidative damage. The CAT-deficient mutants (*cat2*) upon prolonged irradiation

exhibited severe oxidative stress underlining the importance of CAT in protection against photo-oxidative stress (Queval et al., 2007).

Even in our experiments, HL conditions up-regulated the expression of *CAT2*, *APX* isoforms and *GR2* transcript levels, particularly in *aox1a* and *vtc1* mutants. Among APX isoforms, the *cAPX* appears to be more up-regulated than the other isoforms (Figure 5.6). Our results on *aox1a* and *vtc1* mutants, suggests that the upregulation of these antioxidant enzymes is not sufficient to counteract the photo-oxidative stress. In contrast, unaltered expression of transcript levels of *CAT2*, *APX* isoforms and *GR2* of *nadp-mdh* mutants, this indicates these mutants are not subjected to photo-oxidative stress (Hebbelmann et al., 2012).

Up-regulation of free proline content and the key gene involved in proline synthesis

Accumulation of proline in higher plants is considered as an indication of perturbed osmotic environment, triggered by water/salinity stress. Exposure of plants to different environmental stress conditions leads to increase in the free proline content and induction of transcript levels of its related biosynthetic genes (Verbruggen and Hermans, 2008; Szabados and Savouré, 2010). Of late, there have been suggestions that proline also can be an efficient redox buffer (Hare and Cress, 1997; Moustakas et al., 2011). In the present experiments, the HL enhanced the accumulation of free proline content and up-regulated Δ*P5CS1* gene in all the three mutants of *Arabidopsis.* These responses were more pronounced in *nadp-mdh* than those in *aox1a* and *vtc1* mutants (Table 5.2; Figure 5.7). Our study therefore suggests that the proline may act as an alternative protective mechanism to minimize the excess reducing equivalents thereby offering protection to plants from photo-oxidative stress.

Conclusions:

1. The susceptibility of photosynthetic performance in *vtc1* or *aox1a* and sustained photosynthesis of *nadp-mdh* in HL suggested that *vtc1* and *aox1a* mutants were quite sensitive to photo-oxidative stress while *nadp-mdh* mutants were tolerant.

2. Excess accumulation of ROS, despite enhanced activities of APX, GR and catalase in *vtc1* or *aox1a* mutants imply that antioxidant defense mechanisms are not robust enough to keep ROS levels low in these mutants.
3. The low levels of ROS and no significant change in CAT, APX and GR activity in *nadp-mdh* mutants indicate that the AsA-glutathione cycle related enzymes may not be crucial in their role in redox balance.
4. Increased levels of CAT, APX, GR proteins and upregulation of their respective gene transcripts in *vtc1* or *aox1a* mutants indicate the requirement of these antioxidant enzymes to scavenge the excess ROS generated in these mutants, while the unchanged protein levels and unaltered gene expression of CAT, APX and GR enzymes indicate that *nadp-mdh* mutants are not proned to photo-oxidative stress.
5. Enhanced accumulation of free proline content and upregulation of gene involved proline synthesis, especially in *nadp-mdh* mutants, at HL suggest the operation of alternative protective mechanisms in *nadp-mdh* mutants besides the well-known AsA or glutathione based antioxidant defense systems in protection of plant against photo-oxidative stress.

****

Chapter 6

Importance of photorespiration and alternative oxidase in *nadp-mdh* mutants

Chapter 6

Importance of photorespiration and alternative oxidase in *nadp-mdh* mutants

INTRODUCTION

Plants utilize multiple mechanisms to minimize the oxidative damage, which include: D1 protein turnover, non-photochemical energy quenching, xanthophyll cycle, chlororespiration, cyclic electron transport, and the Mehler's reaction. Besides these mechanisms located in chloroplasts, there are additional extra-chloroplastic systems, such as alternative oxidase (AOX) and photorespiration, to protect plant cells against oxidative stress. The mitochondrial oxidative metabolism was important for neutralizing excess of photosynthetic reducing power, preventing oxidative damage of thylakoid membranes and other cellular components (Raghavendra and Padmasree, 2003; Yoshida and Noguchi, 2010; Xu et al., 2011).

Alternative oxidase (AOX) pathway play a major role in relieving the over-reduction of chloroplasts. Several reports demonstrated that inhibition of AOX led to a decrease in the photosynthetic rate and the over-reduction of the photosynthetic electron transport chain in leaves and in protoplasts (Padmasree and Raghavendra, 1999; Bartoli et al., 2005). The amount and activity of AOX dramatically increased in high-light (HL) conditions (Yoshida et al., 2006; Noguchi and Yoshida, 2008). It is expected that AOX would function as a outlet for excess reducing equivalents generated in the chloroplasts and serves as a protective mechanism in dissipation of excess redox.

Photorespiration could also facilitate as an efficient outlet for dissipation excess reducing equivalents from chloroplasts thereby optimizing the photosynthesis (Igamberdiev et al., 2001; Foyer et al., 2009). In chloroplasts, photorespiration consumes reducing equivalents for refixation of CO_2. Additional chloroplastic ATP is consumed for

phosphorylation of glycerate to 3-phosphoglycerate (PGA) in the glycolate cycle. During the refixation of CO_2, twice as much NADPH and ATP was consumed in the Calvin cycle, thus photorespiration serves as an energy-dissipating mechanism which helps in protection of chloroplasts from photoinhibition (Wingler et al., 2000; Bauwe et al., 2010; Takahashi and Badger, 2011).

In the present study, we have chosen *nadp-mdh* mutants of *Arabidopsis thaliana* lacking chloroplastic NADP-malate dehydrogenase. The *aox1a* mutants were not used, because the response of *aox1a* mutant towards the photorespiratory inhibitors was studied earlier. The *aox1a* mutants attempted to increase their capacity for photorespiration (Strodtkötter et al., 2009), when the function of AOX was suppressed. In this study, we examined the photosynthetic performance and antioxidant defense systems in mesophyll cell protoplasts of *nadp-mdh* mutants under restricted conditions of photorespiration and mitochondrial respiratory electron transport system. The photorespiration was decreased either by lowering O_2 or by using photorespiratory inhibitors. The present findings with *nadp-mdh* mutants suggests that when there is a suppressed function of malate valve or photorespiration or AOX, the role of antioxidant defense systems get pronounced.

RESULTS

Effect of lowering O_2 on photosynthesis and sensitivity to photorespiratory inhibitors

Photosynthesis was monitored at either normal O_2 (~410 nmoles O_2 ml^{-1}) or low O_2 (~85 nmoles O_2 ml^{-1}) levels in mesophyll cell protoplasts of WT and *nadp-mdh* mutants of *Arabidopsis*. The photosynthetic rates in WT were not significantly changed at low O_2 compared to ambient O_2 at an optimum bicarbonate level (1 mM) in the assay medium. While in the mutants photosynthesis was significantly lowered at low O_2 (by > 40 %) compared to normal air (Figure 6.1). This decrease in photosynthetic oxygen evolution was significant in

nadp-mdh mutant compared to WT, particularly at high bicarbonate levels (10 mM) (Figure 6.1).

At normal O_2, the photorespiratory (aminoacetonitrile, AAN and glycine hydroxamate, GHA) and mitochondrial respiratory inhibitors (antimycin A and salicyl hydroxamate, SHAM) significantly decreased the photosynthetic rates of WT and *nadp-mdh* mutants. This decrease in photosynthesis was higher in *nadp-mdh* mutants on exposure to AAN or GHA (by >30 %) and SHAM (by >40 %) than that in WT. At low O_2, exposure to photorespiratory and mitochondrial respiratory inhibitors led to a marginal decrease in the photosynthetic rates, but was not significant in WT and *nadp-mdh* mutants (Table 6.1).

Effect of photorespiratory inhibitors and mitochondrial respiratory inhibitors on antioxidant content

Ascorbate (AsA): Exposure to AAN or GHA stimulated the total AsA both in WT and *nadp-mdh* mutants, but this stimulation was not significant (Figure 6.2A). The redox ratios of AsA (reduced AsA/total AsA) slightly dropped in both WT and *nadp-mdh* mutants on treatment with AAN or GHA, this decrease in redox ratio of AsA was slightly high in *nadp-mdh* mutants (from 0.9 to 0.7) compared to WT (Figure 6.2B).

The antimycin A or SHAM slightly stimulated the total AsA in WT and *nadp-mdh* mutants (Figure 6.2A). The redox ratio of AsA decreased in WT and *nadp-mdh* mutants on exposure to antimycin A or SHAM, this decrease was more pronounced in *nadp-mdh* mutants particularly on exposure to SHAM (from 0.9 to 0.7) compared to WT (Figure 6.2B).

Glutathione (GSH): The AAN or GHA exposure marginally decreased the total GSH contents, particularly in *nadp-mdh* mutants compared to WT, this decrease was not significant (Figure 6.3A). Exposure to AAN or GHA led to decrease in the redox ratios of GSH (reduced GSH/total GSH) in *nadp-mdh* mutants (from 0.9 to 0.7) compared to WT (Figure 6.3B).

The antimycin A or SHAM led to slight stimulation in the total GSH contents in both WT and *nadp-mdh* mutants (Figure 6.3A). The redox ratios of GSH decreased marginally on treatment with antimycin A or SHAM in both WT and *nadp-mdh* mutants, this decrease was more pronounced in *nadp-mdh* mutants particularly upon treatment with SHAM (from 0.9 to 0.7) (Figure 6.3B).

Effect of photorespiratory inhibitors and mitochondrial respiratory inhibitors on antioxidant enzyme activities

Exposure to AAN or GHA, enhanced the activities of three enzymes: ascorbate peroxidase (APX) by >8-fold, glutathione peroxidase (GR) by >1-fold and catalase (CAT) by >1-fold in *nadp-mdh* mutants compared to WT (Table 6.2 to 6.4). Similarly, SHAM also enhanced these enzyme activities: ascorbate peroxidase (APX) by >4-fold, glutathione peroxidase (GR) by >2-fold and catalase (CAT) by >2-fold in *nadp-mdh* mutants especially on treatment with SHAM compared to WT (Table 6.2 to 6.4).

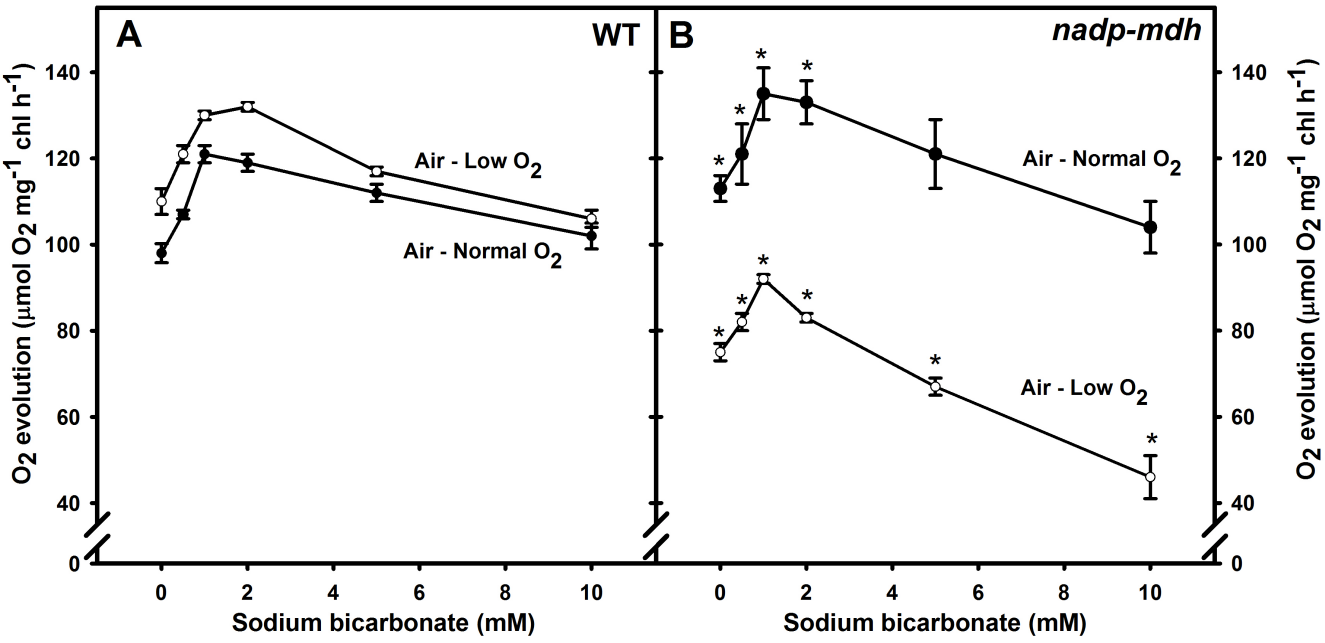

Figure 6.1. Photosynthetic performance of protoplasts in relation to varying bicarbonate and at normal (●) or low O_2 (○) in the reaction medium. The measurements were made with protoplasts from leaves of WT (A) and of *nadp-mdh* mutants (B). The level of O_2 in normal air-equilibrated reaction medium was ~410 nmoles O_2 ml^{-1}, in contrast to medium bubbled with N_2, resulting in low O2 (~85 nmoles O_2 ml^{-1}). The light intensity used was 700 µmol m^{-2} s^{-1}. Data represent mean values (± SE) from at least four independent experiments. Asterisks indicate statistically significant differences ($P< 0.05$) between the WT and *nadp-mdh* mutants, as determined by one way ANOVA (Student-Newman-Keuls method).

Table 6.1. Rates of photosynthetic O_2 evolution by protoplasts from WT and *nadp-mdh* knockout mutants at an optimal bicarbonate concentration (1 mM) under either normal O_2 (~410 nmoles O_2 ml^{-1}) or low O_2 (~85 nmoles O_2 ml^{-1}). Photosynthesis was determined in the absence or in presence of photorespiratory and mitochondrial respiratory inhibitors (AAN, GHA, Antimycin A and SHAM) for 5 min dark and 10 min light (700 µE m^{-2} s^{-1}) incubation. Data represent mean values (± SE) from at least four independent experiments.

Treatment	**O_2 evolution (µmol O_2 mg^{-1} chl h^{-1})**			
	WT		***nadp-mdh***	
	Rate	**%**	**Rate**	**%**
Normal O_2 (~ 415 nmol O_2 ml^{-1})				
None	135 ± 5	100	146 ± 4	100
AAN (8 mM)	63 ± 1	47	55 ± 3	38
GHA (10 mM)	63 ± 3	47	44 ± 6	30
Antimycin A (400 nM)	69 ± 6	51	85 ± 4	58
SHAM (600 µM)	62 ± 1	46	40 ± 8	27
Low O_2 (~ 85 nmol O_2 ml^{-1})				
None	122 ± 3	100	84* ± 4	100
AAN (8 mM)	109 ± 4	89	79* ± 2	94
GHA (10 mM)	113 ± 6	93	78* ± 2	93
Antimycin A (400 nM)	59 ± 1	48	74 ± 6	88
SHAM (600 µM)	75 ± 4	61	50* ± 5	60

*Asterisks indicate that the differences ($P< 0.05$) between the WT and *nadp-mdh* mutants are statistically significant as determined by one way ANOVA (Student-Newman-Keuls method).

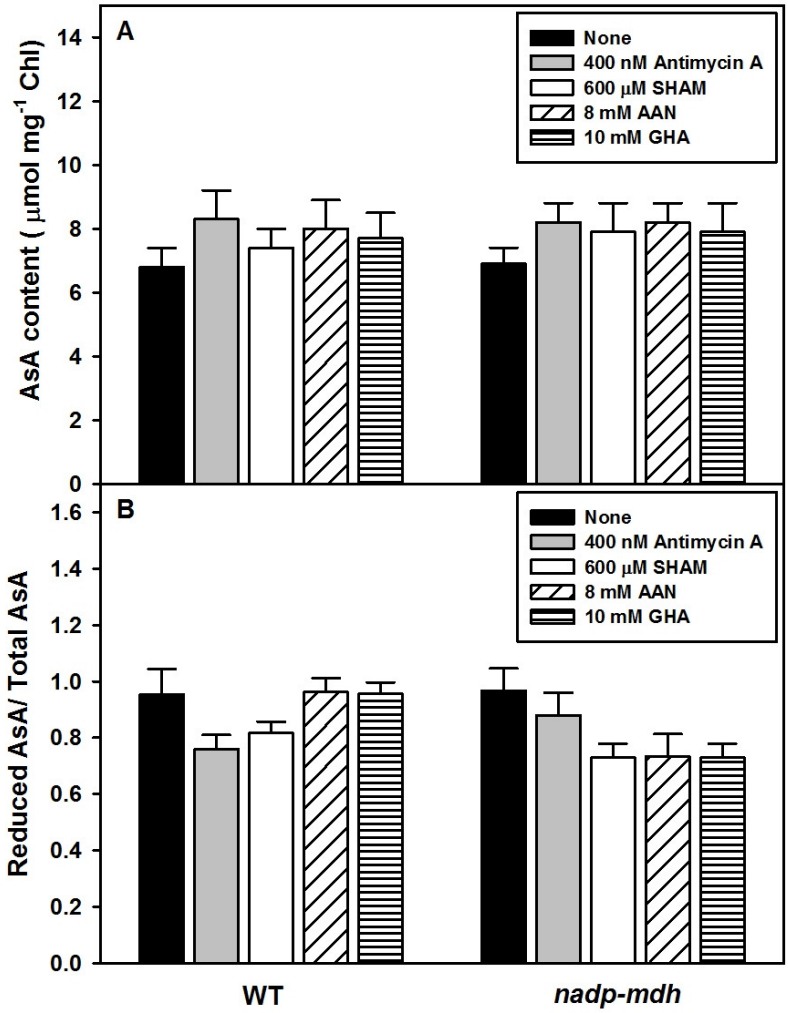

Figure 6.2. AsA content and its redox status determined in mesophyll cell protoplasts of WT and, *nadp-mdh* knock out mutant of *Arabidopsis thaliana* upon treatment with mitochondrial respiratory inhibitors (Antimycin A and SHAM) and photorespiratory inhibitors (AAN and GHA) incubated at a 5 min dark and 10 min light (700 µE m^{-2} s^{-1}). Data represent mean values (± SE) from at least four independent experiments. Statistical analysis was performed by one way ANOVA (Student-Newman-Keuls method), but none of the changes were statistically significant.

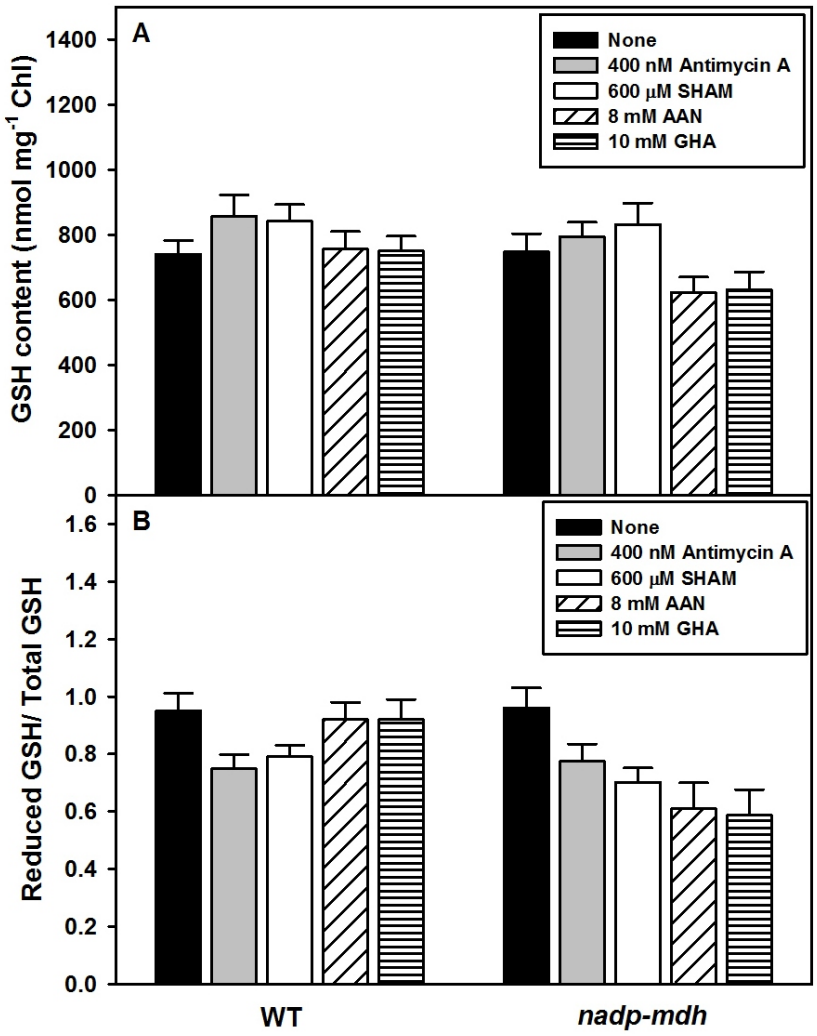

Figure 6.3. Glutathione content and its redox status determined in mesophyll cell protoplasts of WT and *nadp-mdh* knock out mutant of *Arabidopsis thaliana* upon treatment with mitochondrial respiratory inhibitors (Antimycin A and SHAM) and photorespiratory inhibitors (AAN and GHA) incubated at 5 min dark and 10 min light (700 µE m^{-2} s^{-1}). Data represent mean values (± SE) from at least four independent experiments. Statistical analysis was performed by one way ANOVA (Student-Newman-Keuls method), but none of the changes were statistically significant.

Table 6.2. Ascorbate Peroxidase (APX) activity in mesophyll cell protoplasts of wild type and *nadp-mdh* mutants of *Arabidopsis thaliana* on treatment with photorespiratory inhibitors (8 mM AAN, 10 mM GHA) and mitochondrial respiratory inhibitors (400 nM antimycin A and 600 µM SHAM) for 5 min dark and 10 min light (700 µE m^{-2} s^{-1}). Data represent mean values (± SE) from at least four independent experiments.

Treatment	**APX activity** ($\mu mol\ H_2O_2\ mg^{-1}$ **protein** min^{-1})			
	Wild type	**%**	***nadp-mdh***	**%**
None	0.75 ± 0.1	100	0.64 ± 0.4	100
+ 8 mM AAN	1.72 ± 0.1	229	5.63* ± 0.3	880
+ 10 mM GHA	1.77 ± 0.3	236	5.45* ± 0.8	851
+ 400 nM Antimycin A	2.33 ± 0.05	311	1.61* ± 0.2	252
+ 600 µM SHAM	1.66 ± 0.09	221	2.58* ± 0.2	403

*Asterisks indicate that the differences ($P < 0.05$) between the WT and *nadp-mdh* mutants are statistically significant as determined by one way ANOVA (Student-Newman-Keuls method).

Table 6.3. Glutathione reductase (GR) activity in mesophyll cell protoplasts of wild type and *nadp-mdh* mutants of *Arabidopsis thaliana* on treatment with photorespiratory inhibitors (8 mM AAN, 10 mM GHA) and mitochondrial respiratory inhibitors (400 nM antimycin A and 600 μM SHAM) for 5 min dark and 10 min light (700 μE m^{-2} s^{-1}). Data represent mean values (± SE) from at least four independent experiments.

Treatment	**GR activity (μmol mg^{-1} protein min^{-1})**			
	Wild type	**%**	***nadp-mdh***	**%**
None	0.368 ± 0.01	100	0.380 ± 0.07	100
+ 8 mM AAN	0.421 ± 0.03	114	0.520 ± 0.06	137
+ 10 mM GHA	0.452 ± 0.01	123	0.555 ± 0.06	146
+ 400 nM Antimycin A	0.690 ± 0.05	188	0.634 ± 0.04	167
+ 600 μM SHAM	0.503 ± 0.05	137	0.961* ± 0.06	252

*Asterisks indicate that the differences (P< 0.05) between the WT and *nadp-mdh* mutants are statistically significant as determined by one way ANOVA (Student-Newman-Keuls method).

Table 6.4. Catalase activity in mesophyll cell protoplasts of wild type and *nadp-mdh* mutants of *Arabidopsis thaliana* on treatment with photorespiratory inhibitors (8 mM AAN, 10 mM GHA) and mitochondrial respiratory inhibitors (400 nM antimycin A and 600 µM SHAM) for 5 min dark and 10 min light (700 µE m^{-2} s^{-1}). Data represent mean values (± SE) from at least four independent experiments.

Treatment	**Catalase activity (µmol mg^{-1} protein min^{-1})**			
	Wild type	**%**	***nadp-mdh***	**%**
None	71 ± 5	100	84 ± 7	100
+ 8 mM AAN	72 ± 7	101	113* ± 10	135
+ 10 mM GHA	77 ± 3	108	127* ± 8	151
+ 400 nM Antimycin A	92 ± 6	130	122* ± 3	145
+ 600 µM SHAM	67 ± 4	94	193* ± 8	230

*Asterisks indicate that the differences ($P < 0.05$) between the WT and *nadp-mdh* mutants are statistically significant as determined by one way ANOVA (Student-Newman-Keuls method).

DISCUSSION

Restriction of photorespiration and AOX pathway increased the sensitivity of photosynthesis in *nadp-mdh* mutants

Low O_2 levels or high CO_2 at the vicinity of Rubisco restrict the oxygenation reaction thereby lowering the photorespiration (Wingler et al., 2000). Many researchers employed AAN or GHA, the competitive inhibitors of glycine decarboxylase activity to inhibit the photorespiration (Lawyer and Zelitch, 1979; Créach et al., 1982). The significant decrease in photosynthesis in *nadp-mdh* mutants upon restricting photorespiration either by low O_2 or presence of AAN or GHA (Figure 6.1 and Table 6.1) signifies the importance of photorespiration in protection of *nadp-mdh* mutants when function of malate valve was suppressed.

Earlier reports suggested that AOX can dissipate the excess reducing equivalents, which are transported from the chloroplasts, and helps in optimizing photosynthesis against photoinhibition (Yoshida et al., 2007; Strodtkötter et al., 2009; Talla et al., 2011). The greater susceptibility of photosynthesis in *nadp-mdh* mutants towards the mitochondrial respiratory inhibitors (Figure 6.1 and Table 6.1), especially SHAM, suggests the importance of mitochondrial AOX in compensating the impaired function of chloroplastic NADP-MDH.

Inhibition of photorespiration and AOX pathway enhanced the accumulation of antioxidants accompanied by low redox ratios in *nadp-mdh* mutants

The antioxidant metabolites such as AsA and GSH accumulate at greater extent in chloroplasts under stressful conditions and considered to function together in the AsA-GSH cycle to metabolize ROS and to dissipate excess excitation energy in chloroplasts (Asada, 2006; Foyer and Shigeoka, 2011). In this study, the restriction of photorespiration and AOX pathway in *nadp-mdh* mutants led to slight stimulation in total AsA and GSH contents with a slight decrease in the redox ratios signifying the sensitivity of *nadp-mdh* mutants to oxidative

stress (Figure 6.2 and Figure 6.3). This sensitivity of *nadp-mdh* mutants to oxidative stress and insignificant response of antioxidants and their redox ratios upon restriction of photorespiration and AOX pathway mechanisms signifies the importance of photorespiration and AOX pathway in counteracting oxidative stress (Hebbelmann et al., 2012) and there was further requirement of antioxidants performance is necessary to minimize the oxidative stress.

Enhanced activities of APX, GR and CAT upon restriction of photorespiration and AOX pathway in *nadp-mdh* mutants

The impairment in the function of photorespiration and AOX leads to enhancement of ROS production (Queval et al., 2007; Zhang et al., 2010). The enhanced activity of antioxidant enzymes can minimize such excess ROS. In the present study, there was a significant increase in the activities of APX, GR and CAT in *nadp-mdh* mutants upon treatment with AAN or GHA or SHAM (Table 6.2 to 6.4). The increased performance of antioxidant defense systems in *nadp-mdh* mutant indicates that there is a high flexibility of antioxidant defense systems to minimize oxidative stress. Our results emphasize that the role of antioxidant defense systems gets pronounced in order to minimize the excess ROS when function of malate valve or AOX or photorespiration is suppressed.

Conclusions:

1. Marked inhibition of the photosynthesis in mesophyll protoplasts of *nadp-mdh* mutants by low O_2 or photorespiratory inhibitors and AOX pathway inhibitors suggests that photorespiration and AOX pathway may play crucial role in optimizing photosynthesis, when function of malate valve was compromised.
2. Enhanced antioxidant levels and activities of APX, GR and catalase in *nadp-mdh* mutants upon treatment with photorespiratory inhibitors and mitochondrial respiratory inhibitors especially SHAM suggest that the antioxidant defense systems are not able to minimize oxidative stress.

3. Our results emphasize that the plants which have suppressed function of malate valve or photorespiration or AOX pathway, need to have a pronounced role of antioxidant enzymes, rather than the levels of antioxidant in leaves.

******

Chapter 7

Effects of supraoptimal bicarbonate in *nadp-mdh* and *vtc1* mutants of *Arabidopsis*

Chapter 7

Effects of supraoptimal bicarbonate in *nadp-mdh* and *vtc1* mutants of *Arabidopsis*

INTRODUCTION

Being a major metabolic process, photosynthesis responds to various environmental conditions, which often cause over-reduction of the electron transport system, leading to oxidative stress. Among the environmental conditions, elevated CO_2 levels could also induce oxidative stress in plant cells (Kolla et al., 2007; Qiu et al., 2008). In long-term, exposure to high CO_2 at the vicinity of Rubisco resulted in decline of its protein and transcript levels and then decreased photosynthetic performance. High CO_2 conditions would also restrict the photorespiratory pathway by limiting the oxygenation of Rubisco (Sheen, 1990; Stitt, 1991).

In order to combat oxidative stress, plants have developed several different protective mechanisms, such as: antioxidants defense systems, D1 protein turnover, state transitions, non-photochemical energy quenching, xanthophyll cycle, chlororespiration, cyclic electron transport and Mehler's reaction (Nunes-Nesi et al., 2008; Foyer and Noctor, 2009). Additionally, extra-chloroplastic mechanisms operate to protect from oxidative stress which include malate valve, alternative oxidase (AOX) and photorespiration (Scheibe et al., 2005; Wilhelm and Selmar, 2010).

In the present study, we have chosen mesophyll protoplasts, as they allow free diffusion of O_2 or CO_2, and maintain closeness to the *in vivo* situation, unlike isolated organelles. Qiu et al. (2008) suggested that, the elevated CO_2 would cause oxidative stress in plants by increasing leaf protein carbonylation, leading to loss of leaf chlorophyll and decrease in photosynthetic rate. Very little information is available on the exact role of crucial redox components in response to elevated CO_2. A recent report on *aox1a* mutant

revealed that AOX could help in optimization of photosynthesis under high CO_2 concentrations (Gandin et al., 2012). We have therefore chosen the mutants lacking or deficient of crucial redox components to investigate the response of their redox components towards elevated CO_2. The *nadp-mdh* mutants lack chloroplastic NADP-malate dehydrogenase (NADP-MDH) and *vtc1* mutants are deficient of ascorbate (AsA) with 30 % of AsA compared to wild type. During this study, the elevated CO_2 was mimicked by using 10 mM bicarbonate, which would be equivalent to 741 μM CO_2.

Our results emphasize the increased susceptibility of *nadp-mdh* mutants towards oxidative stress caused by supra-optimal bicarbonates levels. This was indicated by an imbalance inside the cell, one of them likely to be the redox state. Although there were significant changes in photosynthesis, the antioxidant levels were not much altered.

RESULTS

Effect of varying bicarbonate on photosynthesis

In *nadp-mdh* and *vtc1* mutants, the photosynthetic oxygen evolution gradually increased to reach maximum at bicarbonate level of 1 mM. Such increase was more pronounced in *nadp-mdh* mutant. Further increase of bicarbonate 1 to 10 mM decreased the photosynthetic rates in *nadp-mdh* mutants. The *vtc1* mutants exhibited low photosynthetic rates throughout, at all bicarbonate levels (Figure 7.1).

Effect of varying bicarbonate on antioxidant content

Ascorbate (AsA) and glutathione (GSH): Exposure to high bicarbonate levels did not alter the total content and redox ratios of AsA (reduced AsA/total AsA) in both *nadp-mdh* and *vtc1* in comparison to WT (Figure 7.2A, B). Even the total GSH and their redox ratios remained unchanged in *nadp-mdh* or *vtc1* mutants compared to WT at high bicarbonate levels (Figure 7.3A, B).

Effect of varying bicarbonate on antioxidant enzymes

Enzyme activities

At endogenous levels when no bicarbonate added, the activity of ascorbate peroxidase (APX) was low in both *nadp-mdh* and *vtc1* mutants in comparison with WT. While exposure to high bicarbonate levels (10 mM), the activity of APX significantly enhanced in *nadp-mdh* (>3-fold) and *vtc1* mutant (>2-fold) (Table 7.1). The glutathione peroxidase (GR) activity was decreased in *nadp-mdh* and remained unchanged in *vtc1* mutants compared to WT plants at endogenous bicarbonate levels. The GR activity was increased in *nadp-mdh* and *vtc1* mutants (<2-fold) at high bicarbonate levels (Table 7.1). Endogenous bicarbonate levels decreased the activity of catalase (CAT) of *nadp-mdh* and enhanced the activity of CAT of *vtc1* mutants in comparison to WT. At high bicarbonate levels, *nadp-mdh* mutants exhibited enhanced CAT activity which was significant (≤2-fold) (Table 7.1).

Protein levels

The high bicarbonate levels enhanced the accumulation CAT proteins in *nadp-mdh* compared to WT. In *vtc1* mutants, the accumulation CAT protein was unaltered at high bicarbonate levels (Figure 7.4). Exposure to high bicarbonate enhanced the accumulation of four isoforms of APX proteins (especially in chloroplast localized *tAPX* and *sAPX* proteins) in *nadp-mdh* compared to WT (Figure 7.4). The *vtc1* mutants lower accumulation of *APX* isoforms at high bicarbonate levels. At higher bicarbonate levels, the accumulation of GR proteins enhanced in both *nadp-mdh* and *vtc1* mutants compared to WT (Figure 7.4).

mRNA transcript levels

Under endogenous bicarbonate levels, the expression of *CAT2* gene was down-regulated in *nadp-mdh* mutants and up-regulated in *vtc1* mutants in comparison to WT. In contrast, at higher bicarbonate levels (10 mM) the expression of *CAT2* gene was up-regulated in *nadp-mdh* mutant (>6-fold) and down-regulated in *vtc1* mutants (Figure 7.5).

At endogenous bicarbonate levels, the expression of all APX isoforms were down-regulated in both *nadp-mdh* and *vtc1* mutants in comparison to WT. High bicarbonate levels, induced up-regulation in the expression of all three isoforms *APX*, especially *sAPX* and *cAPX* (<5-fold) in *nadp-mdh*, without altering the expression of *APX* genes in *vtc1* mutant (Figure 7.5).

Down-regulation of expression *GR2* gene was observed in *nadp-mdh* or *vtc1* mutants in comparison with WT, at endogenous bicarbonate levels. While high bicarbonate levels, up-regulated the expression of *GR2* gene in *nadp-mdh* (>3-fold), without altering *GR2* gene expression of *vtc1* mutant (Figure 7.5).

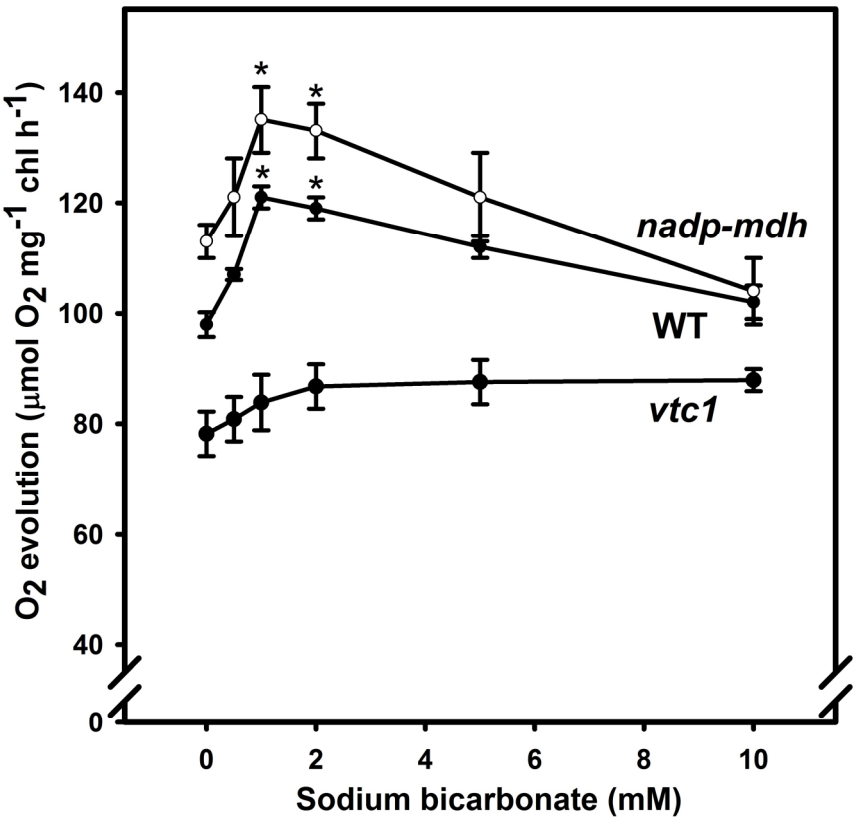

Figure 7.1. Photosynthetic performance of protoplasts in relation to varying bicarbonate in WT, *nadp-mdh* and *vtc1* mutants. The light intensity used was 700 μmol m^{-2} s^{-1}. Data represent mean values (± SE) from at least four independent experiments. *Asterisks indicate statistically significant differences ($P< 0.05$) in response to bicarbonate in WT and *nadp-mdh* or *vtc1* mutants, as determined by one way ANOVA (Student-Newman-Keuls method).

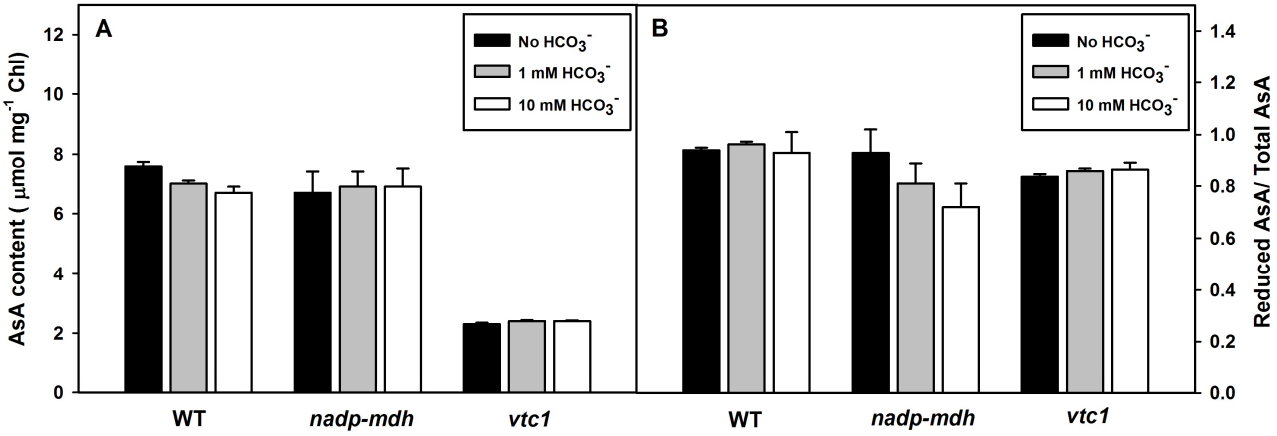

Figure 7.2. AsA content (A) and its redox status (B) determined in mesophyll cell protoplasts of WT, *nadp-mdh* and *vtc1* mutants of *Arabidopsis thaliana* upon treatment with different bicarbonate levels incubated at a 5 min dark and 10 min light (700 µE m^{-2} s^{-1}). Data represent mean values (± SE) from at least four independent experiments. Statistical analysis was performed by one way ANOVA (Student-Newman-Keuls method), but none of the changes was statistically significant.

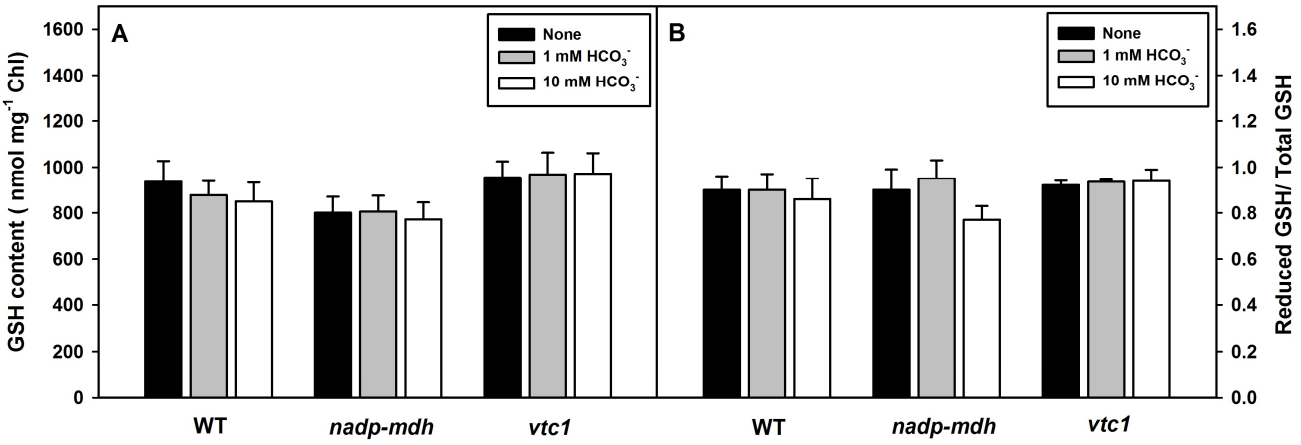

Figure 7.3. GSH content (A) and its redox status (B) determined in mesophyll cell protoplasts of WT, *nadp-mdh* and *vtc1* mutants of *Arabidopsis thaliana* upon treatment with different bicarbonate levels incubated at a 5 min dark and 10 min light (700 µE m^{-2} s^{-1}). Data represent mean values (± SE) from at least four independent experiments. Statistical analysis was performed by one way ANOVA (Student-Newman-Keuls method), but none of the changes was statistically significant.

Table 7.1. APX, GR and CAT activity in mesophyll cell protoplasts of WT, *nadp-mdh* and *vtc1* mutants of *Arabidopsis thaliana* upon 5 min dark and 10 min light (700 μE m^{-2} s^{-1}) incubation upon treatments with varying concentrations of bicarbonate. Data represent mean values (± SE) from at least four independent experiments.

Treatment	**CAT activity (μmol H_2O_2 mg^{-1} protein min^{-1})**					
	Wild type	**%**	***nadp-mdh***	**%**	***vtc1***	**%**
None	83 ± 8	100	71 ± 9	100	95 ± 5	100
+ 1 mM HCO_3^-	70 ± 3	84	84 ± 6	118	75 ± 4	79
+ 10 mM HCO_3^-	56 ± 2	67	115* ± 7	162	60 ± 5	63
	APX activity (μmol H_2O_2 mg^{-1} protein min^{-1})					
None	1.53 ± 0.2	100	1.21 ± 0.2	79	0.35 ± 0.02	23
+ 1 mM HCO_3^-	1.25 ± 0.1	82	2.94* ± 0.3	243	0.60 ± 0.04	171
+ 10 mM HCO_3^-	1.02 ± 0.1	67	3.44* ± 0.7	284	0.85* ± 0.04	243
	GR activity (μmol mg^{-1} protein min^{-1})					
None	0.432 ± 0.04	100	0.331 ± 0.05	100	0.433 ± 0.01	100
+ 1 mM HCO_3^-	0.380 ± 0.01	88	0.380 ± 0.07	115	0.550 ± 0.01	127
+ 10 mM HCO_3^-	0.340 ± 0.01	79	0.490 ± 0.04	148	0.570 ± 0.01	132

*Asterisks indicate that the differences ($P < 0.05$) in response to bicarbonate in WT and *nadp-mdh* or *vtc1* mutants are statistically significant as determined by one way ANOVA (Student-Newman-Keuls method).

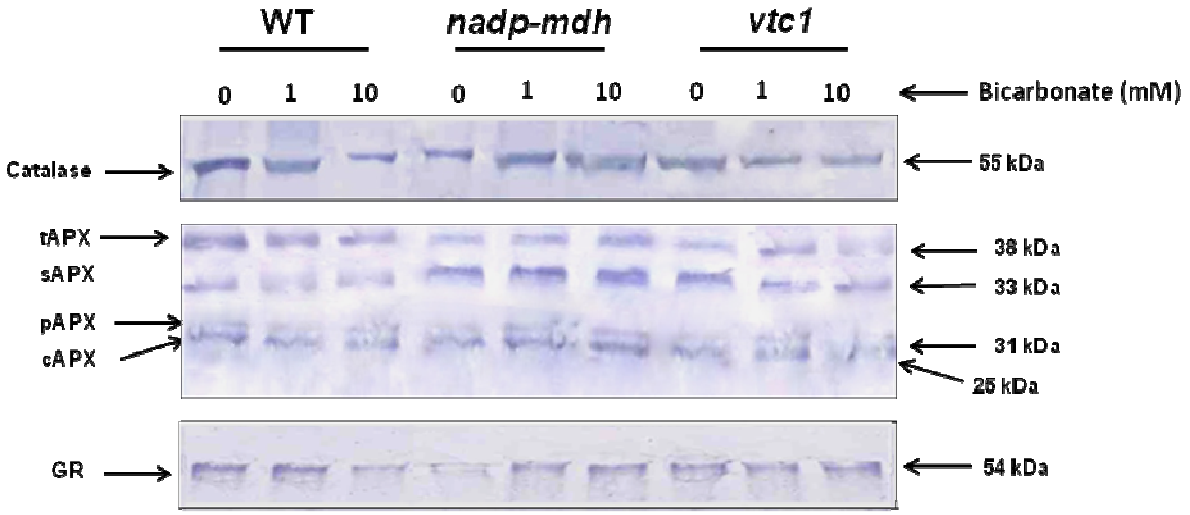

Figure 7.4. Effect of bicarbonate on protein levels of CAT, sAPX, tAPX, peroxisomal APX, cAPX and GR in mesophyll cell protoplasts of WT, *nadp-mdh* and *vtc1* mutants of *Arabidopsis thaliana* after incubation with 5 min dark and 10 min light (700 µE m^{-2} s^{-1}) exposure.

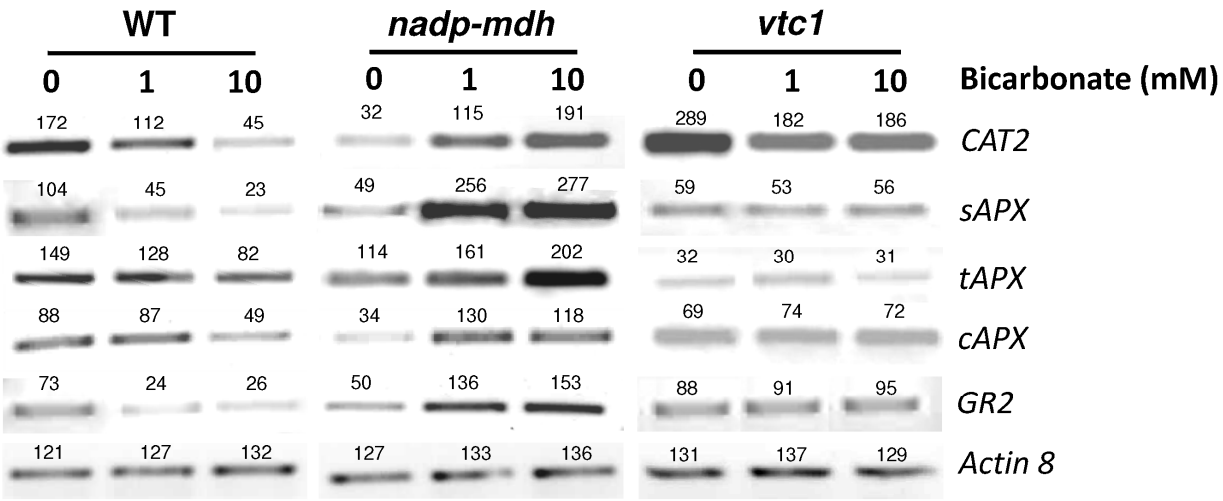

Figure 7.5. Effect of bicarbonate on gene expression of *CAT2, sAPX, tAPX, cAPX* and *GR2* in mesophyll cell protoplasts of WT, *nadp-mdh* and *vtc1* mutants of *Arabidopsis thaliana* after incubation with 5 min dark and 10 min light (700 µE m^{-2} s^{-1}) exposure. *ACTIN 8* was used as a loading control. Relative band intensities are indicated by the numbers on top of each band.

DISCUSSION

Photosynthesis was inhibited in *nadp-mdh* and remained low in *vtc1* mutants at supraoptimal bicarbonate

Studies on plants grown under elevated CO_2 concentrations revealed that, after an initial stimulation of photosynthetic rates, the carboxylation capacity of plants stabilizes at lower levels after long-term exposure (Ainsworth et al., 2007; Aranjuelo et al., 2008). The plants appear to suffer from oxidative stress at high CO_2 levels and exhibit enhanced protein carbonylation, loss of leaf chlorophyll and decrease of leaf photosynthetic rate (Qiu et al., 2008). In our experiments too, the high bicarbonate levels inhibited the photosynthetic performance in WT and *nadp-mdh* mutants (Figure 7.1).

At high CO_2 conditions, there would be higher requirement of NADPH so as to drive CO_2 assimilation process. As per the suggestions of Scheibe et al. (2005), NADP-MDH plays a key role in recycling NADPH, especially when the production of reducing equivalents was in excess than required for the photosynthetic CO_2 assimilation. In *nadp-mdh* mutants, the photorespiratory pathway may play a compensatory role in protecting plants, by dissipating the excess reducing equivalents (Hebbelmann et al., 2012). Even *aox1a* mutant exhibited reduced state of the chloroplasts and excitation pressure under high CO_2, suggesting a need for increased Mal–OAA shuttle activity compared to WT (Gandin et al., 2012).

Our data indicate that, supraoptimal levels of bicarbonate led to the decrease in the photosynthetic rates of *nadp-mdh* mutants. Such decrease may be due to the disturbance in the *nadp-mdh*-based mechanism of dissipating excess reducing equivalents and subsequent oxidative stress (Figure 7.1). The combined effect of suppressed malate valve and restricted photorespiration might be a cause for accumulation of excess reducing equivalents in *nadp-mdh* mutants. In contrast, *vtc1* mutant exhibited undisturbed photosynthetic rates on exposure to elevated bicarbonate levels (Figure 7.1). We suggest that the restriction of photorespiration

may possibly benefit the *vtc1* mutant as it was deficient of AsA which was a major ROS scavenging antioxidant to minimize the photorespiratory H_2O_2.

Low response of antioxidants towards supraoptimal bicarbonate in *nadp-mdh* and *vtc1* mutants

The levels of antioxidants are usually enhanced under oxidative stress conditions. However, the total content and redox ratios of AsA or GSH were not much changed in response to high bicarbonate levels in both *nadp-mdh* and *vtc1* mutants (Figure 7.2A, B and Figure 7.3A, B). Marginal decrease in the total GSH contents and their redox ratios at elevated CO_2 in *nadp-mdh* may be due to suppression of the photorespiratory carbon cycle, which helps in the synthesis of glutathione, by reduced availability of serine and glycine and then glutathione (Noctor et al., 1999; Foyer and Noctor, 2000).

Activities of APX, GR and CAT enzymes enhanced in *nadp-mdh* and unchanged in *vtc1* mutants at supraoptimal bicarbonate levels

The upregulation in the activities of antioxidant defense systems in plants is common under oxidative stress conditions, including even the elevated CO_2 (Qiu et al., 2008). In the present study also, at supraoptimal bicarbonate, the *nadp-mdh* mutants exhibited enhanced APX, GR and CAT enzyme activities, protein levels and gene expression (Table 7.1; Figure 7.4 & 7.5). Such enhanced activities of antioxidant enzymes in *nadp-mdh* mutants signify the need for antioxidant systems to protect plants against oxidative stress caused by high bicarbonate. No significant change in APX, GR and CAT activities towards high bicarbonate in *vtc1* mutants signifies that these mutants exhibit the least response to oxidative stress.

Plants grown under elevated CO_2 concentrations exhibited lower activities of superoxide dismutase or catalase than from plants grown under ambient CO_2 concentrations (Schwanz et al., 1996; Queval et al., 2007). In our results too, at supraoptimal bicarbonate,

the activities, protein levels and gene expression of APX, GR and CAT enzymes decreased in WT plants.

Conclusions:

1. Supraoptimal bicarbonate levels decreased the photosynthetic performance of mesophyll protoplasts of WT and *nadp-mdh* mutants, indicating that high bicarbonate levels may cause some kind of stress in WT and *nadp-mdh* due to accumulation. This could be, for example, due to imbalance in reducing equivalents in chloroplasts.
2. High bicarbonate levels elevated the antioxidant enzymes in *nadp-mdh* mutants compared to WT and *vtc1* mutants suggesting adjust severity of oxidative stress and the importance of malate valve in exporting excess reducing equivalents.
3. The *vtc1* mutants had already low rates of photosynthesis and were not affected by oxidative stress caused by bicarbonate. The patterns of antioxidant enzyme activities also did not exhibited much change in this mutant.
4. The decreased expression of catalase suggests that at high bicarbonate in *vtc1* mutant may be due to the restriction of photorespiration.

****

Chapter 8

General Discussion and Conclusions

Chapter 8

General Discussion and Conclusions

When plants are exposed to varying environmental conditions in nature, there is often a disturbance in their cellular redox balance. To maintain redox homeostasis, a delicate metabolic equilibrium operates between the key compartments within plant cells including chloroplasts, mitochondria and cytosol. This helps in optimizing photosynthesis as well as protection against oxidative stress. A major factor in metabolic equilibrium between intracellular organelles is the exchange of several metabolites. Besides metabolites, ascorbate (AsA), nitric oxide and the cytosolic pH may also serve as signals (Raghavendra and Padmasree, 2003; Noguchi and Yoshida, 2008; Nunes-Nesi et al., 2008). Adjustments in extra-chloroplastic components such as malate valve, photorespiration and alternative oxidase (AOX) pathway also help in optimizing the photosynthesis (Wingler et al., 2000; Gardeström et al., 2002; Scheibe, 2004; Yoshida and Noguchi, 2010). Despite their expected importance, the detailed roles of several of these components have not been studied.

In the present study, we aimed at elucidating the role of AsA, malate valve, photorespiration and AOX in optimizing photosynthesis under oxidative stress conditions. We employed leaf discs or mesophyll protoplasts from mutants of *Arabidopsis thaliana* deficient in crucial redox components: *vtc1,* deficient in AsA; *nadp-mdh,* lacking NADP-malate dehydrogenase, a crucial enzyme of malate valve and *aox1a,* lacking the leaf form of AOX1a.

Role of AsA during interorganelle interaction in optimizing photosynthesis against photoinhibition in wild type and AsA-deficient mutants of *Arabidopsis thaliana*

In the first part of study, we investigated the possible role of L-ascorbate (AsA) as a key component during the interorganelle interaction in leaf discs of *Arabidopsis thaliana*,

particularly between mitochondria and chloroplasts. The leaf discs of *vtc1* mutants when exposed to mitochondrial respiratory inhibitors, exhibited enhanced sensitivity of photosynthesis particularly at high light (HL). The effect of SHAM was more pronounced than that of antimycin A (Figure 4.4A). These results support the previous findings in which the AsA-deficient plants are hypersensitive to photoinhibition and oxidative damage (Müller-Moulé et al., 2003, 2004). The AOX pathway has been suggested to help in photoprotection of *Arabidopsis thaliana* leaves (Bartoli et al., 2006).

The AOX pathway capacity was high in *vtc1* mutants compared to WT, even in normal conditions (Figure 4.2A). This might be due to severe oxidative stress in *vtc1* mutants, due to deficiency in AsA. Our findings complement the observations of Yoshida et al. (2007) and Bartoli et al. (2005), that the AOX capacity increases, when ROS levels are high. In *vtc1* mutants, the total AsA levels were stimulated in presence of antimycin A or SHAM (Figure 4.3A, B). This stimulation in total AsA signifies the attempt by the cell to counter the oxidative stress, as a consequence of inhibition of mitochondrial electron transport. Besides the increased levels of AsA, the redox status of AsA could also be crucial in mediating the crosstalk between mitochondria and chloroplasts and thus protecting photosynthesis from photoinhibition.

Our data indicate that the levels and redox state of AsA could modify the pattern of modulation of photosynthesis by mitochondrial metabolism. The role of AsA becomes more pronounced at HL, when the AOX pathway is inhibited. While not ignoring the importance of the COX pathway, we hypothesize that AsA and the AOX pathway may complement each other to protect photosynthesis against photoinhibition. The role of AOX pathway in redox signaling has been pointed out (Nunes-Nesi et al., 2005; Vidal et al., 2007).

Effect of high light on ROS-levels and antioxidant enzymes in three mutants of *Arabidopsis* (*nadp-mdh*, *vtc1* and *aox1a* mutants)

In the second part of study, we evaluated the response of three Arabidopsis mutants: *nadp-mdh* or *vtc1* or *aox1a* mutants to HL conditions. Photosynthesis, on exposure to HL, was quite susceptible in *vtc1* or *aox1a* mutants, while photosynthesis in *nadp-mdh* mutant was sustained (Figure 5.1). Our results are similar to observations of Müller-Moulé et al. (2004) and Zhang et al. (2010) who found that, *vtc1* or *aox1a* mutants are quite sensitive to photoinhibition. The *vtc1* or *aox1a* mutants on exposure to HL led to accumulation of ROS (Figure 5.2) and enhanced activities of APX, GR and catalase (Table 5.1), while the *nadp-mdh* mutants kept up the levels of ROS low, with no significant change in APX or GR activity, even at HL. Laisk et al. (2007) suggested that plants with low amounts of NADP-MDH could sustain photosynthesis possibly due to utilization of energy-dissipating cycles at PSI and PSII.

Accumulation of free proline (Table 5.2) and upregulation of Δ*P5CS1,* were noticeable, especially in *nadp-mdh* mutants at HL (Figure 5.7). Increase in proline appears to be one of the strategies for protection of plant against photo-oxidative stress in *nadp-mdh* mutants (Hebbelmann et al., 2012). Osmotic stress often results in induction of transcript levels of proline biosynthetic genes (Verbruggen and Hermans, 2008; Szabados and Savouré, 2009). There were suggestions that proline can be an efficient redox buffer (Hare and Cress, 1997; Moustakas et al., 2011) and this must be the basis of proline increase in stress.

Our findings reveal that, exposure to HL led to marked inhibition of photosynthesis and the enhanced response of antioxidant defense systems in *vtc1* or *aox1a* mutants, while *nadp-mdh* mutants exhibited sustained photosynthesis and least response of antioxidant defense systems. This implies that antioxidant defense mechanisms are not robust enough to

keep ROS levels low in *vtc1* or *aox1a* mutants and the AsA-glutathione cycle related enzymes do not play a major role in redox balance in *nadp-mdh* mutants. We conclude that, the *vtc1* or *aox1a* mutants are unable to adapt due to insufficient protective mechanisms to combat against photo-oxidative stress and thus are highly susceptible. The *nadp-mdh* mutants are tolerant, due to operation of efficient alternative protective mechanisms.

Importance of photorespiration and AOX in *nadp-mdh* mutants

In the third part of our study, we examined the photosynthetic performance and antioxidant defense systems in mesophyll cell protoplasts of *nadp-mdh* mutants under restricted conditions of photorespiration and mitochondrial respiratory electron transport system. The inhibition of photosynthetic rates (Figure 6.1 and Table 6.1) and enhanced activities of APX, GR and catalase enzymes in *nadp-mdh* mutants (Table 6.2 to 6.4), upon exposure to low O_2, photorespiratory inhibitors and AOX pathway inhibitor, suggest that there was a high flexibility of antioxidant defense systems to minimize oxidative stress.

Photorespiration and malate valve help in preventing the over-reduction of the photosynthetic electron transport chain and photoinhibition thus serving as efficient dissipatory mechanisms of excess reducing equivalents from the chloroplast (Wingler et al., 2000; Scheibe, 2004; Wilhelm and Selmar, 2011). We assume that restriction of photorespiration may lead to oxidative stress in plants. Inhibition of AOX pathway, would lead to susceptibility of plant to oxidative stress due to failure of dissipating the excess reducing equivalents from chloroplasts (Yoshida et al., 2007; Strodtkötter et al., 2009; Talla et al., 2011).

Effects of supraoptimal bicarbonate in *nadp-mdh* and *vtc1* mutants of *Arabidopsis*

In last part of study, we examined the response of *nadp-mdh* or *vtc1* mutants, to supra-optimal bicarbonate (elevated CO_2 was mimicked by using 10 mM bicarbonate). Photosynthesis and the carboxylation capacity in plants grown under elevated CO_2

concentrations were stimulated initially but decreased during long-term exposure (Ainsworth et al., 2007; Aranjuelo et al., 2008). High CO_2 levels can induce oxidative stress in plants and show up protein carbonylation of leaf proteins (Qiu et al., 2008). In our experiments too, the high bicarbonate levels inhibited the photosynthetic performance in WT and *nadp-mdh* mutants, without disturbing the photosynthetic rates of *vtc1* mutants which remain low (Figure 7.1).

The decreased photosynthesis in *nadp-mdh* mutants may be due to their inability to dissipate excess reducing equivalents in chloroplasts, leading to oxidative stress (Figure 7.1). The combined effect of suppressed malate valve and restricted photorespiration might be a cause for accumulation of excess reducing equivalents in *nadp-mdh* mutants. The upregulation in the activities of antioxidant defense systems under oxidative stress conditions is well known (Gill and Tuteja, 2010; Foyer and Shigeoka, 2011). In our study, the *nadp-mdh* mutants had enhanced enzyme activities, protein levels and gene expression of APX, GR and CAT (Table 7.1; Figure 7.4 & Figure 7.5) at supraoptimal bicarbonate. Such enhanced responses of antioxidant enzymes in *nadp-mdh* mutant emphasize the requirement of antioxidant defense systems, to protect plants even under high bicarbonate.

No significant change in photosynthesis and APX, GR and catalase activities (Figure 7.1 and Table 7.1) towards high bicarbonate in *vtc1* mutants suggests that this mutant is unable to respond to oxidative stress. Our experiments emphasize that the *nadp-mdh* mutants are more sensitive to supra-optimal bicarbonate than the *vtc1* mutant.

Varied response of *nadp-mdh* or *vtc1* or *aox1a* mutants towards stress conditions:

The responses of three mutants employed in this study, varied depending on the cellular site of stress. The *nadp-mdh* mutant lacking NADP-MDH enzyme, a crucial enzyme of malate valve localized in chloroplast exhibited tolerance on exposure to HL stress, while exhibited sensitivity to supraoptimal bicarbonate levels. The *vtc1* mutant carrying altered

function of AsA biosynthesis localized mainly in cytosol and mitochondria exhibited high sensitivity to HL stress and exhibited least response to supraoptimal bicarbonate levels. The *aox1a* mutant lacking AOX1a which was localized in mitochondria exhibited high sensitivity to HL stress.

On exposure to HL, the *nadp-mdh* mutants had adjustments in extra-chloroplastic components, involving photorespiration and proline, which all help in dissipating the excess reducing equivalents in chloroplasts. The reduction in photosynthetic rates of *nadp-mdh* at supra-optimal bicarbonate might be due to the restriction of photorespiration, as photorespiration was a major protection mechanism in *nadp-mdh* mutants. The photorespiratory pathway was mainly localized in peroxisomes. The varied responses of mutants towards stress conditions, such as HL or supra-optimal bicarbonate, suggest that leaves employ multiple modes of adaptation, which may involve all cellular compartments, namely chloroplasts, mitochondria, peroxisomes and cytosol.

The following conclusions can be derived from the present study.

1. Ascorbate is a key player in the inter-organelle interaction and may complement AOX in optimizing photosynthesis against photoinhibition.
2. The enhanced activities of antioxidant enzymes are not sufficient enough to combat against photo-oxidative stress in *vtc1* and *aox1a* while efficient additional protective mechanisms operate in *nadp-mdh* mutants.
3. The antioxidant defense systems become quite pronounced in terms of enzyme activity, protein levels and transcription of antioxidant enzymes on restriction of malate valve or photorespiration or alternative oxidase pathway.
4. The oxidative stress caused by supra-optimal bicarbonate leads to the enhanced antioxidant activities in *nadp-mdh* mutants, while no significant changes occur in

antioxidant activities in *vtc1* mutants; all implying that *vtc1* mutant is unable to respond the oxidative stress caused by high bicarbonate.

5. The three mutants used in this study exhibited varied responses to stresses such as HL or supra-optimal bicarbonate, suggesting that leaves employ multiple modes of adaptation, which may involve all cellular compartments, namely chloroplasts, mitochondria, peroxisomes and cytosol.

****

Chapter 9

Literature Cited

Chapter 9

Literature Cited

Ahn JH (2002) Noncompetitive RT-PCR. In: Arabidopsis: A Laboratory Manual. Weigel D, Glazebrook J (Eds.) Cold Spring Harbor Laboratory Press, NY, pp. 174–176

Ainsworth EA, Rogers A (2007) The response of photosynthesis and stomatal conductance to rising [CO_2]: mechanisms and environmental interactions. Plant Cell Environ **30:** 258-270

Alhagdow M, Mounet F, Gilbert L, Nunes-Nesi A, Garcia V, Just D, Petit J, Beauvoit B, Fernie AR, Rothan C, Baldet P (2007) Silencing of the mitochondrial ascorbate synthesizing enzyme L-galactono-1,4-lactone dehydrogenase affects plant and fruit development in tomato. Plant Physiol **145:** 1408–1422

Ali MB, Eun-Joo Hahn EJ, Paek KY (2005) Effects of temperature on oxidative stress defense systems, lipid peroxidation and lipoxygenase activity in *Phalaenopsis.* Plant Physiol Biochem **43:** 213–223

An CI, Sawada A, Fukusaki E, Kobayashi A (2003) A transient RNA interference assay system using *Arabidopsis* protoplasts. Biosci Biotechnol Biochem **67:** 2674–2677

Aono M, Kubo A, Saji H, Tanaka K, Kondo N (1993) Enhanced tolerance to photooxidative stress of transgenic *Nicotiana tabacum* with high chloroplastic glutathione reductase activity. Plant Cell Physiol **34:** 129–135

Aranjuelo I, Erice G, Nogués S, Morales F, Irigoyen JJ, Sánchez-Díaz M (2008) The mechanism(s) involved in the photoprotection of PSII at elevated CO_2 in nodulated alfalfa plants. Environ Exp Bot **64:** 295–306

Arnon DI (1949) Copper enzymes in isolated chloroplasts. Polyphenol oxidase in *Beta vulgaris*. Plant Physiol **24:** 1-15

Asada K (2006) Production and scavenging of reactive oxygen species in chloroplasts and their functions. Plant Physiol **141:** 391–396

Bartoli CG, Gomez F, Gergoff G, Guiamét JJ, Puntarulo S (2005b) Up-regulation of the mitochondrial alternative oxidase pathway enhances photosynthetic electron transport under drought conditions. J Exp Bot **56:** 1269–1276

Bartoli CG, Guiamet JJ, Kiddle G, Pastori GM, Di Cagno R, Theodoulou FL, Foyer CH (2005a) Ascorbate content of wheat leaves is not determined by maximal L-galactono-1, 4-lactone dehydrogenase (GalLDH) activity under drought stress. Plant Cell Environ **28:** 1073–1081

Bartoli CG, Pastori GM, Foyer CH (2000) Ascorbate biosynthesis in mitochondria is linked to the electron transport chain between complexes III and IV. Plant Physiol **23:** 335-343

Bartoli CG, Yu JB, Gomez F, Fernandez L, McIntosh L, Foyer CH (2006) Inter-relationship between light and respiration in the control of ascorbic acid synthesis and accumulation in *Arabidopsis thaliana* leaves. J Exp Bot **57:** 1621-1631

Bauwe H, Hagemann M, Fernie AR (2010) Photorespiration: players, partners and origin. Trends Plant Sci **15:** 330-336

Becker B, Holtgrefe S, Jung S, Wunrau C, Kandlbinder A, Baier M, Dietz KJ, Backhausen JE, Scheibe R (2006) Influence of the photoperiod on redox regulation and stress responses in *Arabidopsis thaliana* L. (Heynh.) plants under long- and short-day conditions. Planta **224:** 380–393

Chang CCC, Ball L, Fryer MJ, Baker NR, Karpinski S, Mullineaux PM (2004) Induction of ascorbate peroxidase 2 expression in wounded *Arabidopsis* leaves does not involve known wound-signalling pathways but is associated with changes in photosynthesis. Plant J **38:** 499–511

Chen C, Dickman MB (2005) Proline suppresses apoptosis in the fungal pathogen *Colletotrichum trifolii*. Proc Natl Acad Sci **102:** 3459-3464

Chen X , Li W , Lu Q, Wen X, Li H, Kuang T, Li Z , Lu C (2011) The xanthophyll cycle and antioxidative defense system are enhanced in the wheat hybrid subjected to high light stress. J Plant Physiol **168:** 1828– 1836

Chomczynski P, Sacchi N (1987) Single-step method of RNA isolation by acid guanidinium thiocyanate phenol chloroform extraction. Anal Biochem **162:** 156–159

Conklin P, Norris SR, Wheeler GL, Williams EH, Smirnoff N, Last RL (1999) Genetic evidence for the role of GDP-mannose in plant ascorbic acid (vitamin C) biosynthesis. Proc Natl Acad Sci USA **96:** 4198-4203

Cornic G, Bukhov NG, Wiese C, Bligny R, Heber U (2000) Flexible coupling between light-dependent electron and vectorial proton transport in illuminated leaves of C3 plants. Role of photosystem I-dependent proton pumping. Planta **210:** 468–477

Corpas FJ, Palma JM, Sandalio LM, Valderrama R, Barroso JB, del Río LA (2008) Peroxisomal xanthine oxidoreductase: characterization of the enzyme from pea (*Pisum sativum* L.) leaves. J Plant Physiol **165:** 1319–1330

Créach E, Stewart CR (1982) Effects of aminoacetonitrile on net photosynthesis, ribulose-1,5-bisphosphate levels, and glycolate pathway intermediates. Plant Physiol **70:** 1444 1448

Creissen GP, Broadbent P, Kular B, Reynolds H, Wellburn AR, Mullineaux PM (1994) Manipulation of glutathione reductase in transgenic plants: Implications for plant responses to environmental stress. Proc R Soc Edinb **102:** 167-175

De Gara L, Locato V, Dipierro S, de Pinto MC (2010) Redox homeostasis in plants. The challenge of living with endogenous oxygen production. Resp Physiol Neurobiol **173:** 13–19

Edwards EA, Rawsthorne S, Mullineaux PM (1990) Subcellular distribution of multiple forms of glutathione reductase in leaves of pea (*Pisum sativum* L.). Planta **180:** 278-284

Endo T, Shikanai T, Sato F, Asada K (1998) NAD(P)H dehydrogenase dependent, antimycin A-sensitive electron donation to plastoquinone in tobacco chloroplasts. Plant Cell Physiol **39:** 1226–1231

Fabro G, Kovács I, Pavet V, Szabados L, Alvarez ME (2004) Proline accumulation and AtP5CS2 gene activation are induced by plant-pathogen incompatible interactions in *Arabidopsis*. Mol Plant Microbe Interact **17:** 343–350

Fernandez-García N, Martí MC, Jimenez A, Sevilla F, Olmos E (2009) Sub-cellular distribution of glutathione in an *Arabidopsis* mutant (*vtc1*) deficient in ascorbate. J Plant Physiol **166:** 2004-2012

Foyer CH, Bloom AJ, Queval G Noctor G (2009) Photorespiratory metabolism: genes, mutants, energetics, and redox signaling. Annu Rev Plant Biol **60:** 455–484

Foyer CH, Noctor G (2000) Oxygen processing in photosynthesis: regulation and signaling. New Phytol **146:** 359–388

Foyer CH, Noctor G (2003) Redox sensing and signalling associated with reactive oxygen in chloroplasts, peroxisomes and mitochondria. Physiol Plant **119:** 355-364

Foyer CH, Noctor G (2009) Redox regulation in photosynthetic organisms: Signaling, acclimation, and practical implications. Antioxid Redox Signal **11:** 861-913

Foyer CH, Noctor G (2011) Ascorbate and glutathione: the heart of the redox hub. Plant Physiol **155:** 2–18

Foyer CH, Shigeoka S (2011) Understanding oxidative stress and antioxidant functions to enhance photosynthesis: Update on oxidative stress and photosynthesis. Plant Physiol **155:** 93–100

Foyer CH, Rowell J, Walker D (1983) Measurement of the ascorbate content of spinach leaf protoplasts and chloroplasts during illumination. Planta **157:** 239-244

Galvez-Valdivieso G, Mullineaux PM (2010) The role of reactive oxygen species in signalling from chloroplasts to the nucleus. Physiol Plant **138:** 430–439

Gandin A, Duffes C, Day DA, Cousins AB (2012) The absence of alternative oxidase AOX1A results in altered response of photosynthetic carbon assimilation to increasing CO_2 in *Arabidopsis thaliana*. Plant Cell Physiol **53:** 1627–1637

Gao Q, Zhang L (2008) Ultraviolet-B-induced oxidative stress and antioxidant defense system responses in ascorbate deficient *vtc1* mutants of *Arabidopsis thaliana*. J Plant Physiol **165:** 138–148

Gardeström P, Igamberdiev AU, Raghavendra AS (2002) Mitochondrial functions in light and significance to carbon–nitrogen interactions. In: Advances in Photosynthesis and Respiration: Photosynthetic nitrogen assimilation and associated carbon metabolism, Vol. **12**. Foyer CH, Noctor G (Eds.) Kluwer Acad Pub, The Netherlands, pp. 151-172

Gatzek S, Wheeler GL, Smirnoff N (2002) Antisense suppression of L-galactose dehydrogenase in *Arabidopsis thaliana* provides evidence for its role in ascorbate synthesis and reveals light modulated L-galactose synthesis. The Plant J **30:** 541-553

Giacomelli L, Masi A, Ripoll RLee M, Wijk KJ (2007) *Arabidopsis thaliana* deficient in two chloroplast ascorbate peroxidases shows accelerated light induced necrosis when levels of cellular ascorbate are low. Plant Mol Biol **165:** 627–644

Gill SS, Tuteja N (2010) Reactive oxygen species and antioxidant machinery in abiotic stress tolerance in crop plants. Plant Physiol Biochem **48:** 909-930

Gillespie KM, Rogers A, Ainsworth EA (2011) Growth at elevated ozone or elevated carbon dioxide concentration alters antioxidant capacity and response to acute oxidative stress in soybean (*Glycine max*). J Exp Bot **62:** 2667–2678

Griffith OW (1980) Determination of glutathione and glutathione disulfide using glutathione reductase and 2-vinyl-pyridine. Anal Biochem **106:** 207-212

Guy RD, Vanlerberghe GC (2005) Partitioning of respiratory electrons in the dark in leaves of transgenic tobacco with modified levels of alternative oxidase. Physiol Plant **125:** 171–180

Halliwell B (2006) Reactive species and antioxidants. Redox biology is a fundamental theme of aerobic life. Plant Physiol **141:** 312-322

Halliwell B, Foyer CH (1976) Ascorbic acid, metal ions and the superoxide radical. Biochem J **155:** 697–700

Han RM, Zhang JP, Skibsted LH (2012) Reaction dynamics of flavonoids and carotenoids as antioxidants. Molecules **17:** 2140-2160

Hare PD, Cress WA (1997) Metabolic implications of stress-induced proline accumulation in plants. Plant Growth Regul **21:** 79–102

Hebbelmann I, Selinski J, Wehmeyer C, Goss T, Voss I, Mulo P, Kangasjarvi S, Aro EM, Oelze ML, Dietz KJ, Nunes-Nesi A, Phuc TD, Fernie AR, Talla SK, Raghavendra AS, Linke V, Scheibe R (2012) Multiple strategies to prevent oxidative stress in *Arabidopsis* plants lacking the malate valve enzyme NADP-malate dehydrogenase. J Exp Bot **63 (3):** 1445-1459

Hernández JA, Escobar C, Creissen G, Mullineaux PM (2006) Antioxidant enzyme induction in pea plants under high irradiance. Biol Plant **50:** 395-399

Hernández JA, Ferrer MA, Jiménez A, Barceló AR, Sevilla F (2001) Antioxidant systems and $O_2^{\cdot-}/H_2O_2$ production in the apoplast of pea leaves. Its relation with salt-induced necrotic lesions in minor veins. Plant Physiol **127:** 817–831

Huang C, He W, Guo J, Chang, X, Su P, Zhang L (2005) Increased sensitivity to salt stress in an ascorbate-deficient *Arabidopsis* mutant. J Exp Bot **422:** 3041–3049

Igamberdiev AU, Bykova NV, Lea PJ, Gardeström P (2001) The role of pho-torespiration in redox and energy balance of photosynthetic plant cells: a study with a barley mutant deficient in glycine decarboxylase. Physiol Plant **111:** 427–438

Ishikawa T, Shigeoka S (2008) Recent advances in ascorbate biosynthesis and the physiological significance of ascorbate peroxidase in photosynthesizing organisms. Biosci Biotechnol Biochem **72:** 1143–1154

Jiang M, Zhang J (2001) Effect of abscissic acid on active oxygen species, antioxidative defense system and oxidative damage in leaves of maize seedlings. Plant Cell Physiol **42:** 1265-1273

Kangasjärvi S, Lepistö A, Hännikäinen K, Piippo M, Luomala EM, Aro EM, Rintamäki E (2008) Diverse roles for chloroplast stromal and thylakoid-bound ascorbate peroxidases in plant stress responses. Biochem J **412:** 275–285

Karpinski S, Escobar C, Karprinska B, Creissen G, Mullineaux PM (1997) Photosynthetic electron transport regulates the expression of cytosolic ascorbate peroxidase genes in *Arabidopsis* during excess light stress. Plant Cell **9:** 627–640

Khan TA, Mazid M, Mohammad F (2011) A review of ascorbic acid potentialities against oxidative stress induced in plants. J Agrobiol **28:** 97–111

Klotz KL, Finger FL, Anderson MD (2008) Respiration in postharvest sugarbeet roots is not limited by respiratory capacity or adenylates. J Plant Physiol **165:** 1500-1510

Kolla VA, Vavasseur A, Raghavendra AS (2006) Hydrogen peroxide production is an early event during bicarbonate induced stomatal closure in abaxial epidermis of *Arabidopsis*. Planta **225:** 1421–1429

Koornneef M, Meinke D (2010) The development of *Arabidopsis* as a model plant. Plant J **61:** 909–921

Laemmli UK (1970) Cleavage of structural proteins during the assembly of the head of bacteriophage T4. Nature **227:** 680-685

Laisk A, Eichelmann H, Oja V, Talts E, Scheibe R (2007) Rates and roles of cyclic and alternative electron flow in leaves. Plant Cell Physiol **48:** 1575–1588

Lawyer AL, Zelitch I (1979) Inhibition of glycine decarboxylation and serine formation in tobacco by glycine hydroxamate and its effect on photorespiratory carbon flow. Plant Physiol **64:** 706-11

Li JF, Bush J, Xiong Y, Li L, McCormack M (2012) Large-scale protein-protein interaction analysis in *Arabidopsis* mesophyll protoplasts by split firefly luciferase complementation. PLoS One **6:** e27364.

Li Y, Zhou Y, Wang Z, Sun X, Tang K (2010) Engineering tocopherol biosynthetic pathway in *Arabidopsis* leaves and its effect on antioxidant metabolism. Plant Sci **178:** 312–320

Li Z, Wakao S, Fischer BB, Niyogi KK (2009) Sensing and responding to excess light. Annu Rev Plant Biol **60:** 239–60

Linster CL, **Clarke SG (2008)** L-Ascorbate biosynthesis in higher plants: The role of VTC2. Trends Plant Sci **13:** 567–573

Lowry OH, Rosebrough NJ, Farr AL, Randall RJ (1951) Protein measurement with the folin phenol reagent. J Biol Chem **193:** 265-275

Lu P, Sang WG, Ma KP (2008) Differential responses of the activities of antioxidant enzymes to thermal stresses between two invasive *Eupatorium* Species in China. J Integr Plant Biol **50:** 393-401

Mano J, Hideg E, Asada K (2004) Ascorbate in thylakoid lumen functions as an alternative electron donar to photosystem II and I. Arch Biochem Biophys **429:** 71-80

Maruta T, Tanouchi A, Tamoi M, Yabuta Y, Yoshimura K, Ishikawa T, Shigeoka S (2010) *Arabidopsis* chloroplastic ascorbate peroxidase isoenzymes play a dual role in photoprotection and gene regulation under photooxidative stress. Plant Cell Physiol **51:** 190–200

Maxwell DP, Wang Y, Lee MI (1999) The alternative oxidase lowers mitochondrial reactive oxygen production in plant cells. Proc Natl Acad Sci **96:** 8271-8276

Mhamdi A, Queval G, Chaouch S, Vanderauwera S, Van Breusegem F, Noctor G (2010) Catalase function in plants: A focus on *Arabidopsis* mutants as stress-mimic models. J Exp Bot **61:** 4197–4220

Millar AH, Mittova V, Kiddle G, Heazlewood JL, Bartoli CG, Theodoulou FL, Foyer CH (2003) Control of ascorbate synthesis by respiration and its implications for stress responses. Plant Physiol **133:** 443-447

Mittler R, Vanderauwera S, Gollery M, Breusegem FV (2004) Reactive oxygen gene network of plants. Trends Plant Sci **9:** 490-498

Moller I M, Bkrczi A, Linus HW, Plas V, Lambers H (1988) Measurement of the activity and capacity of the alternative pathway in intact plant tissues: Identification of problems and possible solutions. Physiol Plant **72:** 642-454

Moustakas M, Sperdouli I, Kouna T, Antonopoulou CI, Therios I (2011) Exogenous proline induces soluble sugar accumulation and alleviates drought stress effects on photosystem II functioning of *Arabidopsis thaliana* leaves. Plant Growth Regul **65:** 315–25

Müller-Moulé P, Golan T, Niyogi KK (2004) Ascorbate deficient mutants of *Arabidopsis* grow in high light despite chronic photoxidative stress. Plant Physiol **134**: 1163-1172

Müller-Moulé P, Havaux M, Niyogi KK (2003) Zeaxanthin deficiency enhances the high light sensitivity of an ascorbate-deficient mutant of *Arabidopsis*. Plant Physiol **133:** 748-760

Mullineaux P, Ball L, Escobar C, Karpinska B, Creissen G, Karpinski S (2000) Are diverse signalling pathways integrated in the regulation of *Arabidopsis* antioxidant defence gene expression in response to excess excitation energy? Phil Trans R Soc Lond Biol **355:** 1531-1540

Mullineaux PM, Rausch T (2005) Glutathione, photosynthesis and the redox regulation of stress-responsive gene expression. Photosynth Res **86:** 459–474

Murchie EH, Niyogi KK (2011) Manipulation of photoprotection to improve plant photosynthesis. Plant Physiol **155:** 86–92

Nakano Y, Asada K (1981) Hydrogen peroxide is scavenged by Ascorbate-specific peroxidase in spinach chloroplasts. Plant Cell Physiol **22:** 867-880

Noctor G, Arisi CM, Jouanin L, Foyer CH (1999) Photorespiratory glycine enhances glutathione accumulation in both the chloroplastic and cytosolic compartments. J Exp Bot **50:** 1157–1167

Noctor G, De Paepe R, Foyer CH (2007) Mitochondrial redox biology and homeostasis in plants. Trends Plant Sci **12:** 125-134

Noctor G, Foyer CH (1998) Ascorbate and glutathione: keeping active oxygen under control. Annu Rev Plant Physiol Plant Mol Biol **49:** 249–279

Noguchi K, Yoshida K (2008) Interaction between photosynthesis and respiration in illuminated leaves. Mitochon **8:** 87–99

Nunes-Nesi A, Carrari F, Lytovchenko A, Smith AMO, Loureiro ME, Ratcliffe RG, Sweetlove LJ, Fernie AR (2005) Enhanced photosynthetic performance and growth

as a consequence of decreasing mitochondrial malate dehydrogenase activity in transgenic tomato plants. Plant Physiol **137**: 611–622

Nunes-Nesi A, Sulpice RR, Gibon Y, Fernie AR (2008) The enigmatic contribution of mitochondrial function in photosynthesis. J Exp Bot **59:** 1675-1684

Oelze ML, Kandlbinder A, Dietz KJ (2008) Redox regulation and over-reduction control in the photosynthesizing cell: Complexity in redox regulatory networks. Biochim Biophy Acta **1780:** 1261–1272

Oelze ML, Vogel MO, Alsharafa K, Kahmann U, Viehhauser A, Maurino VG, Dietz KJ (2012) Efficient acclimation of the chloroplast antioxidant defence of Arabidopsis thaliana leaves in response to a 10-or 100-fold light increment and the possible involvement of retrograde signals. J Exp Bot **63:** 1297–1313

Padmasree K, Padmavathi L, Raghavendra AS (2002) Essentiality of mitochondrial oxidative metabolism for photosynthesis: Optimization of carbon assimilation and protection against photoinbition. Crit Rev Biochem Mol Biol **37:** 71-119

Padmasree K, Raghavendra AS (1999) Response of photosynthetic carbon assimilation in mesophyll protoplasts to restriction on mitochondrial oxidative metabolism: metabolites related to the redox status and sucrose biosynthesis. Photosynth Res **62:** 231–239

Padmasree K, Raghavendra AS (2001) Restriction of mitochondrial oxidative metabolism leads to suppression of photosynthetic carbon assimilation but not of photochemical electron transport in pea mesophyll protoplasts. Curr Sci **81:** 680-684

Patterson BD, Payne LA, Chen Y, Graham D (1984) An inhibitor of catalase induced by cold chilling-sensitive plants. Plant Physiol **76:** 1014-1018

Pignocchi C, Foyer CH (2003) Apoplastic ascorbate metabolism and its role in the regulation of cell signalling. Curr Opin Plant Biol **6:** 379-389

Pineau B, Layoune O, Danon A, de Paepe R (2008) L-galactono-1, 4-lactone dehydrogenase is required for the accumulation of plant respiratory complex I. J Biol Chem **283:** 32500-32505

Pospíšil P (2012) Molecular mechanisms of production and scavenging of reactive oxygen species by photosystem II. Biochim Biophys Acta **1817:** 218-231

Qiu, QS, Huber JL, Booker FL, Jain V, Leakey ADB, Fiscus EL, Yau PM, Ort DR, Huber SC (2008) Increased protein carbonylation in leaves of Arabidopsis and soybean in response to elevated [CO_2]. Photosynth Res **97:** 155–166

Queval G, Issakidis-Bourguet E, Hoeberichts FA, Vandorpe M, Gakiere B, Vanacker H, Miginiac-Maslow M, Breusegem FV, Noctor G (2007) Conditional oxidative stress responses in the Arabidopsis photorespiratory mutant cat2 demonstrate that redox state is a key modulator of daylength-dependent gene expression, and define photoperiod as a crucial factor in the regulation of H_2O_2-induced cell death. The Plant J **52:** 640–657

Raghavendra AS, Padmasree K (2003) Beneficial interactions of mitochondrial metabolism with photosynthetic carbon assimilation. Trends Plant Sci **8:** 546-553

Rao ASVC, Reddy AR (2008) Glutathione reductase: A putative redox regulatory system in plant cells. In: Sulfur Assimilation and Abiotic Stresses in Plants, Vol. **10**. Khan NA, Singh S, Umar S (Eds.) Springer, The Netherlands, pp. 111-147

Rayapati PJ, Stewart CR, Hack E (1989) Pyrroline-5-carboxylate reductase is in pea (*Pisum sativum* L.) leaf chloroplasts. Plant Physiol **91:** 581– 586

Reddy AR, Raghavendra AS (2006) Photooxidative stress. In: Physiology and Molecular Biology of Stress Tolerance in Plants. Madhava Rao KV, Raghavendra AS, Reddy KJ (Eds.) Springer, The Netherlands, pp. 157-186

Riazunnisa K, Padmavathi L, Schiebe R, Raghavendra AS (2007) Preparation of Arabidopsis mesophyll protoplasts with high rates of photosynthesis. Physiol Plant **129:** 679–686

Robinson SP, Walker DA (1979) Rapid separation of the chloroplast and cytoplasmic fraction from intact leaf protoplasts. Arch Biochem Biophys **196:** 319-323

Robson CA, Vanlerberghe GC (2002) Transgenic plant cells lacking mitochondrial alternative oxidase have increased susceptibility to mitochondria- dependent and independent pathways of programmed cell death. Plant Physiol **129:** 1908–1920

Romero-Puertas MC, Palma JM, Gomez M, Del Rio LA, Sandalio LM (2002) Cadmium causes the oxidative modification of proteins in pea plants. Plant Cell Environ **25:** 677-686

Rozen S, Skaletsky HJ (2000) Primer3 on the WWW for general users and for biologist programmers. In: Bioinformatics Methods and Protocols: Methods in molecular biology. Krawetz S, Misener S (Eds.) Humana Press, Totowa, NJ, pp. 365-386

Scandalios G, Guan L, Polidoros AN (1997) Catalases in plants: Gene structure, properties, regulation and expression. In: Oxidative Stress and the Molecular Biology of Antioxidants Defenses, Vol. **34**. Scandalios JG (Eds.) Cold Spring Harbor Lab Press, New York, USA, pp. 343–406

Schacter B, Bassham JA (1972) Antimycin A sensitive stimulation of rate-limiting steps of photosynthesis in isolated spinach chloroplasts. Plant Physiol **49:** 411–416

Scheibe R (2004) Malate valves to balance cellular energy supply. Physiol Plant **120:** 21-26

Scheibe R, Backhausen JE, Emmerlich V, Holtgrefe S (2005) Strategies to maintain redox homeostasis during photosynthesis under changing conditions. J Exp Bot **56:** 1481-1489

Scheibe R, Dietz KJ (2012) Reduction–oxidation network for flexible adjustment of cellular metabolism in photoautotrophic cells. Plant Cell Environ **35:** 202–216

Schwanz P, Haberie KH, Polle A (1996) Inter-active effects of elevated CO_2, ozone and drought stress on the activities of antioxidative enzymes in needles of Norway spruce trees *(Picea abies L.* Karsten) grown with luxurious N-supply. J Plant Physiol **148:** 351 -35

Sheen J (1990) Metabolic repression of transcription in higher plants. Plant Cell **2:** 1027–1038

Sheen J (2001) Signal transduction in maize and Arabidopsis mesophyll protoplasts. Plant Physiol **127:** 1466-1475

Sicher RC (1999) Photosystem-II activity is decreased by yellowing of barley primary leaves during growth in elevated carbon dioxide. Int J Plant Sci **160:** 849–854

Smirnoff N (2000) Ascorbic acid: metabolism and functions of a multi-facetted molecule. Curr Opin Plant Biol **3:** 229-235

Smirnoff N, Conklin PL, Loewus FA (2001) Biosynthesis of ascorbic acid in plants: a renaissance. Annu Rev Plant Physiol Plant Mol Biol **52:** 437–467

Smirnoff N, Wheeler GL (2000) Ascorbic acid in plants: Biosynthesis and function. Crit Rev Biochem Mol Biol **35:** 291–314

Somerville CR, Ogren WL (1982) Isolation of photorespiration mutants in *Arabidopsis thaliana*: In Methods in Chloroplast Biology, Edelman M, Hallick RB, Chua NH (Eds). Amsterdam: Elsevier Biomed Press, pp 129–138

Stitt M (1991) Rising CO_2 levels and their potential significance for carbon flow in photosynthetic cells. Plant Cell Environ **14:** 741–762

Stitt M, Lunn J, Usadel B (2010) Arabidopsis and primary photosynthetic metabolism - more than the icing on the cake. The Plant J **61:** 1067-1091

Storozhenko S, De Pauw P, Van Montagu M, Inzé D, Kushnir S (1998) The heat-shock element is a functional component of the Arabidopsis APX1 gene promoter. Plant Physiol **118:** 1005-1014

Strodtkötter I, Padmasree K, Dinakar C, Speth B, Niazi PS, Wojtera J, Voss I, Do PT, Nunes-Nesi A, Fernie A R, Linke V, Raghavendra AS, Scheibe R (2009) Induction of the AOX1D isoform of alternative oxidase in *A. thaliana* T-DNA insertion lines lacking isoforms AOX1A is insufficient to optimize photosynthesis when treated with antimycin A. Mol Plant **2:** 284–297

Szabados L, Savoure´ A (2009) Proline: a multifunctional amino acid. Trends Plant Sci **15:** 89–97

Szalai G, Kellős T, Galiba G, Kocsy G (2009) Glutathione as an antioxidant and regulatory molecule in plants under abiotic stress conditions. J Plant Growth Regul **28:** 66–80

Szoke A, Miao GH, Hong Z, Verma DP (1992) Subcellular location of delta-pyrroline-5-carboxylate reductase in root/nodule and leaf of soybean. Plant Physiol **99:** 1642–1649

Takahashi S, Badger MR (2011) Photoprotection in plants: a new light on photosystem II damage. Trends Plant Sci **16**: 53-60

Talla SK, Riazunnisa K, Padmavathi L, Sunil B, Rajsheel P, Raghavendra AS (2011) Ascorbic acid is a key participant during the interactions between chloroplasts and mitochondria to optimize photosynthesis and protect against photoinhibition. J Biosci **36:** 163–173

Tambussi EA, Bartoli CG, Beltrano J, Guiamet JJ, Araus JL (2000) Oxidative damage to thylakoid proteins in water-stressed leaves of wheat (*Triticum aestivum*). Physiol Plant **108:** 398–404

Taniguchi M, Miyake H (2012) Redox-shuttling between chloroplast and cytosol: integration of intra-chloroplast and extra-chloroplast metabolism. Curr Opin Plant Biol **15:** 1–9

Towbin H, Staehlin T, Gordon J (1979) Electrophoretic transfer of proteins from polyacrylamide gels to nitrocellulose sheets. Procedure and some applications. Proc Natl Acad Sci USA **76:** 4350-4354

Vandenabeele S, Vanderauwera S, Vuylstecke M, Rombauts S, Langebartels C, Seidlitz HK, Zabeau M, Van Montagu M, Inzé D, Van Breusegem F (2004) Catalase deficiency drastically affects gene expression induced by high light in *Arabidopsis thaliana*. Plant J **39:** 45–58

Veljovic-Jovanovic SD, Pignocchi C, Noctor G, Foyer CH (2001) Low ascorbic acid in the *vtc1* mutant of *Arabidopsis* is associated with decreased growth and intracellular redistribution of the antioxidant system**.** Plant Physiol **127:** 426–435

Verbruggen N, Hermans C (2008) Proline accumulation in plants: a review. Amino Acids **35:** 753–759

Vidal G, Carbo MR, Garmier M, Dubertret G, Rasmusson AG, Mathieu C, Foyer CH, Paepe RD (2007) Lack of respiratory chain complex I impairs alternative oxidase engagement and modulates redox signalling during elicitor induced cell death in tobacco. Plant Cell **19:** 640–655

Walker D (1988) The Use of the Oxygen Electrode and Fluorescence Probes in Simple Measurements of Photosynthesis. University of Sheffield Press, Sheffield, UK

Wilhelm C, Selmar D (2011) Energy dissipation is an essential mechanism to sustain the viability of plants: The physiological limits of improved photosynthesis. J Plant Physiol **168:** 79-87

Willekens H, Chamnongpol S, Davey M, Schraudner M, Langebartels C, Van Montagu M, Inzé D, Van Camp W (1997) Catalase is a sink for H_2O_2 and is indispensable for stress defence in C-3 plants. EMBO J **16:** 4806–4816

Willekens H, Inze D, Van Montagu M, Van Camp W (1995) Catalases in plants. Mol Breeding **1:** 207–228

Wingler A, Lea PJ, Quick WP, Leegood RC (2000) Photorespiration-metabolic pathways and their role in stress protection. Phil Trans R Soc London B **355:** 1517–1529

Winkel-Shirley B (2002) Biosynthesis of flavonoids and effects of stress, Curr Opin Plant Biol **5:** 218-223

Xu F, Yuan S, Lin HH (2011) Response of mitochondrial alternative oxidase (AOX) to light signals. Plant Signal Behav **6:** 55-58

Yabuta Y, Mieda T, Madhusudhan R, Ayana N, Motoki T, Maruta T, Yoshimura K, Ishikawa T, Shigeoka S (2007) Light regulation of ascorbate biosynthesis is dependent on the photosynthetic electron transport chain but independent of sugars in *Arabidopsis*. J Exp Bot **5:** 2661-2671

Yabuta Y, Motoki T, Yoshimura K, Takeda T, Ishikawa T, Shigeoka S (2002) Thylakoid membrane-bound ascorbate peroxidase is a limiting factor of antioxidative systems under photo-oxidative stress. Plant J **32:** 915–925

Yang SL, Lan SS, Gong M (2009) Hydrogen peroxide-induced proline and metabolic pathway of its accumulation in maize seedlings. J Plant Physiol **166:** 1694–1699

Yoshida K, Noguchi K (2010) Interaction between chloroplasts and mitochondria: activity, function and regulation of the mitochondrial respiratory system during photosynthesis. In Kempken F (Eds). Plant Mitochondria: Adv Plant Biol **1** NY: Springer, pp. 383–410.

Yoshida K, Terashima I, Noguchi K (2006) Distinct roles of the cytochrome pathway and alternative oxidase in leaf photosynthesis. Plant Cell Physiol **47:** 22-31

Yoshida K, Terashima I, Noguchi K (2007) Up-regulation of mitochondrial alternative oxidase concomitant with chloroplast over-reduction by excess light. Plant Cell Physiol **48:** 606–614

Yoshida K, Watanabe CK, Kato Y, Sakamoto W, Noguchi K (2008) Influence of chloroplastic photo-oxidative stress on mitochondrial alternative oxidase capacity and respiratory properties: a case study with *Arabidopsis* yellow variegated 2. Plant Cell Physiol **49:** 592–603

Yoshimura K, Yabuta Y, Ishikawa T, Shigeoka S (2000) Expression of spinach ascorbate peroxidase isoenzymes in response to oxidative stresses. Plant Physiol **123:** 223–234

Zhang DW , Xu F, Zhang ZW, Chen Ye, Du JB, Jia SD, Yuan S, Lin HH (2010) Effects of light on cyanide-resistant respiration and alternative oxidase function in *Arabidopsis* seedlings. Plant Cell Environ **33:** 2121-2131

Zhang LT, Zhang ZS, Gao HY, Xue ZC, Yang C, Meng XL, Meng QW (2011) Mitochondrial alternative oxidase pathway protects plants against photoinhibition by alleviating inhibition of the repair of photodamaged PSII through preventing formation of reactive oxygen species in *Rumex* K-1 leaves. Physiol Plant **143:** 396–407

****

Appendix

Research Articles Published and Meetings Attended By

Sai Krishna Talla

(First pages of the article are attached)

Research Publications:

1. Inga Hebbelmann, Jennifer Selinski, Corinna Wehmeyer, Tatjana Goss, Ingo Voss, Paula Mulo, Saijaliisa Kangasjärvi, Eva-Mari Aro, Marie-Luise Oelze, Karl-Josef Dietz, Adriano Nunes-Nesi, Phuc T. Do, Alisdair R. Fernie, **Sai K. Talla**, Agepati S. Raghavendra, Vera Linke and Renate Scheibe (2012) "Multiple strategies to prevent oxidative stress in Arabidopsis plants lacking the malate valve enzyme NADP-malate dehydrogenase" *Journal of Experimental Botany* **63:** 1445–1459
2. **Sai Krishna Talla,** K. Riazunnisa, L. Padmavathi, B. Sunil, RajSheel Pidakala and Agepati. S. Raghavendra (2011) "Ascorbic acid is a key participant during the cross-talk between chloroplasts and mitochondria to optimize photosynthesis at high light and protect against photoinhibition" *Journal of Bioscience* **36:** 163–173
3. Sunil Bobba, K Riazunnisa, **T Sai Krishna**, Gert Schansker, Reto J Strasser, Agepati S Raghavendra and Prasanna Mohanty (2008) "Application of fast chlorophyll *a* fluorescence transient (OJIP) analysis to monitor functional integrity of pea *(Pisum sativum)* mesophyll protoplasts during isolation" *Indian Journal of Biochemistry and Biophysics* **45:** 37-43

Posters Presented at the Conferences:

1. Poster presentation on "Components of redox homeostasis to optimize photosynthesis in mesophyll cell protoplasts of *nadp-mdh* knock out mutants of *Arabidopsis thaliana"* **Sai Krishna Talla** and Agepati S. Raghavendra in International conference on *"Plant Science in post genomic era (ICPSPGE-2011)"* held on 17th-19th February 2011, Sambalpur University, Jyoti Vihar, Odissa, India
2. Poster presentation on "Role of ascorbate during the interorganelle interactions of chloroplasts and mitochondria in optimizing photosynthesis and protection against photoinhibition" **Sai Krishna Talla** and Agepati S. Raghavendra in "*The 6th SPPS PhD Student Conference"* 2nd -5th September 2010, Espoo, Finland
3. Poster presentation on "Role of ascorbate during optimization of photosynthesis and protection against photoinhibition by mitochondrial metabolism" **Sai Krishna Talla,** K. Riazunnisa, Rajsheel Pidakala, Bakka Kavya and Agepati S. Raghavendra in *"4th Asia-Oceanic conference on Photobiology"*. 24th – 26th Nov, 2008, BHU, Varanasi, India
4. Poster presentation on " Role of ascorbate during optimization of photosynthesis and protection against photoinhibition by mitochondrial metabolism" K. Riazunnisa, **Sai Krishna Talla,** B. Sunil, Rajsheel Pidakala and Agepati S. Raghavendra in *"2nd International conference on Trends in Cellular and Molecular Biology"*. 2nd- 5th January 2008, JNU, New Delhi, India
5. Poster presentation on "Low carbon requirement for photosynthesis by mesophyll protoplasts of pea (*Pisum sativum*): possible roles of photorespiratory CO_2 and carbonic anhydrase" **Sai Krishna Talla**, K. Riazunnisa, B. Sunil and Agepati S. Raghavendra in *"XVIII International Symposium on Light and Life"*. August 2007, University of Hyderabad, Hyderabad.